Numerical Modelling of High Bit-rate Dispersion Managed Systems

Mobasshir Mushtaq
Master of Philosophy

Aston University

June 2001

Aston University
Numerical Modelling of High Bit-rate Dispersion Managed Systems

Mobasshir Mushtaq

Master of Philosophy

June 2001

This thesis presents the results of numerical modelling of the propagation of dispersion managed solitons, in standard fibre using fibre grating for dispersion compensation. The theory of optical fibre and propagation in single mode optical fibre is introduced, followed by numerical technique to solve the nonlinear Schrödinger equation. The recent development in the use of dispersion managed solitons are discussed before the numerical results are presented.

The work in this thesis covers the upgrade of the installed standard fibre network to higher data rates through the use of solitons and dispersion management.

The use of dispersion management has been investigated using fibre grating for dispersion compensation, both as single pulse and for the transmission of a 10 Gbit/sec data pattern. It has been found that by placing the amplifier and grating at an optimum position stable propagation is possible at high data rates.

The interest has increased over recent years in use of EDFAs and dispersion management to upgrade installed standard fibre network to higher data rates. This thesis presents a study of propagation of data at both 10 Gbit/sec and 40 Gbit/sec. Propagation over Trans-oceanic distances is possible for 10 Gbit/sec and for more than 1500km at 40 Gbit/sec. The use of dispersion managed solitons in the future of optical communication systems is discussed in the thesis conclusions.

Additional Keywords and phrases

Optical solitons, dispersion management, fibre grating

Acknowledgement

There are several people who have provided valuable assistance during the course of my studies. I would firstly like to thank my supervisor Wladek Forsiak for his help and support throughout my time at Aston. I would also like to thank Finlay Knox who provided a good deal of guidance during my second year. I would also like to thank all my friends and other past and present members of photonics research group for their help and friendship.

Finally my thanks go to Wladek Forsiak for reading this thesis.

for Mum, Dad, Aisha, Fatima, Sarah and Ahmed

Table of Contents

List of Figures

Chapter 1

Introduction to optical fibre communication system

1.1 Introduction

Recent years have seen rapid progress in the research and development of lightwave communication systems. The reason behind this is the increasing demand for telecommunication services. Most of the practical and research work has been directed towards two goals: the development of long-haul optical fibre communication systems and the upgrade of existing terrestrial fibre network. The developments in light wave systems have been revolutionised by the deployment of erbium-doped fibre amplifiers, providing periodic amplification of optical signals. The purpose of this thesis is study of one potential method to increase the capacity and accuracy of existing optical communication systems, making use of fibre non-linearity and optical solitons.

1.2 Optical fibre characteristics

Optical fibre consists of a central core surrounded by a cladding layer whose refractive index is slightly lower then that of the core. These are referred to as step index fibre to distinguish them from graded-index fibres in which the refractive index of the core decreases gradually from centre of the core boundary. This encasing of slightly high refractive index within a lower refractive index cladding optical signal is guided through the glass medium. Naturally the electric field transverses this boundary but is contained by the core cladding boundary which then in turns guides the signal through the fibre.

The core size is the main difference between the single-mode and multi-mode fibres. The multi-mode fibres have core radius of ~ 25-30 μm, where as single mode fibres with typical value of relative core cladding index difference (Δ) ~ 3 x 10^{-3} require radius to be in the range 2-4 μm. The outer radius should be large enough to confine the fibre modes entirely. Typically, outer radius is 50-60 μm for both single mode and multi-mode fibres. Recent developments in fibre fabrication technology has enabled us to make the core so narrow that it is possible to have fundamental single mode HE_{11}. The core radius for single mode fibre is given by normalised frequency V

$$V = k_0 \quad a \left(n_1^2 - n_2^2\right)^{1/2} \tag{1.1}$$

Where $k_0 = 2\pi/\lambda$, 'a' is core radius and λ is the wavelength of light.

The relative core-cladding index difference Δ is defined by

$$\Delta = \frac{n_1 - n_2}{n_1} \tag{1.2}$$

The parameter V determines the number of modes supported by the fibre. The step index fibres support a single mode if $V < 2.405$, and the fibres designed to satisfy this condition are called single mode fibres. Since non-linear effects are mostly studied using single mode fibres, the term optical fibre normally refers to single-mode fibres unless noted otherwise.

1.2.1 Fibre loss

A measure of power loss during transmission of optical signals inside the fibre is an important fibre parameter. If P_0 is the power launched at the input of a fibre of length L, the transmitted power P_T is given by

$$P_T = P_0 \exp(-\alpha L) \tag{1.3}$$

Where α is the attenuation constant, commonly referred to as the fibre loss. It is customary to express the fibre loss in the units of dB/km by using the relation

$$\alpha_{dB} = -\frac{10}{L}\log\left[\frac{P_T}{P_0}\right] = 4.343\alpha \quad (1.4)$$

Where equation (1.4) was use to relate α_{dB} and α.

Fibre pulling techniques have enabled us to reduce the loss so that only three type of loss are important. First, one is the fundamental intrinsic loss due to Rayleigh scattering, which depends on the constituents of fibre random density fluctuations of silica. These fluctuations depend on wavelength λ^{-4}, which is dominant for short wavelengths beyond 1.6 μm. The other losses are the electronic infrared absorption losses and OH absorption losses. These losses could be reduced be take more care during the manufacturing process. Figure (1.1) shows the loss profile of single mode optical fibre:

The loss profile is the deciding factor in operating window for the long distance transmission systems. The first window 980 μm not shown in the figure 1.1, is not applicable for the long distance transmission systems however it is good for short distance systems due to the availability of cheap and simple electronics for transmitters and receivers. Second window is at 1.3 μm, which is used, in installed fibre due to the low dispersion of step index fibre.

The third window 1.55 μm has the lowest loss. This thesis concentrate on third window at 1.55 μm that has opened system design through two developments namely the dispersion shifted fibre and Erbium doped fibre amplifiers.

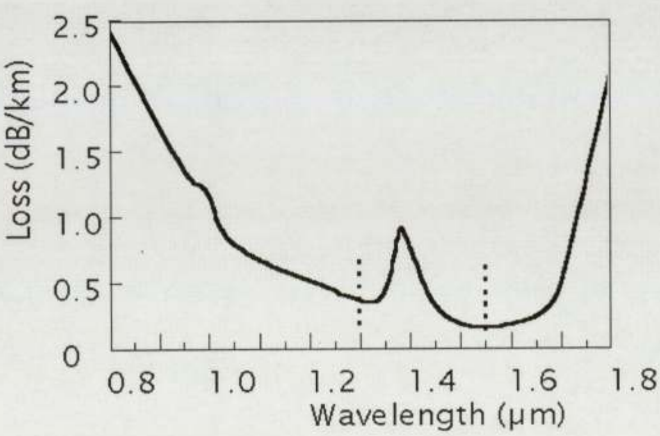

Figure 1.1: Measured loss profile of a single mode optical fibre, from [1], pp 6. The dashed curve is the intrinsic loss from Rayleigh scattering and infrared absorption of pure silica, the solid line is the

measured profile clearly showing a peak in the loss from the OH-absorption at 1.4 μm and a smaller peak at 1.25 μm.

1.3 Chromatic Dispersion

The second characteristic of optical fibres is their chromatic dispersion. This results due to the interaction of electromagnetic waves with bound electrons of the medium, which then results frequency dependency of the refractive index $n(\omega)$. This dependence affects the propagation of optical pulses as the propagation speed of their constituent frequency component is given by $c/n(\omega)$. This results in components arriving at different times producing a temporal

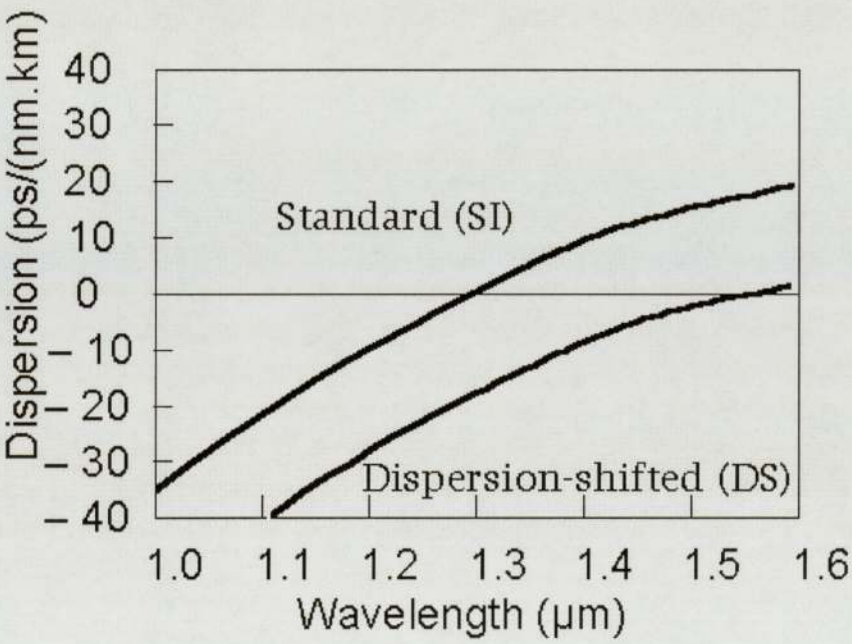

dispersion of the pulse. This can be a serious limitation to the optical system.

Figure 1.2: Variation of the dispersion parameter D_2 with wavelength for a step-index single-mode fibre, taken from [1], pp.11

The rate of this dispersion is described by the dispersion parameter D_2, essentially the second derivative of the refractive index with respect to wavelength. Figure 1.2 shows a typical dispersion profile for a standard step index fibre.

In the standard fibre, the dispersion is mainly due to the chromatic dispersion of the optical fibre although there is a small contribution from the waveguiding effect of the fibre called waveguide dispersion. The dispersion zero wavelength can be tailoring the fibre core and cross-section profile to increase the wave guide dispersion. One of the examples is moving the dispersion zero into the second window to give "dispersion shifted fibres: (DSFs) which permits long distance transmission. Secondly by moving the dispersion zero beyond 1.6 μm produces Dispersion compensating fibres (DCFs) which are of great interest currently [2,3].

1.3.1 Fibre Nonlinearity

The third fibre characteristic is it's nonlinearly. From the earliest proposals of the application of fibres in communication systems, it has been recognised that non-linear optical processes would present an operation limit on the fibre length and power levels to be transmitted. For example self-phase modulation gives rise to spectral broadening, this together with the dispersion in fibre temporally broadens the transmitted pulses and limits the maximum achievable information transmission rate. Similarly, the non-linear process of stimulated Raman scattering would act to limit the maximum operational power levels or give rise to information loss and introduce noise into the system. With present developments in optical communications, particularly towards long distance, single mode, repeaterless submarine cable systems, it is necessary to consider the use of low-loss mid infrared fibres or to increase the transmitted power levels. Under these circumstances, it is highly likely that detrimental non-linear effects cannot be neglected.

The nonlinearity of optical fibre comes from the third order susceptibility $\chi^{(3)}$, of the silica and can result in effects such as four wave mixing and non-linear refraction. Four-wave mixing occurs between the co-propagating waves of different frequencies resulting in generation of new frequencies. We will only concentrate on non-linear refraction as we are only considering single wavelength. This occurs both through the self-action of waves on itself as well as between different waves and polarization. This results in a non-linear variation of the refractive index $\bar{n}(\omega, |E|^2)$ of the fibre with intensity $|E|^2$ [1], pp.16.

Although optical fibres have very small non-linear index coefficient, over long transmission distances this intensity dependence of the refractive index leads to effects such as self-phase modulation and cross-phase modulation.

1.3.2 Fibre birefringence

The final fibre characteristic of interest is the fibre birefringence. Coupling between the polarization modes of a single mode fibre can be reduced to zero by making the fibre perfectly cylindrical. However manufacturing defects lead to deviation from cylindrical symmetry and hence results in birefringence. For a constant difference in the refractive indices of the two modes, there is a fast and a slow axis, with the fast axis having lower refractive index. Generally, however local fluctuations in the core and hence in the local birefringence are introduced by imperfections in the manufacturing process. Light launched into a single mode fibre, reaches quickly to some arbitrary polarization due to the resultant mixing of the polarization modes. The implication of optical transmission systems is that ordinary fibres will not be able to support polarization division multiplexing, as the signals will mix on propagation and the data will be corrupted although some success has been found [4][5]. A strong and essential constant birefringence can be induced by tailoring the fibre cross-sectional profile to create "polarization maintaining fibres" which should allow polarization multiplexing. The birefringence is also responsible for polarization mode dispersion (PMD), which is currently presenting limitations for upgrading existing standard fibre systems, as low birefringence and hence low PMD was not specified when fibre was commissioned.

1.4 All optical systems

The fibre loss is no longer the major limitation in optical fibre transmission and the performance of optical amplifier systems is then limited by chromatic dispersion and non-linearity. Optical SNR also plays an important role, low average dispersion does reduce the timing jitter but it degrades OSNR, hence increasing the probability of error. These limitations can be overcomed either by linear or non-linear methods. In the first approach both the chromatic dispersion and nonlinearity are considered to be detrimental factors, where as in the later the non-linear and dispersive effects are counter balanced. Non-linear effects that are detrimental in the "Linear" systems can be used to improve the transmission characteristics of intensity-modulated direct detection optical communication systems. In the long haul light wave communication systems, the utilisation of in line erbium doped fibre optical amplifiers (EDFA's) is assumed to be used to compensate for the attenuation in the carrier signal in the transmission fibre. Average slow dispersive broadening of the pulse propagating in the anomalous dispersion region can be exactly compensated for by the non-linear phase shift. Thus traditional fundamental solitons rely on a balance between the self-phase modulation and anomalous second order dispersion that allows the preservation of carrier signal over thousands of kilometres. The important feature of traditional non-linear systems is the considerable shorter amplifier spacing than the dispersion and non-linear lengths, and hence both dispersion and nonlinearity can be treated as perturbations on the scale of one amplification period. In the leading order, only the fibre loss and the periodic amplifications are significant factors effecting pulse evolution between two consecutive amplifiers. These factors cause power oscillations, while the form of pulse during one amplification period approximately remains unchanged. The nonlinearity and dispersion come into play on the larger scales and pulse propagation in such communication systems is described by the well-established guiding centre (path averaged) soliton theory. The average dynamics of the optical signal in this case is given in the leading order by the integrable non-linear Schödinger equation (NLSE). This gives an additional advantage to the use of well-developed mathematical technique for analysing effect of numerous practical perturbations and boundary conditions. The penalty in using the soliton approach is that the broader optical spectrum of RZ pulses is more susceptible to the spontaneous emission noise introduced by optical amplifiers. This results in amplitude fluctuations and a timing jitter known as Gordon-Haus effect. However on the other hand is good news for WDM systems where broader spectrum means more channels. Additionally the need to balance the nonlinearity with the dispersion for any given pulse width prevents arbitrary increase in the transmitted signal power. The increase in the launch power by selection of the pulse width or fibre dispersion improves the signal to noise ratio, which results in worse timing jitter, thus limiting the benefits obtainable from optimisation of these parameters. To overcome this problem much effort has been placed in the development of soliton control techniques. These rely on the placement of additional components within the transmission path to suppress the accumulation of timing and amplitude errors. The two most common approaches are spectral filtering of either fixed or sliding variants and synchronous modulation. Fixed filtering [69]uses identical band pass filters placed at regular intervals along the fibre produces small performance improvements, although there have been recent suggestions that better filter characteristics could be beneficial. The sliding filter approach involves displacing the centre of passband successively along the fibre, thereby achieving a more effective separation between the signal and the noise. The second common control mechanism places phase [101] and or intensity modulators within the transmission path driven synchronously with the bit rate. This can result in effectively unlimited propagation distances. However, both spectral filtering and modulation raise serious issues of component count, cost, complexity and reliability due to addition under water components required.

The above mentioned fibre characteristics can lead to signal degradation in an optical transmission system. To date all optical transmission systems have relied on a linear transmission format, where non-linear effects are avoided through the use of square pulses filing the bit period, known as non-return-to-zero (NRZ) transmission [3,6,7,8]. In these systems, the detrimental effects the pulses experience are not significant over a single amplifier span. The pulses are detected electronically at the end of each span, and re-timed, amplified, reshaped and then transmitted. High-speed electronics are required after each fibre span adding unwanted expense and complexity at each fibre node. These systems are also restricted in operation to single data rate because in order to upgrade the system by increasing the data rate would mean replacing all the electronics. This will be very expensive and complex and hence not practical.

Dispersion compensation is rapidly emerging as alternative strategy for improving the performance of soliton transmission. The idea is to adopt non-uniform dispersion map which contains segments of both normal and anomalous dispersion fibre. The non-linear optical properties of a fibre system can be strongly modified by the periodic alternation of the dispersion sign. With in the soliton transmission short segments of normally dispersive fibres, which might arise due to fluctuation in the fibre fabrication process, are known to be tolerated. Recently this idea was extended to allow discretion allocation of a system to achieve a desired mean dispersion from the concatenation of more than one fibre, thus easing fibre fabrication and selection. Another avenue of development was provided by an investigation of the possibilities of soliton transmission on installed standard fibre using dispersion compensation to reduce the mean dispersion value. Much of the installed step index fibre has a high dispersion ~15-20 ps/nm/km in the 1.55 μm gain window of EDFA's. Upgrading these systems to higher data rates by simply replacing the electronic regenerators with optical amplifiers is highly attractive economically. However, the all optical nature of these amplifiers means that there is no pulse re-shaping as with the electronic regeneration, and hence the converted system will require some dispersion management. Solitons offer this possibility, by offsetting the dispersion against nonlinearity, but present their own problems. In contrast to the long-haul systems, accumulated noise is not the source of the difficulties for these short-haul systems. Instead, the principle constraints are due to the high fibre dispersion. In particular these are the high average powers required to support solitons, the short soliton periods which limit the amplifier spacing and the short soliton interaction distances [101] of closely packed solitons, which limit the total transmission distances.

1.5 Thesis overview

In this chapter, so far general terms and limitations to pulse transmission in fibre optic communications and the place of soliton in such systems have been discussed. In chapter 2, these ideas and some of the limitations to soliton propagation will be discussed in more detail. Different effects such as group velocity dispersion (GVD) and self-phase modulation will be discussed. In chapter 3, the non-linear Schrödinger equation and soliton solution is discussed, with some insight to soliton system design features such as soliton-soliton interaction and Gordon Haus effect. Chapter 4 discusses dispersion management and properties of dispersion managed solitons. With this as our background, we wish to find ways to alleviate some of the problems in order that solitons can be used in real transmission systems. This considers methods of improving soliton propagation in optical fibres using variety of novel techniques, mainly concerning dispersion management of the optical fibre.

In chapter 5, we consider an asymmetric dispersion compensation scheme with fibre grating. The moving of launch point with in the dispersion map to average over the pulse shape changes as well as power in highly perturbed systems is discussed. It then goes on to show possibility of soliton propagation at 10Gbit/s with long spans of standard fibre.

Chapter 6 discusses the upgradation of existing fibre links with the use of chirped pulse at the input and fibre gratting, and compares the performance of such system with the one discussed in chapter 5.

In chapter 7, the possibility of upgrading the links composed of standard fibre, to high data rates of 40Gbit/s with 100-km section of standard fibre. This shows a novel RZ pulse propagation regime where pulses can be transmitted jitter free for more than global distances. Finally chapter 8 summarises the conclusion of this work and considers the current and future positions of dispersion managed solitons in the world of fibre optic communication.

Chapter 2

Propagation in Optical Fibres

2.1 Introduction

A mathematical model is required to study the propagation of pulses in optical fibre systems. The simplest model of non-linear pulse propagation in an optical fibre is the Non-linear Schödinger (NLS) equation. This section outlines the derivation, from Maxwell's equations, of the NLS equation which describes pulse propagation in a dispersive medium and will be used to investigate two important effects, group velocity dispersion (GVD) and self phase modulation (SPM). These effects will be introduced and investigated separately before their combined effect will be studies, which leads to formation of optical solitons. Other effects on soliton system performance are also discussed and dispersion compensating systems, which use fibre grating, will be introduced.

2.2 The non-linear Schödinger equation

The basic wave equation used in deriving the NLS equation is

$$\nabla^2 E - \frac{1}{c^2}\frac{\partial^2 E}{\partial t^2} = \mu_0 \frac{\partial^2 P_L}{\partial t^2} + \mu_0 \frac{\partial^2 P_{NL}}{\partial t^2} \tag{2.1}$$

Where E(r, t) is the electric field, c is the speed of light, μ_0 is the permeability of free space and P_L, P_{NL} are the linear and non-linear parts of the induced polarisation P(r, t)

$$P(r, t)=P_L(r, t)+ P_{NL}(r, t) \tag{2.2}$$

The linear and non-linear induced polarisation fields are related to E(r, t) through the dielectric tensors $\chi^{(1)}$ and $\chi^{(3)}$ respectively [1], pp28.

In order to solve equation 2.1 three approximation are required to simplify the problem: the non-linear polarisation P_{NL} is taken only a small perturbation to the linear polarisation P_L; it is assumed that the polarisation of the optical field does not change as it propagates along the fibre-thus a scalar approaches valid and finally, it is assumed that the optical field is quasi-monochromatic, i.e. $\Delta\omega/\omega_0 << 1$ where $\Delta\omega$ is the spectral width and ω_0 is the central frequency. E(r, t) can then be written as

$$E(r,t) = \frac{1}{2}\hat{x}\left[\overline{E}(r,t)\exp(-i\omega_0 t) + c.c\right] \tag{2.3}$$

Where c.c. denotes the complex conjugate, $\hat{x}$ is the polarisation unit vector of the propagating light and $\overline{E}(r,t)$ is a slowly varying function of time compared to the optical period. P_L, P_{NL} can be represented in a similar way. The nonlinearity is taken to be instantaneous, in order obtain non-linear polarisation form electric field, which is generally valid for optical fibres for pulse widths greater than 0.1 ps [1], pp.36.

Since the amplitude E(r, t) varies slowly, hence is given by using the Fourier transform, which is valid when PNL is taken as a small perturbation. This wave equation is given by

$$\nabla^2 \widetilde{E} + \varepsilon(\omega) k_0^2 \widetilde{E} = 0 \tag{2.4}$$

Where $k_0 = 2\pi/\lambda$ is the propagation constant at wavelength λ and $\varepsilon(\omega)$ is the dielectric constant which is related to dielectric tensor and allows us to find the

Coefficient of nonlinearity n_2 as [1], pp.37

$$n_2 = \frac{3}{8n} \chi^{(3)}_{xxxx} \tag{2.5}$$

By using the definition

$$\overline{n}(\omega, |E|^2) = n(\omega) + n_2 |E|^2 \tag{2.6}$$

Equation (2.6) shows the nature of the nonlinearity, as a modification to the linear refractive index, n (ω), depending on the square of the electric field, the intensity. This intensity dependent refractive index change, known as non-linear refraction, gives rise to the effect of self-phase modulation.

Equation (2.4) could be solved to give

$$\widetilde{E}(r, \omega - \omega_0) = \int_{-\infty}^{\infty} \overline{E}(r, y) \exp\left[i(\omega - \omega_0)t\right] dt \tag{2.7}$$

By separating the variables for the electric field we get

$$\widetilde{E}(r, \omega - \omega_0) = F(x, y) \widetilde{A}(Z, \omega - \omega_0) \exp(i\beta_0 z) \tag{2.8}$$

Where $\widetilde{A}(Z, \omega - \omega_0)$ varies slowly with Z and F (x, y) contains the lateral fibre mode dependence, approximately Gaussian for a single mode fibre and unaffected by changes in the refractive index hence ignored below, and β_0 is the propagation constant. Using this substitution, the propagation equation (2.4) becomes

$$\frac{\partial \widetilde{A}}{\partial Z} = i[\beta(\omega) + \Delta\beta - \beta_0]\widetilde{A} \tag{2.9}$$

Where $\Delta\beta$ is found from the modal distribution through F (x, y). The temporal solution of the slowly varying amplitude A (Z, t) could be obtained by taking the inverse transform of equation (2.7), for which it is useful to expand $\beta(\omega)$ as a Taylor series about the carrier frequency ω_0 as

$$\beta(\omega) = \beta_0 + (\omega - \omega_0)\beta_1 + \frac{1}{2}(\omega - \omega_0)^2 \beta_2 + \frac{1}{6}(\omega - \omega_0)^3 \beta_3 + \cdots \tag{2.10}$$

Where

$$\beta_n = \frac{\partial^n \beta}{\partial \omega^n} \tag{2.11}$$

With β_0 , β_1 , β_2 and β_3 the propagation constant, inverse group velocity, group velocity dispersion and the third order dispersion respectively. The cubic and higher order terms are generally negligible if the spectral width is much less than the carrier frequency ($\Delta\omega << \omega_0$). The cubic term can become significant if $\beta_2 \cong 0$.

Substituting this and performing Fourier transform on equation (2.9) and evaluating $\Delta\beta$, which includes the effects of fibre loss and nonlinearity, we get [1], pp.40

$$\frac{\partial A}{\partial Z} + \beta_1 \frac{\partial A}{\partial t} + \frac{i}{2}\beta_2 \frac{\partial^2 A}{\partial t^2} + \frac{\alpha}{2} A = i\gamma |A|^2 A \tag{2.12}$$

Where the non-linear coefficient γ is defined as

$$\gamma = \frac{n_2 \omega_0}{c A_{eff}} \tag{2.13}$$

Where A_{eff} is the effective core area of the fibre, the area of the core and cladding within which signal propagates. As there is still some discussion, the value of n2 is known to be around 2.5 x 10-20m2W-1. Typically the effective core area at 1.55 μm is 50 - 80 ,μm^2, depending on the fibre type. Another simplification is to move to a frame of reference, moving with the pulse, we wish to study at the group velocity $v_g = 1/\beta_1$ by making the transformation

$$T = t - \frac{Z}{v_g} = t - \beta_1 Z \qquad (2.14)$$

This gives equation (2.12) as

$$i\frac{\partial A}{\partial Z} = -\frac{i}{2}\alpha A +_2 \frac{1}{2}\frac{\partial^2 A}{\partial T^2} - \gamma|A|^2 A \qquad (2.15)$$

This is known as the generalised non-linear Schödinger equation. If the loss is taken as $\alpha=0$ it is known simply as the non-linear Schödinger equation (NLSE). Loss aside, equation (2.15) gives four regimes of operation to consider when studying optical pulse propagation. These can be loosely defined through the use of two length scales, the dispersion length L_D and the non-linear length L_{NL}:

$$L_D = \frac{\tau_0^2}{|\beta_2|} \qquad (2.16)$$

$$L_{NL} = \frac{1}{\gamma P_0} \qquad (2.17)$$

Where P_0 is the peak power of the pulse of width τ_0 and γ is the non-linear coefficient.

The relative magnitudes of these two length scales compared with the transmission distance L give the four regimes of operation. If $L << L_D, L_{NL}$, the pulse does not experience significant linear or non-linear effects, but this regime requires long pulses (>100 ps) at low peak powers (<0.1 mW) which are not of interest for high speed communications. The remaining operating regimes, where dispersion dominates ($L \geq L_D$, $L << L_{NL}$), nonlinearity dominates (dominates ($L \geq L_{NL}$, $L << L_D$) and where both nonlinearity and dispersion are significant (dominates ($L \geq L_D, L_{NL}$) are outlined below.

2.3 Group velocity dispersion

The operating regime in which $L > L_D$ and $L << L_{NL}$, dispersion has a significant effect on the optical pulse. Different optical wavelengths travel at a slightly different velocity in any medium due to the variation in the refractive index with wavelength. This means that the constituent wavelengths of a pulse arrive at slightly different times, giving a temporal dispersion known as group velocity dispersion (GVD). This can be understood by the refraction of a white light source through a prism splitting the light into its constituent colours and revealing the optical spectrum. This well-known effect is the result of the difference in refraction experienced by the colours of the light due to the refractive index variation.

Mathematically, we start from the NLSE with loss as defined by equation (2.16). If the effects due to nonlinearity are assumed to be negligible, n_2 and hence γ are set equal to zero removing this term. It is not necessary to exclude the effect of loss as it has no effect on pure dispersion and can be removed through the use of a normalised pulse envelope U (Z, T) with,

$$A(Z,T) = \sqrt{P^0}\exp\left(-\frac{\alpha Z}{2}\right)U(Z,T) \tag{2.18}$$

Thus normalised version of equation (2.15) in the dispersive regime is

$$i\frac{\partial U}{\partial Z} = \frac{1}{2}\beta_2\frac{\partial^2 U}{\partial T^2} \tag{2.19}$$

This equation can be solved using the Fourier method. If $\widetilde{U}(Z,\omega)$ is the Fourier transform of U (Z, T) such that,

$$U(Z,T) = \frac{1}{2\pi}\int_{-\infty}^{\infty}\widetilde{U}(Z,\omega)\exp(-i\omega T)d\omega \tag{2.20}$$

Then it will satisfy the ordinary differential equation

$$i\frac{\partial \widetilde{U}}{\partial Z}=\frac{1}{2}\beta_2\omega^2\widetilde{U} \tag{2.21}$$

Giving the solution

$$\widetilde{U}(Z,\omega)=\widetilde{U}(0,\omega)\exp\left(\frac{i}{2}\beta_2\omega^2 Z\right) \tag{2.22}$$

Where $\widetilde{U}(0,\omega)$ is the Fourier transform of the input pulse at Z=0 given by

$$\widetilde{U}(0,\omega)=\frac{1}{2\pi}\int_{-\infty}^{\infty}U(0,T)\exp(i\omega T)dT \tag{2.23}$$

Equation (2.23) gives the relative phase of the pulse spectral components change as a function of propagation distance and the square of the frequency of that component. The spectral contents of the pulse are not however altered by these phase changes, but they do change the shape of the pulse. The general solution of the equation (2.19) can be obtained by substituting equation (2.22) into equation (2.20) to give

$$U(Z,T)=\frac{1}{2\pi}\int_{-\infty}^{\infty}\widetilde{U}(0,\omega)\exp\left(\frac{i}{2}\beta_2\omega^2 Z-i\omega T\right)dT \tag{2.24}$$

The effect of GVD on a pulse can be explained by considering an input transform-limited Gaussian pulse of the form

$$U(0,T)=\exp\left(\frac{T^2}{2\tau_0^2}\right) \tag{2.25}$$

Where τ_0 is the input 1/e half width of the pulse, related to the full width at half maximum (FWHM) pulse width through $\tau_f=2\sqrt{\ln 2}\tau_0\approx 1.665\tau_0$. Equation (2.23) and (2.24) could be integrated after substitution to give solution for a pulse after a given propagation distance as

$$U(Z,T) = \left(\frac{\tau_0^2}{\tau_0^2 - i\beta_2 Z} \right)^{1/2} \exp\left(\frac{T^2}{2\left(\tau_0^2 - i\beta_2 Z\right)} \right) \tag{2.26}$$

On propagation, Gaussian temporal profile is preserved but the peak intensity drops and the pulse becomes broader such that after some distance Z the pulse width τ_1 is

$$\tau_1 = \tau_0 \sqrt{1 + \left(\frac{Z}{L_D} \right)^2} \tag{2.27}$$

This can be seen in Figure 2.1(a), which shows the input pulse and profiles after propagation through the fibre. The diagram shows the intensity against time, in a frame moving with the pulsed at group velocity, with increasing distance.

Equation (2.27) shows the extent of the temporal broadening varies as β_2 and is inversely dependent on the input pulse width τ_0. This results in more quickly broadening of the shorter pulses as broader spectral range is required to support a shorter transform limited pulse.

As the pulse broadens a chirp is accumulated across it. This can be found mathematically by separating the pulse envelope into the amplitude and phase parts

$$U(Z,T) = |U(Z,T)| \exp(i\varphi(Z,T)) \tag{2.28}$$

Which gives the phase $\varphi(Z, T)$ as

$$\varphi(Z,T) = -\frac{\mathrm{sgn}(\beta_2)(Z/L_D)}{1 + (Z/L_D)^2} \frac{T^2}{\tau_0^2} + \tan^{-1}\left(\frac{Z}{L_D} \right) \tag{2.29}$$

With sgn (β_2) signifies the sign of β_2. The instantaneous frequency difference across the pulse $\delta\omega$ is then given by

$$\delta\omega = -\frac{\partial\phi}{\partial T} \tag{2.30}$$

$$= 2\frac{\mathrm{sgn}(\beta_2)(Z/L_D)}{1 + (Z/L_D)^2} \frac{T}{\tau_0^2} \tag{2.31}$$

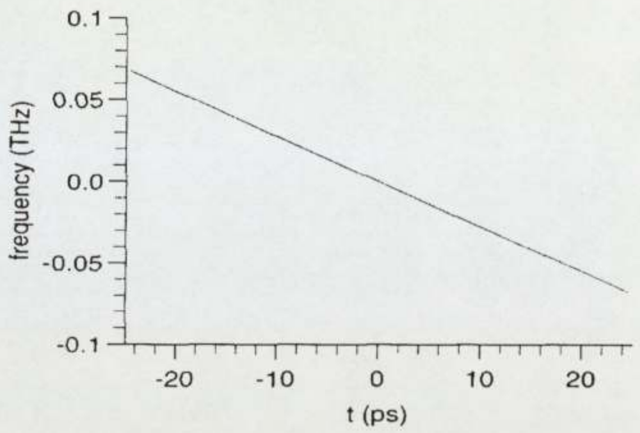

(a)

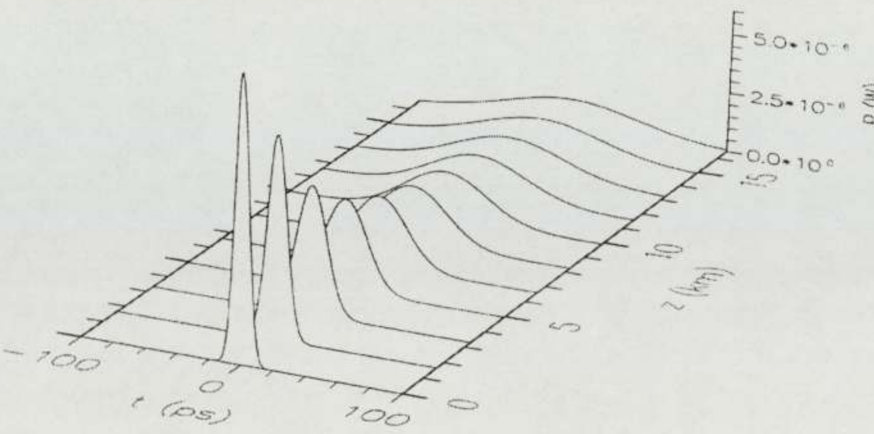

(b)

Figure 2.1: Dispersion induced broadening of a 10 ps Gaussian pulse (Z=0) with propagation over 10 L_D *in optical fibre with a GVD of* β_2*=21.8 ps²/km (or* D_2*=17 ps/nm/km), and loss* α*=0. (a) Temporal shape after each* L_D *=1.651 km. (b) chirp after 10* L_D*.*

This shows the linear frequency change across the pulse, a linear frequency chirp, as shown in figure 2.1(b). The sign of the GVD parameter β_2 through the definition of L_D determines the sign of chirp. This results in the blue components of the pulse faster than the red in the anomalous dispersion regime ($\beta_2<0$).

If the pulse has some initial chirp and is not transform limited the effect of GVD becomes more complex. While the dispersive effects remains the same, the temporal broadening experienced by the given pulse depends on its initial chirp as compared to the dispersive chirp accumulated on propagation.

For the case of linearly chirped Gaussian pulses, the incident field is given by

$$U(0,T) = \exp\left[-\frac{(1+iC)}{2}\frac{T^2}{\tau_0^2}\right] \tag{2.32}$$

Where C is the chirp parameter.

Using equation 2.32 in equation 2.23 and equation 2.24 we get the relationship of Gaussian field after z km propagation.

$$U(z,T) = \frac{\tau_0}{\left[\tau_0^2 - i\beta_2 z(1+iC)\right]^{1/2}}\exp\left[-\frac{(1+iC)T^2}{2\left[\tau_0^2 - i\beta_2 z(1+iC)\right]}\right] \tag{2.33}$$

Even though the pulse shape still remains Gaussian but it accumulates a chirp. Now the pulse width after propagation is given by

$$\frac{\tau_1}{\tau_0} = \left[\left(1+\frac{C\beta_2 z}{\tau_0^2}\right)^2 + \left(\frac{\beta_2 z}{\tau_0^2}\right)^2\right]^{1/2} \tag{2.34}$$

This equation shows that the pulse broadening depends on the related sign of the GVD parameter β_2 and the chirp parameter C.

The pulse whose frequency increases from leading to trailing edge i.e., the up-chirped pulse, in normal dispersion fibre broadens more quickly than an un-chirped pulse as the frequency continue to spread away in the same temporal direction as the initial chirp. Similar phenomenon occurs for down chirped pulses in the anomalous dispersion regime.

The reverse of these two cases is where initial chirp of the pulse effectively had to be "undone" before pulse broadening occurs, which leads to pulse compression. This important result could be exploited to in compressing down-chirped DFB [3] pulses through in normal dispersion fibre.

The dispersion characteristic of the pulse also depends on the pulse profile. Thus for pulses having smooth profile, such as Gaussian, tend to maintain a smooth shape under dispersive broadening. On the other hand pulses with sharp profiles such as super Gaussian can develop oscillations in the trailing edges of the pulse. This happens because more complex spectrum required to support such a pulse shape disperses [1], pp.67.

The higher order terms in the Taylor expansions of equation (2.10) were ignored during the derivation of NLSE, as they are insignificant compared with the second derivative, the group velocity term β_2. However the third order term β_3 becomes significant when second order term is small ($\beta_2 \cong 0$). The third order effects will be noticeable by defining another length scale $L'_D = \tau_0^3 / |\beta_3|$, when $L'_D \leq L_D$ or equivalently $\tau_0^3 |\beta_2 / \beta_3| \leq 1$ which requires a very low dispersion of $\beta_2 \leq 0.01 ps/nm/km$ [1], pp.65. Thus another term is introduced in the equation (2.18) due to the effect of β_3

$$i\frac{\partial U}{\partial Z} = \frac{1}{2}\beta_2 \frac{\partial^2 U}{\partial T^2} + \frac{1}{6}\beta_3 \frac{\partial^3 U}{\partial T^3} \qquad (2.35)$$

Which can be solved using Fourier technique. This extra term introduces asymmetric pulse shaping and an oscillatory temporal pulse structure [1], pp.66. This is however not generally a problem as GVD is so low. For two notations used in thesis for GVD are group velocity dispersion parameter (β_2) and group delay dispersion (D_2). The later tends to be more useful quantity from practical point of view; the difference being this is the second derivative of the refractive index with respect to the wavelength rather than frequency. The relationship between group delay and group velocity dispersion is

$$D_2 = \frac{-2\pi c}{\lambda^2}\beta_2 \qquad (2.36)$$

2.4 Self-phase modulation

Self-phase modulation (SPM) is the most relevant non-linear effect as far as soliton formation is concerned. When the length scales are $L_D \leq L_{NL}$ and $L << L_D$, non-linear effects are the most significant effects experienced by the pulse being transmitted along an optical fibre. In this section we consider GVD to be negligible and take β_2=0,in order to concentrate on the effect of SPM. Thus by applying the normalisation of amplitude (equation (2.18)) to the NLSE with loss (equation (2.15) we get the partial differential equation

$$\frac{\partial U}{\partial Z} = \frac{i}{L_{NL}}\exp(-\alpha Z)|U^2|U \qquad (2.37)$$

The point to be noted here is, the loss coefficient α is still contained in the equation despite the amplitude normalisation, as the nonlinearity is intensity dependent, loss reduces its effect. This can easily be solved to get

$$U(Z,T) = U(0,T)\exp(i\varphi_{NL}(Z,T)) \qquad (2.38)$$

Where U (0,T) is the input pulse amplitude and the non-linear phase term ϕ_{NL} given by

$$\varphi_{NL}(Z,T) = |U(Z,T)|^2\left(\frac{Z_{eff}}{L_{NL}}\right) \qquad (2.39)$$

And the effective length Z_{eff} is

$$Z_{eff} = \frac{1}{\alpha}(1-\exp(-\alpha Z)) \qquad (2.40)$$

This gives a reduced length that in turns re-scales the non-linearity for the presence of fibre loss.

The effect of SPM is to induce an intensity dependent non-linear phase shift across the pulse, through the dependence on $|U(Z,T)|^2$, increasing the propagation distance, as shown in equation (2.38). The frequency chirp this phase shift induces across the pulse is obtained from equation (2.29)

$$\delta\omega = -\frac{\partial \varphi_{NL}}{\partial T} = \frac{\partial |U(Z,T)|^2}{\partial} \frac{Z_{eff}}{L_{NL}} \tag{2.41}$$

This frequency chirp, through the $\frac{\partial |U(Z,T)|^2}{\partial T}$ differential is dependent on the shape of the input pulse and in particular the rate of change of the pulse shape.

This chirp generates new frequencies at the edges of the pulse spectrum, redistributing the pulse energies to these frequencies. As the propagation distance increases, the chirp increases in magnitude, exceeding the bandwidth of original pulse and hence self generate new frequencies by the pulse. The difference in this case as compared to the GVD is that it does not introduce additional frequencies but merely realigns their relationship to each other as they propagate at different velocities. Thus self-phase modulation causes spectral broadening of the pulse.

Now let us consider Gaussian input pulse of equation (2.25), propagating in the presence of non-linearity we get the spectral broadening shown in figure 2.2(a).

If the loss were to be ignored (α=0, Z_{eff}=Z), the peak non-linear phase shift experienced by the pulse centre is given by

$$\varphi_{\max}(Z,0) = \frac{Z}{L_{NL}} = \gamma P_0 Z \tag{2.42}$$

The non-linear phase shift increases linearly with distance and peak power P_0. The most important striking feature of the spectral changes induced by SPM is the oscillatory nature of the spectrum. This can be explained by the temporal variation of the frequency chirp across the pulse as shown in figure 2.2(b), which shows the chirp after a distance of 10 L_{NL} corresponding to the last trace in figure 2.2(a).

This shows the pulse has the same instantaneous frequencies occurring at two points in its temporal profile. This can be explained as two waves of equal frequency but having different phase, these waves can interact with each other, either constructively or destructively depending on the phase difference. It is this interference which results in multiple peaks in the spectrum. If however the pulse used is already chirped, the nature of the SPM induced changes. This change depends on the sign of the chirp, as an un-chirped pulse adds with the SPM induced chirp thus increasing the oscillatory nature of the spectrum, while the opposite is true for the down-chirped pulses [1], pp.84. Secondly the degree of self-phase modulation depends on the rate of change of the pulse intensity.

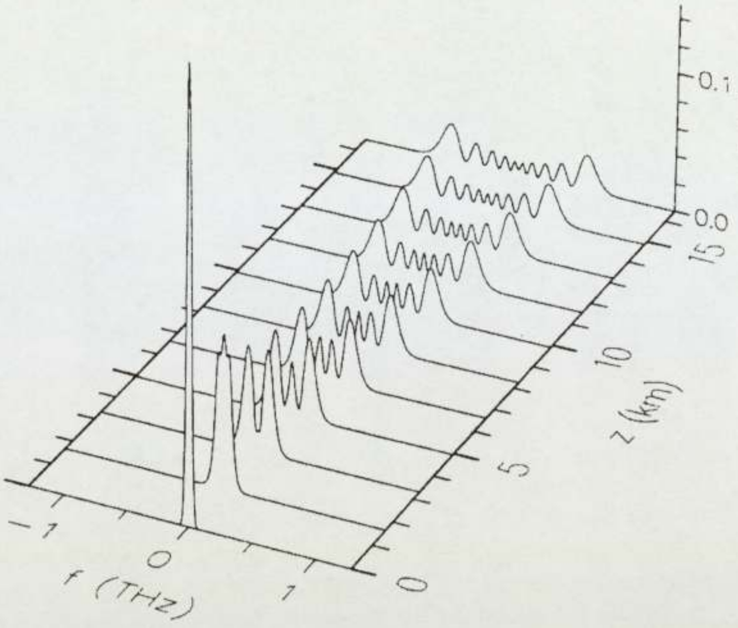

(a)

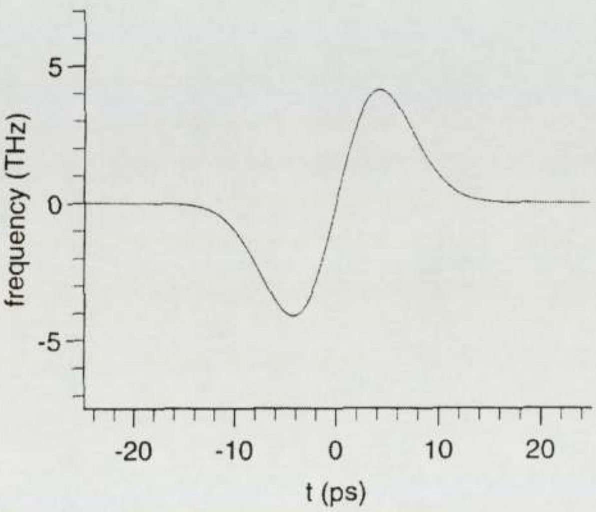

(b)

Figure 2.2: SPM spectrum broadening of a 10 ps Gaussian pulse in the presence of non-linearity but no dispersion or loss for 10 L_{NL}. *(a) Spectrum after each* L_{NL}=1.651 km. *(b) Chirp against time after 10* L_{NL}.

Thus squarer, super-Gaussian pulse will have less variation in the pulse shape over the central part of the pulse and very fast changes in the edges of the pulse. This results in pulse still developing the same number of peaks in its spectral structure where as the majority of the pulse energy experiences little SPM and this energy remains in the spectral peak of the spectrum [1], pp.83. Thus new frequencies are generated due to the wings of the pulse, leading to far lower peaks in the spectrum contrast to that of Gaussian, where outer spectral peak contains the most energy. This is dependence on the pulse shape that leads to the use of squarer pulse in the NRZ transmission systems, as most of the pulse energy remains within the input spectral width.

2.5 Cross-phase modulation and birefringence

Several effects such as polarisation mode dispersion, polarization dependent loss and gain and cross-phase modulation can be a problem given appropriate conditions. Thus again considering the linear effect and ignoring the nonlinearity, the birefringence of optical fibre can be a problem. Due to the imperfections in the manufacturing process, the random variation in the local birefringence breaks the degeneracy of the polarisation modes in nominally cylindrical fibres. Therefore any light launched into the fibre quickly reaches some arbitrary polarisation due to the mixing between the modes. Hence for a randomly oriented input polarisation pulse, the net difference in the group velocities of the slow and fast axes of the two orthogonal polarisation states, if large enough, can result in a pulse splitting. Where as for the spectral components with GVD, the different propagation rates lead to temporal dispersion of the polarisation components. This effect is known as polarisation mode dispersion (PMD). Due to the new improvements in the manufacturing processes, new fibres do not have this problem, but older fibres including a majority of installed fibre base can have very significant PMD and make upgrading to higher data rates with NRZ formats difficult [9]. Other devices used in optical communication, such as optical isolators used to restrict propagation to one direction and eliminate reverse travelling ASE noise from one amplifier interfering with a previous one, can also be affected by PMD significantly. The effect of PMD on solitons will be discussed once non-linear effects have been introduced.

Similarly polarisation dependent loss (PDL) and polarisation dependent gain (PDG), not a problem for fibres now, but when considering older fibres and devices, PDL and PDG do become important [10,11,12,13]. In particular, lithium-niobate modulators, used to impose data on a pulse stream, tend to be highly polarisation sensitive due to waveguiding used for these slab devices, with PDL values around 10 dB. Thus for a single polarisation signal, these high polarisation losses must be avoided, with polarisation controllers used to set the appropriate state for minimum loss. However for systems using polarisation mode multiplexing, more involved solutions are required. Similarly PDG, due to preferential alignment of the erbium ions to one polarisation state during manufacturing of erbium fibre, can become a serious problem. Again this problem have been resolved using improved manufacturing process for erbium fibre, however devices such as semiconductor laser amplifiers can have stronger PDG.

Another non-linear effect which describes the phase modulation of one pulse at frequency ω_1 on co-propagating with another at ω_2 is called cross-phase modulation (XPM). Thus NLSE with XPM can be obtained from wave equation (2.3) by replacing the slowly varying electric field by the following

$$E(r,t) = \frac{1}{2}\hat{x}\left[E_1 \exp(-i\omega_1 t) + E_2 \exp(-i\omega_2 t)\right] + c.c. \quad (2.43)$$

Now by solving for resultant change Δn in the refractive index $n(\omega) = \bar{n} + \Delta n$ which found as [1], pp.175

$$\Delta n_j = n_2\left(\left|E_j\right|^2 + 2\left|E_{3-j}\right|^2\right) \quad (2.44)$$

where j=1,2 for the two wavelengths. The first term E_j is the self-phase modulation term. The second term in E_{3-j} implies that when two waves are co-propagating, the non-linear refractive index change depends not only on their own intensity for SPM, but also on the intensity of other wave. This refractive index change results in phase modulation by one pulse on another, given by

$$\phi_j^{NL} = \frac{\omega_j z}{c}\Delta n_j = \frac{\omega_j z n_2}{c}\left(\left|E_j\right|^2 + 2\left|E_{3-j}\right|^2\right) \qquad (2.45)$$

This equation shows the phase modulation for XPM term to be twice that of the SPM term for the same intensity. This can be obtained by squaring the electric field equation (2.43) for the non-linear polarisation field, giving twice the number of terms for the different frequencies than for one.

When considering XPM, the difference between the group velocities v_{g1} and v_{g2} becomes important. The difference in the group velocity of the co-propagating pulses leads to a walk-off. Once the pulses no longer overlap there will be no cross-phase modulation. Thus the extent of XPM for a given two wavelengths in an optical fibre is limited by the time these pulses overlap. The non-linear effect of birefringence is also an XPM process between two waves of the same frequency but different polarisations.

For solitons, the dispersive and non-linear effects are considered simultaneously. While work continues to understand their effect in the random birefringence of ordinary fibres, consideration of more strongly birefringent fibres gives a qualitative indication of the effect [1], pp.190. If the birefringence is below ~$0.3D_2$ [14] the lower power polarisation component of an elliptically polarised pulse gets "trapped" by the higher power component, thus preventing the pulse from splitting as expected of linear pulse, even though it might lead to timing jitter [15]. If the level of birefringence is very high, the non-linear index change is sufficient enough to balance out the dispersive effect and hence the pulse splits as before. This resilience to PMD pulse splitting is currently creating further interest in solitons for upgrading older systems.

Chapter 3

Optical solitons

3.1 Introduction

The regime where both the linear and non-linear transmission effect are significant is where $L \geq L_D$ in this case the combined effect of GVD and SPM leads to a significantly different variation in the pulse dynamics from either case separately.

Dispersion leads to formation of chirp and temporal broadening of the pulse. SPM leads to Chirp formation and spectrum broadening these two simultaneously occurring, similar size effects will balance provided the chirps are of opposite sense.

3.2 The NLSE and the Soliton solution

The regime where both the linear and non-linear transmission effect are significant is where $L \geq L_D$ in this case the combined effect of GVD and SPM leads to a significantly different variation in the pulse dynamics from either case separately.

Dispersion leads to formation of chirp and temporal broadening of the pulse. SPM leads to Chirp formation and spectrum broadening these two simultaneously occurring, similar size effects will balance provided the chirps are of opposite sense.

First of all considering the lose less case for witch the governing equation is the NLSE of equation (2.15) with lose coefficient α=0 gives

$$i\frac{\partial A}{\partial Z}=\frac{1}{2}\beta_2\frac{\partial^2 A}{\partial t^2}-\gamma|A|^2 A \tag{3.1}$$

The sign of GVD parameter governs the dynamics of equation (3.1).

The continuous wave solution to this equation which is stable for the normal dispersion regime (β_2 >0) but in the anomalous dispersion regime (β_2 < 0) it leads to modulation instability, a modulation to the temporal profile which start simultaneously from noise [1], pp.105. Here we consider only the pulse solutions to the NLSE. In order to simplify the equation (3.1) we introduce

$$u=N\frac{A}{\sqrt{P_0}}, z=\frac{z}{L_D}, \tau=\frac{T}{\tau_0} \tag{3.2}$$

Where the parameter N is defined as

$$N^2=\frac{L_D}{L_{NL}}=\frac{\gamma P_0\tau_0^2}{|\beta_2|} \tag{3.3}$$

Thus we get the standard form of NLSE.

$$i\frac{\partial u}{\partial z}=\frac{1}{2}\frac{\partial^2 u}{\partial \tau^2}+|u|^2 u=0 \tag{3.4}$$

This equation applies in an optical fibre in the negative GVD regime, i.e., for wavelengths longer than the zero dispersion. A minus sign must be used before the second derivative with respect to time for the positive GVD regime. An exact solution to this equation can be found by using inverse scattering transform method in terms of eigenvalues. This method was first proposed by Gardner et al. [16] and was used by Sakharov and Shabat [17] to solve the NLSE in 1973. The method used by them was similar in style to Fourier transform method of solving linear partial differential equations. The higher order solutions exist (N>1), the most important, single eigenvalue solution to this equation which corresponds to N=1 [1],pp.114 has the form

$$u(z,\tau) = 2\xi \sec h(2\xi\tau)\exp(2i\xi^2 z) \tag{3.5}$$

Where ξ is the single eigenvalue. Using normalisation to set u (0,0)=1 by setting $2\xi=1$, a canonical form for the soliton can be found and is given as fundamental soliton solution

$$u(z,\tau) = \sec h(\tau)\exp\left(\frac{iz}{2}\right) \tag{3.6}$$

This pulse thus propagates without change of shape and only accumulates a uniform phase shift proportional to the distance. This non-dispersing pulse is the one sought for communications, as it is invariant in both temporal and spectral width. Equation (3.2) and (3.3) show that this relates in the case of optical fibres, to choosing the input peak power P_0 and pulse width τ_0 such that N=1, i.e., the peak power is set for a given pulse width and fibre parameters is given by

$$P_0 = \frac{|\beta_2|}{\gamma\tau_0^2} \tag{3.7}$$

This gives stable solution, the fundamental soliton, which is supported without change upon transmission. This becomes clear by studying the various dependencies of the soliton solution. Equation (3.5) shows that the eigenvalue ξ links the power, pulse width and phase relationship of the fundamental soliton. However, there is no dependence of this solution with the distance for the pulse width, only for the phase. The hyperbolic secant shape of the pulse remains unchanged with the propagation where as the phase is accumulated across the entire pulse linearly with distance. There is no chirp acquired by the pulse, as phase accumulation does not have a temporal dependence. This can be illustrated by figure (3.1), where temporal evolution of a fundamental soliton with distance and phase of the pulse is shown. This also describes the evolution of the soliton spectrum remaining as invariant due to the non-accumulation of chirp.

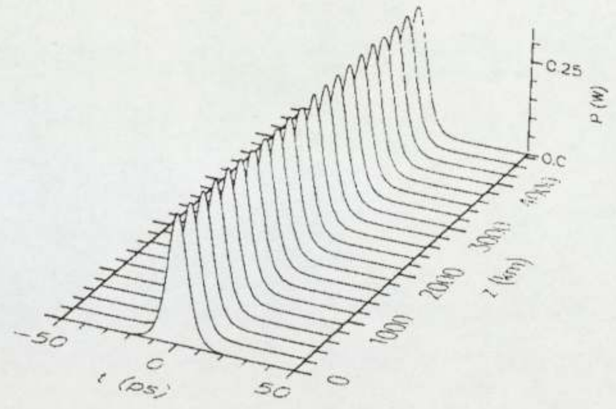

(a)

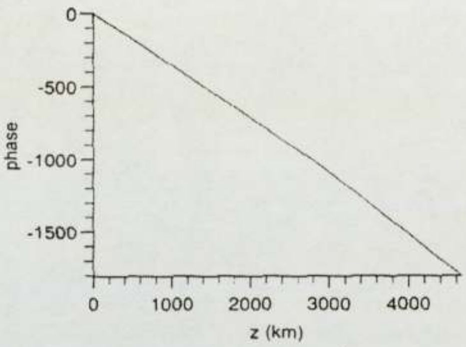

(b)

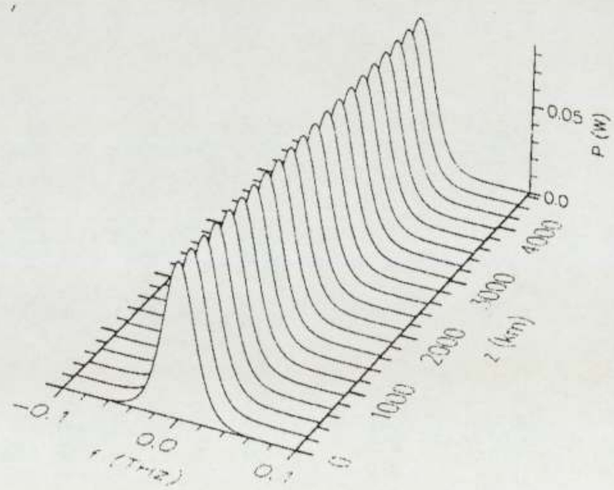

(c)

Figure 3.1: *Evolution of 10 ps fundamental solitons (a) Temporal shape (b) phase and (c) spectrum with distance, in fibre with loss α=0 and D_2=17 ps/nm/km.*

The formation of solitons can also be considered, as found from NLSE, by the chirps imposed on a pulse by GVD and SPM. As shown earlier, the sign of the chirp for GVD depends on the sign of the dispersion parameter β_2, where as the one due to SPM always has the same sign.

This leads the combined and detrimental effects in the normal dispersion regime, but in the anomalous dispersion regime the signs of these two chirps oppose each other.

Thus the formation of soliton can be considered as the pulse shape giving correct frequency chirp balance between GVD and SPM, with pulse width and power chosen such that GVD chirp contribution exactly balances the SPM chirp. As such no temporal chirp gets built up, hence no temporal or spectral broadening occurs.

The soliton period Z_0 could be defined as the distance required for a $\pi/2$ phase rotation, due to the linear increase in phase of a soliton. And is given in normalised units as $z_0 = \pi/2$ or in physical units as

$$Z_0 = \frac{\pi}{2} L_D = \frac{\pi}{2} \frac{\tau_0^2}{|\beta_2|} \tag{3.8}$$

The evolution of soliton under the influence of various effects and perturbations can be described by using the soliton period as length scale. The choice of $z_0 = \pi/2$ is made as this is the period of the shape evolution of higher order solitons [1], pp.115.

Solitons are resilience to perturbations. The NLSE gives a stable solution for the soliton thus if perturbations such as small change in the pulse's temporal or spectral profile is applied to the soliton, it tries to regain the soliton solution. This can be shown mathematically using linear stability analysis and other similar techniques. However there are some unusual and undesirable effects such as Gordon-Haus timing jitter, resulting due to the resilience of solitons, it provides us with an additional advantage in general over other transmission formats. If the input chirps and shapes are in reasonably close to the stable solution, the non-soliton pulses evolve towards the soliton solution due to the stable solution of the NLSE [18,19,20,21].

This is the temporal and spectral invariance that makes solitons an attractive candidate for optical communication systems. The fundamental solitons remain stable for the length of the system, unlike the NRZ transmission systems where GVD and SPM work towards destroying the pulse. So far we have not considered the effect of fibre attenuation, which is discussed in the following section.

3.3 The NLSE with loss

We have already seen the effect of loss for GVD and SPM individually, however their combined effect has different dependence on loss as compared to the individual cases. One of the major problems for soliton in an optical fibre is the decay in non-linear effects due to the decrease in power of the pulse, which in turns removes the balance between the dispersive and non-linear chirps. Thus for a N=1 soliton launched into an optical fibre, this decay in non-linear effect results in pulse broadening as GVD chirp gradually becomes dominant over that for SPM. The must be re-amplified periodically in order to balance out the effect of loss, before the signal is lost to the noise propagating with it [22]. If the dispersion does not destroy the pulse, this can be done all optically in the case of soliton systems using EDFA's [23, 24, 25]. This leads to the effect of average soliton [25], which has major impact on the propagation of solitons in real optical fibres. The EDFA's have been instrumental in the elevation of soliton to a practical transmission format for optical communications. The EDFA's however have their own drawbacks, mainly due to the noise introduced to the optical signal. Here we consider the effect of distributed loss and periodic discrete gain on propagation of solitons. Due to the short length of (a few meters) EDFA's as compared to fibre transmission length between amplifiers (a few 10's of kilometres), they can be considered as discrete amplifiers. Thus considering NLSE with loss and normalising (equation (3.2)) we get

$$i\frac{\partial u}{\partial z}+\frac{1}{2}\frac{\partial^2 u}{\partial \tau^2}+|u|^2 u=-i\Gamma u \tag{3.9}$$

Where normalised loss Γ is given by

$$\Gamma=\frac{\alpha}{2}L_D \tag{3.10}$$

The distributed loss at each fibre section can be exactly compensated for by the discrete gain from the amplifier provided the fields, u_1 and u_2 , before and after each (j^{th}) amplifier respectively, are related by

$$u_2(jz_a)=G^{1/2}u_1(jz_a) \tag{3.11}$$

Where $G=e^{2\Gamma z_a}$ is the power amplification factor required to restore the signal after the exponential loss and $z_a = L_a / L_D$ is the amplifier spacing L_a normalised to the dispersion length. The Equation (3.9) after transformation $u(z,t)=\Lambda(z)R(z,t)$ becomes

$$i\frac{\partial R}{\partial z}+\frac{1}{2}\frac{\partial^2 R}{\partial \tau^2}+\Lambda^2(z)|R|^2 R=0 \tag{3.12}$$

Where

$$\Lambda(z)=\Lambda(0)e^{-\Gamma(z-jz_a)} \tag{3.13}$$

Thus for the periodically forced NLSE, the exponential energy variation is equivalent to an exponential variation $\Lambda^2(z)$, in the non-linear coefficient of the lossless NLSE (equation (3.4) with $\gamma=\Lambda^2(z)$ and $u=R$). Thus average soliton model is obtained provided period of $\Lambda^2(z)$ is short on the characteristic length scale of the soliton evolution ($L_a << Z_0$ or $z_a << \pi/2$) and its average is a good approximation in equation (3.12) [9,10,26]. By equating average variation of $\Lambda^2(z)$ over the first amplifier span (j=0) to the desired normalised average value of 1, we get

$$\langle\Lambda^2(z)\rangle=\frac{1}{z_a}\int_0^{z_a}\Lambda^2(z)dz=1 \tag{3.14}$$

Which gives

$$\Lambda^2(z) = \Lambda_0^2 = \frac{1-e^{-2\Gamma z_a}}{2\Gamma z_a} \tag{3.15}$$

Where Λ_0^2 is the peak amplitude of input average soliton.

For such a system the variation in the soliton energy on propagation along a few amplification periods is shown in figure (3.2). The average soliton model balances the excess non-linear chirp of the initial section of the propagation between amplifiers with the excess dispersive chirp of the second part, so that on average dispersion and non-linearity balances. This is equivalent to the areas above and below the $\Lambda^2(z)=1$ being equal as shown in figure (3.2).

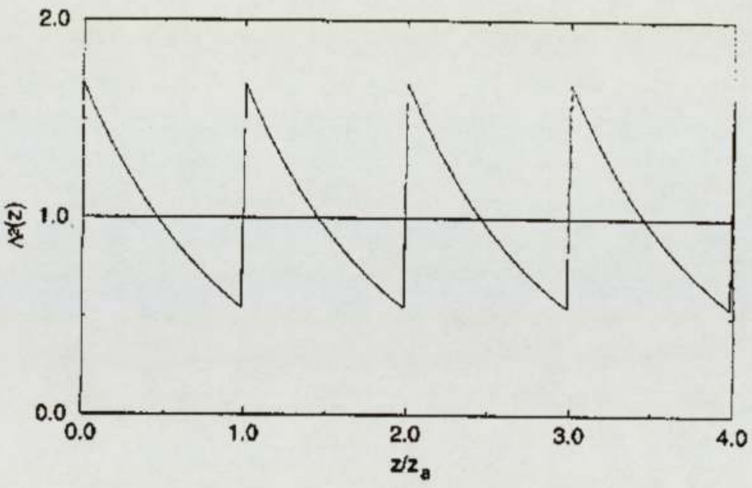

Figure 3.2: Soliton energy variation with propagation distance over 4 amplifier spans each with a net loss of 5 dB. $\Lambda^2(z)=1$ is the energy of an N=1 soliton in a lossless fibre to which the soliton is averaging.

This discussion about loss can be generalised for other perturbation to the soliton transmission system. Thus other periodic variations should have period short compared to the soliton period. Even though the defects from manufacturing process should meet this criteria, however as these defects are generally short compared with any realistic amplification period, designing the system for average soliton also removes their effects.

3.4 Soliton System Design Features

Apart from average soliton considerations, there are other important requirements, specific to solitons, which must be considered in the design of optical soliton transmission system. Any design requires some trade-offs for its competing requirements. Generally, soliton system design can be divided in to two main categories, namely short and long haul systems. Systems with lengths of hundreds of kilometres are here referred to as short haul and with transoceanic lengths (thousands of kilometres) are the long haul systems. As mentioned earlier one very important consideration is that average soliton to amplifier spacing, $L_a << Z_0$, which should be met for any length of soliton system. Typically a factor of 10 is taken to be acceptable, but we consider the full soliton period ($8z_0 = 2\pi$), giving this limit as $L_a < 8/10Z_0$ [27]. Soliton interactions, random timing jitter, the signal to noise ratio (SNR) requirements, acoustic interactions and the average power requirements are also discussed in the following sections.

3.4.1 Soliton-soliton interaction

The solitons have to be placed as close as possible in order to maximise the possible data rate (R) when considering high-speed transmission systems. Thus minimum separation between solitons need to be assessed, without detrimental effects. The nonlinearity, which leads to the existence of solitons also, provides mechanism for interaction between them. A great deal of interest has been shown in this effect and methods of dealing with it [28, 29, 30, 31, 32, 33, 34, 35, 36, 37, 38].

The two main cases to be considered are the ones where solitons have equal frequency or the one where solitons have unequal frequency. The earlier case applies to optical time division multiplexing (OTDM), and the later is used in wavelength division multiplexed (WDM) systems [39, 40, 41].

The equation describing two solitons at the input of a transmission system can be described as

$$u(0,\tau) = \sec h\left(\tau - \frac{T_R/2}{\tau_0}\right) + r \sec h\left(r\left(\tau \frac{T_R/2}{\tau_0}\right)\right)e^{j\theta} \quad (3.16)$$

Where $T_R = 1/R$ is the initial separation, r is the relative amplitude and θ is the relative phase of the two input pulses. The inverse scattering method, perturbation theory as well as numerical simulation [39], can be used to solve NLSE for this input. Solitons with equal amplitude and phase have been shown to attract periodically and collapse upon propagation as shown in figure (3.3).

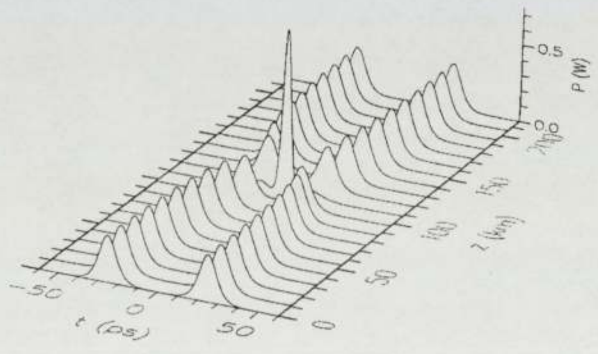

Figure 3.3: Evolution of two in-phase, equal amplitude solitons along a transmission line. The fibre dispersion of 17 ps/nm/km and pulse width of 10 ps gives a collapse distance of 108 km (Z_P =216.7km) at the data rate of 20 Gbit/sec.

For solitons with large separation compared with the pulse width, the pulses collapse and separate with a period [1], pp.132

$$Z_p = Z_0 \exp\left(\frac{1}{2R\tau_0}\right) \tag{3.17}$$

The collapse occurs at $Z_p/2$, in a perfect lossless system. For a perfect pair of soliton in a lossless system, this distance is related to the soliton period Z_0, even though predictable, this behaviour has implications for a soliton system. In order to avoid potential failure mechanism, systems are designed to ensure that this length is shorter than the collapse length. For solitons separated by a sufficient mark to space ratio the exponential of equation (3.16) is large enough to avoid interactions over global distances. Generally mark-to-space ratio is taken to be between 1:6 to 1:10.

For out of phase pulses ($\theta = \pi$) different evolutions occurs in that the pulses don't attract but instead repel, as shown in figure (3.4).

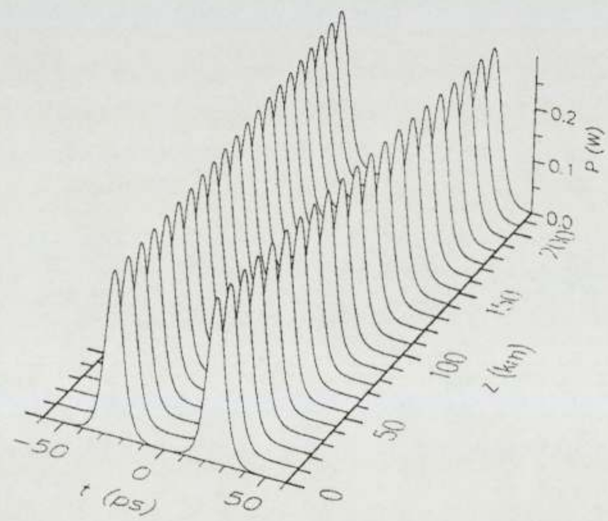

Figure 3.4: Two 10 ps pulses at 20 Gbit/sec in standard fibre, as in figure (3.3), but with a phase difference of π between them.

The repulsion in first glance may seem to be desirable for soliton systems design, as it avoids the pulse collapse of in phase solitons. Due to the fact that pulses continue to separate for the entire system length at the same rate, regardless of how far apart they become, make it a non-desirable effect. This could result in out of phase pulses walking into adjacent bit slots producing errors. It has been suggested that in the context of a pulse stream the mutual repulsion from out of phase pulses on either side will give a stable operating point with no pulse movement [42]. However in the usual amplitude modulation format of a soliton data stream we cannot have pulses either side of every pulse, and hence this method fails.

Recently some interest has been shown in pulses having unequal amplitude [43]-[44]. Unequal pulses introduce an interesting behaviour to a transmission line, in that they essentially eliminate the problem of soliton interaction. The evolution of two such solitons, with an amplitude difference of 10 % is shown in figure (3.5).

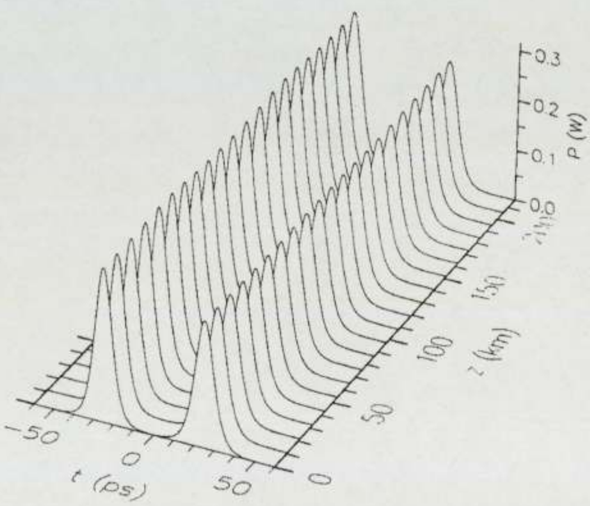

Figure 3.5: Two in-phase, 10 ps pulses at 20 Gbit/Sec in standard fibre, with an amplitude difference of 10%.

The pulses remain in their given time slots, regardless of the interplay between them which is not noticeable of this figure. This behaviour is result of the difference in the evolution rate of the phase of two pulses. The rate of evolution of phase, as given in equation (3.6), is related to the phase amplitude. Thus the phases of pulses with unequal amplitude vary at different rates, constantly going in and out of phase, causing the pulse to attract and repel periodically, hence cancelling out the effect of each other. This effect have been used successfully to propagate solitons over 11500 km at 20 Gbit/sec [45] and 500 km at 80 Gbit/sec [44].

Another distinct soliton interaction case is that of solitons with different frequencies, as used in wavelength division multiplexed systems [39,40]-[43]. Trains of pulses with different frequency travel at different rates due to the difference in the group velocity and hence collide and interfere periodically when in conjunction. After the interaction the pulse emerge unperturbed from the encounter, as illustrated in figure (3.6).

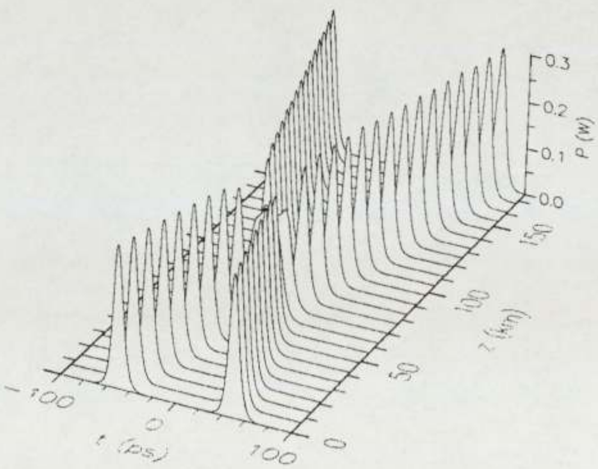

Figure 3.6: Interaction of two 10 ps pulses having different frequency (40 GHz frequency separation) on propagation along an optical fibre.

Even though the pulses do emerge unscathed by their encounter, there is a small modification to the pulse position, resulting from the modification to the refractive index. The manifestation of the refractive index change is that while pulses interfere, the slower pulse gets retarded and the faster pulses advances, by a time proportional to frequency difference [13,26]. Even though both pulses return to their original velocity at the end of interaction, there is implication for data in a WDM transmission system. Due to the random data imposed on the communication data stream, the pulse of one stream may not always encounter a pulse from the other, resulting in random number of temporal shifts any pulse encounters. These temporal shifts can become significant for long haul communication systems, thus limiting separation between the WDM channels. This effect shall be left out of the system design considerations as this thesis considers only single wavelength channel propagation.

3.4.2 Gordon Haus effect

When perturbed, solitons try to retain the stable soliton solution due to their resilience to perturbations. However over long transmission distances this leads to some unusual consequences such as random timing jitter, known as Gordon-Haus effect [46,47]. The resilience mentioned above also leads directly to method for dealing with this timing jitter problem.

The EDFA's introduce ASE noise to the propagating signal resulting in Gordon-Haus effect. This noise effects various parameters defining a soliton such as temporal position, the spectrum, the pulse width and phase. The most important perturbation is found to be experienced by the soliton spectrum [48], pp.130. The pulse tries to absorb this noise component due to the resilience of soliton to perturbations. This absorption results in small change in the soliton spectrum due to the shift in average central frequency by the new induced component of the spectrum, towards or away from the new noise component frequency depending upon the relative phases. Even though this frequency shift could have a profound effect, the problem encountered is however in the temporal domain. The slight change in frequency gives a small change in the group velocity of the pulse. This result in difference in the arrival time of the pulse from centre of its nominal bit slot over a long propagation distance called random timing jitter.

The Gordon-Haus effect results from the change in the group delay of a pulse over one amplifier span L_a of $\Delta t_g = \beta_2 L_a \Delta\omega$ for a frequency change $\Delta\omega$. An estimate of the standard deviation of the pulse arrival time can be derived by considering an ensemble of pulses and summing their variation over the full system length [47] as follows

$$\left\langle t_N^2 \right\rangle = \frac{2\pi n_2 N_{SP} |\beta_2| hc\{G-1\} L^3}{9\tau_0 \lambda^2 A_{eff} \Lambda_o^2} \tag{3.18}$$

Where N_{SP} is the spontaneous emission factor of the amplifiers, G is the amplifier gain, h is the Plank's constant and τ_0 is the pulse width. The deviation of the pulse position and hence jitter experienced is dependent on the system length by $L^{3/2}$. Thus the jitter is low for short systems and does not present a significant problem, but for system with long length the jitter may become significant and can be the limiting factor in long distance system design.

Thus the pulse must arrive with in a time window $\pm t_w$ around its input position, in order for the detector not to receive an error. For Gaussian statistics, a typical acceptable bit-error ratio {BER} of less than 10^{-9} can be obtained by applying the variance to be [13,33]

$$\left\langle t_N^2 \right\rangle = \left(\frac{t_\omega}{6.1} \right)^2 \tag{3.19}$$

The maximum transmission distance allowed for a given set of parameters can be found using equation (3.18) and (3.19) as

$$L_{\max}^3 \leq 0.1372 \frac{\tau_f t_\omega^2 A_{eff} L_a \Lambda_0^2}{N_{SP} n_2 D_2 h(G-1)} \tag{3.20}$$

Where D_2 is the dispersion and $\tau_f = 2\ln(1+\sqrt{2})\tau_0 = 1.763\tau_0$ is the full-width at half maximum for a soliton. Thus shift in the frequency of a signal due to ASE noise and hence the arrival time of the pulse, through the interaction of the pulse with dispersion, limits the maximum allowable length a soliton transmission system.

As this timing jitter appears to limit the possibility of long distance soliton transmission and the data rates of such systems, a great deal of work has been directed to reducing or eliminating its effect. There is an overlap here to other soliton work toward an optical fibre "soliton storage ring" where pulses can be maintained for long times (and hence long distances) in order to provide an optical buffer or memory which obviously suffers similar problems to soliton transmission. One novel result has returned soliton to the fore again. It has been shown that this resilience could lead to a substantial reduction in the ASE noise build-up and the accumulation of timing jitter [55] , by forcing the soliton to follow a change in their central wavelength. By gradually changing the central wavelength of the filters in a transmission line away from the input wavelength. However as the noise is linear it cannot follow the shifting wavelength and will eventually be attenuated by the fibres. This "sliding guiding" filter technique has been used to great effect to propagate soliton of 20 Gbit/s over 14,000 km error free. The advantages found from this form of filtering by far outweigh the disadvantages of the extra gain requirement.

Chapter 4

Dispersion Management

4.1 Introduction

Recent years have seen the potential of constructing a transmission line using section of fibre with different dispersions [49]. This technique is usually referred to as dispersion management. Alternating lengths of normal and anomalous dispersion fibre are used to form the simplest and most successful dispersion map. This results in high local dispersion but low average dispersion. Maps of this sort have been found to support stable non-linear pulses, known as dispersion managed solution [50].

The high local dispersion and low average dispersion of the dispersion-managed system have many advantages. One of the expected advantages of low dispersion is the reduction in Gordon-Haus timing jitter. Equation 3.18 shows how the timing jitter depends on the size of dispersion. The low average dispersion results in the increase in soliton period, which means that the amplifier span length can be increased as a result of the constraints set by the average soliton model (see section 3.2). The high local dispersion means that the four wave mixing is insufficient, as it is phase matched at zero dispersion. There are also less expected advantages that result from using dispersion management, for example dispersion managed solitons demonstrate enhanced pulse energies when compared to average solitons is optical fibre with constant dispersion [50, 51, 52, 53, 54]. This implies that it is possible to use lower average dispersion and so gain further advantage from the reduced Gordon-Haus jitter [55][56][57][58][59] without degrading the signal-to-noise ratio. A further advantage of using dispersion-managed solitons is the possibility to operate at the zero dispersion and even to operate with a normal average dispersion [54][60][61][62][63].

This chapter will give a review of the work that has been done previously on dispersion managed solitons. This will include an examination of the effect of the dispersion map on the properties of solitons such as pulse shape as well as the effect of dispersion management on such things as Gordon-Haus jitter and soliton interactions. There will also be a review of some of experimental and numerical results, published for high bit rate transmission systems, which use dispersion management.

4.2 Background

In the context of this chapter, dispersion management will be taken to mean a transmission line made up of alternating steps of normal and anomalous dispersion fibre. The average dispersion of transmission line is set to be significantly less, in magnitude, than the dispersion of constituent fibres.

An example of the dispersion map is given in figure 4.1. This dispersion map consists on mainly normal dispersion fibre with fibre grating having normal The fibre grating was simulated by a small piece (10 cm) of high normal dispersion fibre. Transmission lines made up of different dispersion fibre have been used for some time. The first dispersion maps were used in an attempt to have a dispersion profile that followed the exponential loss of the fibre. This technique involves minimising the difference between a true exponential dispersion decreasing fibre [64] (which have also been used [65, 66]) and a dispersion profile that decrease in steps and so can be more easily constructed.

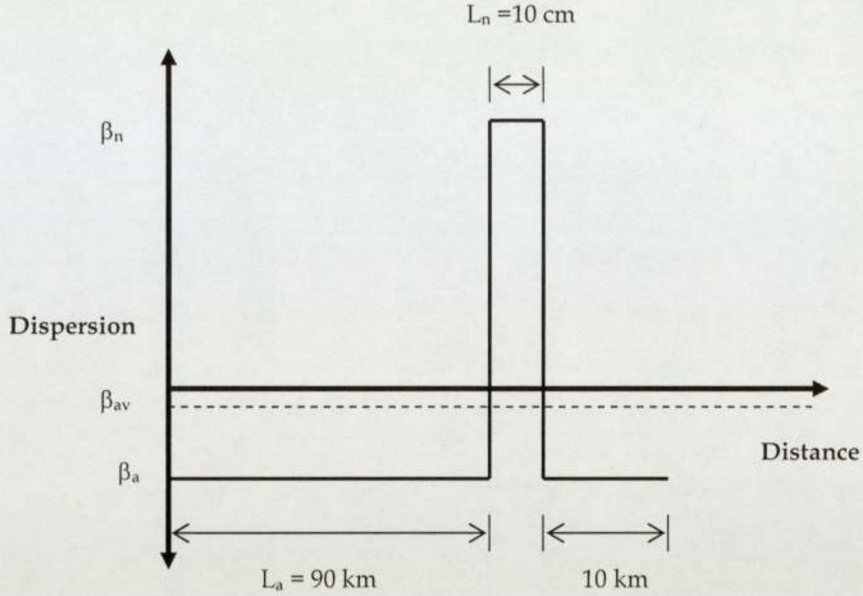

Figure 4.1: *A dispersion map withl lengths of anomalous dispersion fibres followed by fibre grating having normal dispersion.. L_n and β_n are the length and dispersion of fibre grating respectively, and L_a and β_a are the length and dispersion of the anomalous dispersion fibre.*

A second precursor to dispersion management is using dispersion compensating element at the end of the transmission line to remove some of the accumulated timing jitter from the pulses [67]. The idea is that the dispersion of the line is unaffected thus a lower average dispersion could be used without having an effect on the signal-to-noise ratio [67]. In this case the decrease in dispersion at the end of the transmission line is gained at the expense of an increased pulse width, which limit the amount of compensating fibre that can be used.

Dispersion managed solitons were discovered when a transmission line made up of alternating lengths of anomalous and normal dispersion was used. The length of each section of fibre are generally 100km or less so the length of dispersion map in total is of the same order as an amplifier span. One of the major areas where dispersion management is found to be useful is for the upgrade of the standard fibre network. Standard fibre was originally intended for use at a wavelength of 1.3μm and has low dispersion at this wavelength. The invention of Erbium doped fibre amplifiers (EDFA)has made it more attractive to work around 1.55 μm wavelength. It is thus necessary to operate standard fibre at this wavelength, which results in the dispersion of the fibre being between 16 and 20 ps/nm km. Dispersion management could be used for these fibres to reduce the average dispersion, which makes it possible to work at higher data rates, without the use of regenerators. Propagation in standard fibre will be discussed in more detail in chapter 5 and 6.

4.3 Dispersion Managed Solitons

In this section the formation of solitons in a transmission line with dispersion management will be discussed. Prior to examining the pulse shapes and energies found for dispersion managed soliton, it is interesting to see what happens to the pulse width and bandwidth through one dispersion map in order to see how the balance between dispersion and nonlinearity is attained in the case of dispersion managed solitons. Since the average dispersion of the transmission line is much smaller than the local dispersion at any point in the map, thus the powers being used are low relative to the local dispersion, hence the dispersion dominates, however the nonlinearity of the self-phase modulation still has an important role to play in the formation of dispersion managed soliton The traditional soliton transmission lines have constraints such as timing jitter, interaction [*68*].

Let us consider an un-chirped pulse launched into a length of anomalous dispersion fibre with a power less than that required for formation of a soliton. The higher dispersion causes the pulse width to increase as the pulse becomes chirped. Fig 4.2 , 4.3 and 4.4 show the pulse shape, FWHM and chirp of a pulse in a length of anomalous dispersion fibre. The fibre was taken to have no loss and no higher order dispersion.

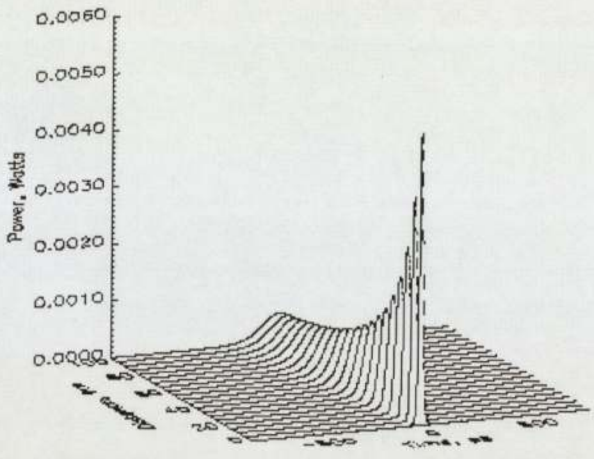

Fig 4.2: The pulse shape evolution of a Gaussian pulse in 100km of anomalous dispersion fibre

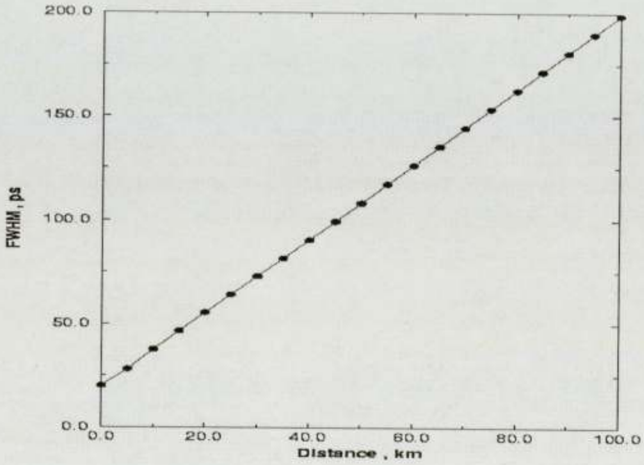

Fig 4.3 The increase in pulse width as the soliton propagate through in 100km of anomalous dispersion fibre

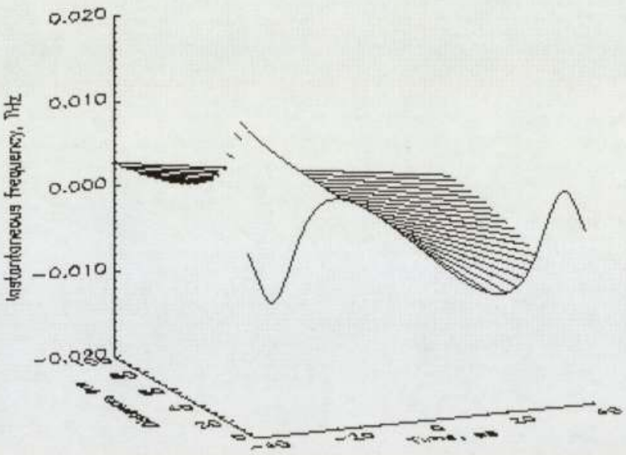

Fig 4.4: The instantaneous frequency across the soliton as it propagates through in 100Km of anomalous dispersion fibre. The accumulation of chirp can be clearly seen as the pulse propagates.

The pulses used are 20 ps Gaussian pulse with a pulse energy of 0.116 pJ in 100 Km of anomalous dispersion fibre with dispersion of 17 ps/nm /km, which is well below the pulse energy for a first order soliton which would be 1.485 pJ. The bandwidth of the same pulse as it propagates over the length of fibre is shown in Fig 4.5. The non-linearity causes the bandwidth of the pulse to decrease as it propagates through the fibre. This decrease in bandwidth of pulses is due to the effect of nonlinearity acting on a chirped pulse.

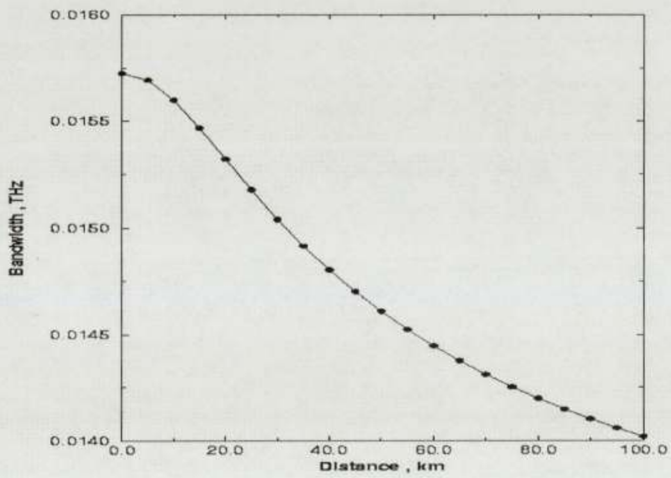

Fig 4.5: The bandwidth of the Gaussian pulse decreasing as it propagates through in 100Km of anomalous dispersion fibre

Due to the domination of dispersion the pulse quickly become chirped in such a way that the leading edge is up shifted in frequency and the trailing edge is down shifted the nonlinearity reduces the frequency of the front of the pulse and increase the frequency of the trailing edge of the pulse. This destroys the extremes of the spectrum, creating frequencies closer to the centre of the pulse bandwidth, thus resulting in a decrease in a bandwidth. The propagation of the same un-chirped Gaussian pulse into a length of normal dispersion fibre is shown in Fig 4.6.

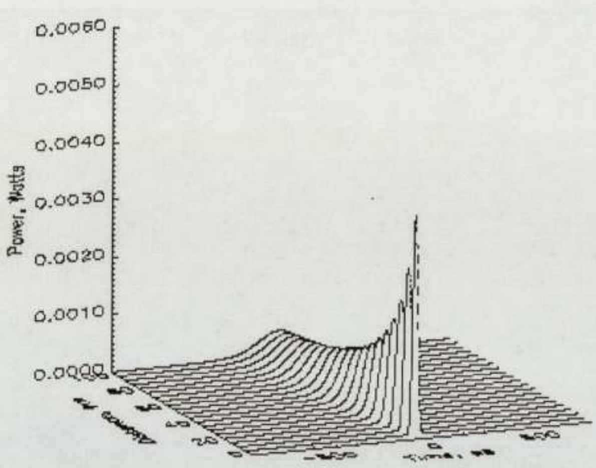

Fig 4.6: The pulse shape evolution of a soliton in 100Km of normal dispersion fibre.

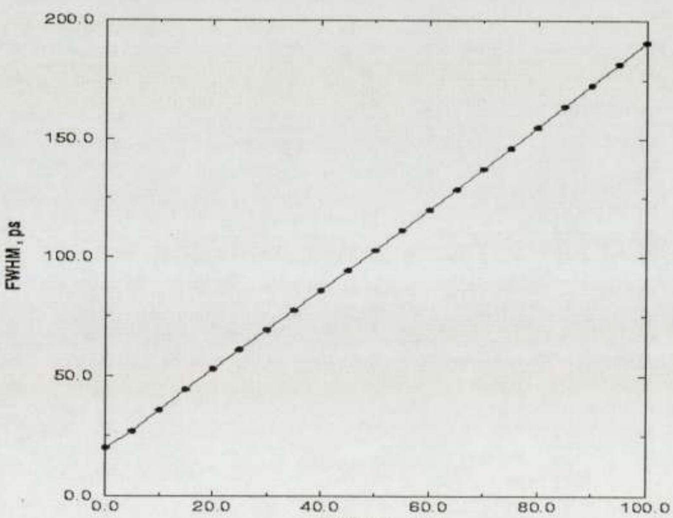

Fig 4.7: The pulse width increases as the soliton propagates through 100 Km of normal dispersion fibre.

The simulation in this case uses the same parameters as those for the anomalous dispersion simulation, however the dispersion of the fibre is -17 ps/nm/*km* . Once again the effect of dispersion on this pulse increases the pulse width, as seen in Fig 4.7. The bandwidth of the pulse in normal dispersion fibre increases due to the fact that the chirp induced on a transformed limited input pulse is of the opposite sense to that found in the anomalous dispersion fibre. This can be seen in the plot of instantaneous frequency given in Fig 4.8.

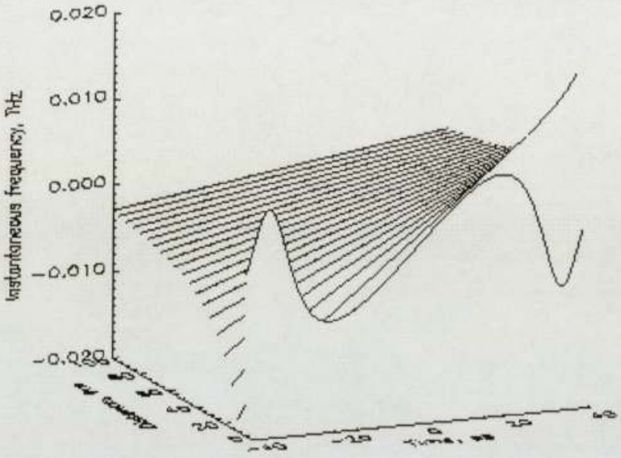

Fig 4.8: The instantaneous frequency across the soliton as it propagates through a 100 Km of normal dispersion fibre. The chirp is of opposite direction to that seen for the pulse in anomalous dispersion

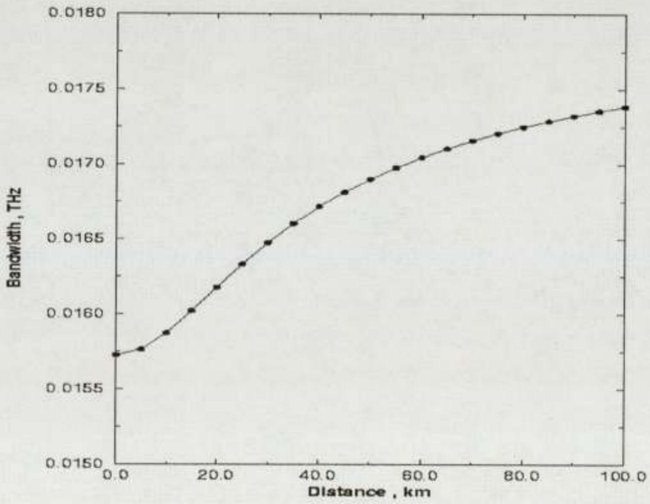

fibre.

Fig 4.9: The bandwidth of the soliton increases as it propagates through a 100 Km of normal dispersion fibre.

This shows that the pulse has lower frequencies in its leading edge and higher frequencies on its trailing edge. As the nonlinearity reduces the frequencies on the leading edge and increases the frequencies at the trailing edge, the overall effect of the normal dispersion fibre is to increase the bandwidth of the chirp free input pulse.

It is also interesting to look at the evolution of the pulse parameters as they vary through out one section of the dispersion map. *[69][70]*. In this simulation, the dispersion map consists of 100 Km of anomalous dispersion fibre with a dispersion of -17 ps/nm/km followed by a 10 cm grating having dispersion of 2.142 x 10^7 ps^2/Km which gives a average dispersion of 0.2 ps^2/km. The input pulse is taken to be 20 ps sech pulse having peak power of 0.6 mw. In this case when the pulse enters the first dispersion segment it is unchirped, and accumulates dispersion induced linear chirp (negative chirp). In the grating this negative chirp is counter balanced by the positive chirp induced by the normal dispersion of the grating and some residual chirp is induced in the opposite direction. When the pulse enters the second segment of the standard fibre, the extra chirped gets compensated. Fig 4.10 shows the pulse as it propagates through this dispersion map.

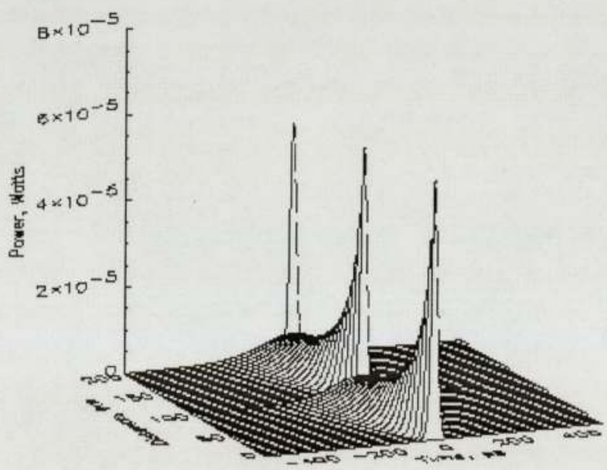

Fig 4.10 Propagation of dispersion managed soliton through one unit cell of the dispersion map this pulse is 20 ps Gaussian with a peak power of a 0.6 mW.

The bandwidth, pulse width and instantaneous frequency for this pulse are shown in Fig 4.11 4.12 and 4.13 respectively.

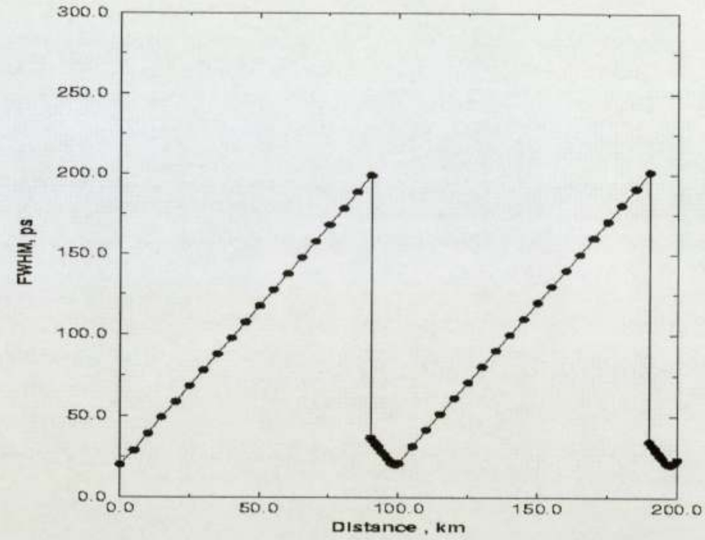

Fig 4.11 The evolution of pulse width for a dispersion managed soliton through one unit cell.

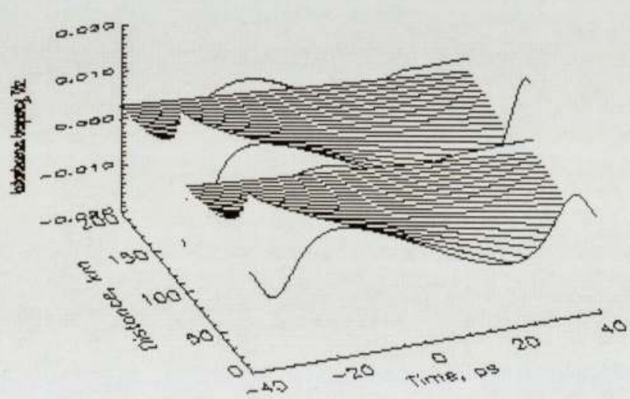

Fig 4.12 The instantaneous frequency through one unit cell for a dispersion managed soliton.

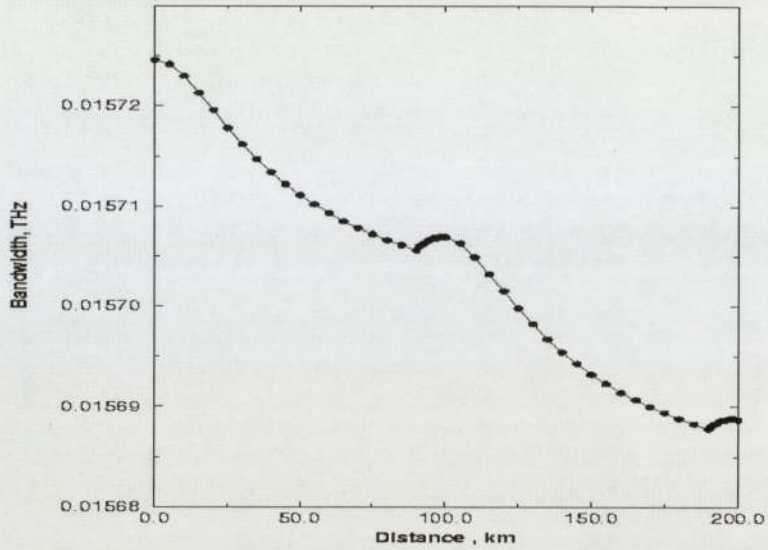

Fig 4.13 The change in bandwidth of a dispersion managed soliton during propagation through one unit cell.

As the pulse propagates through the first section of anomalous dispersion fibre the, pulse width increases because the pulse become chirped. During the same section of the fibre the bandwidth decreases afterwards when the pulse entered the grating having normal dispersion, the pulse width decreases as it become less chirped. Since the sign of the chirped determines whether the bandwidth increases or decreases, the bandwidth continuous to decrease during propagation through grating. At the end of the second section of fibre the pulse width reaches a minimum, as it is un-chirped at this point after the end of the second section of fibre the pulse once again becomes chirped and hence the pulse width increases. Since the chirp is now in the opposite sense the bandwidth also increases during this section of the normal dispersion fibre.

In order to have correct balance between the nonlinearity and the dispersion, it is necessary to have the right pulse shape and energy, as is the case with traditional solitons. *[71]*.

When dispersion management is used, the required pulse shape and energy depends on the dispersion map as well as the pulse width an average dispersion *[12, 25, 52, 72]*.

The dispersion map can be described using average dispersion β_{ave}, the dispersion difference $\Delta\beta$ and the normalised average dispersion given by $D=-\beta_{ave}/\Delta\beta(=D_{ave}/\Delta D)$. Finally the parameter used to describe the dispersion map's strength S, given by [54]

$$S = \frac{|l_n \beta_n - l_g \beta_g|}{T^2} \tag{4.1}$$

Where l_n and β_n are the length and dispersion of normal fibre, l_g and β_g are the length and dispersion of grating and T is the FWHM pulse width. The map strength gives an indication of the amount of pulse spreading the pulse is under go, in the dispersion map. The high dispersion of the fibre or short pulses cause the maps strength to be high, which means that the dispersion length of the pulse is short compare to the length of fibre map's strength up to 12 have been used to give stable propagation *[4, 73]*.

In dispersion managed systems the stable pulses have different pulse shapes from those in constant dispersion systems. The pulse shapes vary from being very close to Sech shaped for

Weak dispersion map to Gaussian pulse and on to pulses with shapes closer to Sinc functions [3,27]. For dispersion managed soliton there is no one set shape, the correct shape of the pulse can be found numerically using an averaging technique first used in reference [4]. If the pulse shape or width of a dispersion managed soliton are not exactly correct, they do not evolved into the correct pulse but oscillate around the correct solution *[74]*. The pulse energy depends on the strength of the dispersion map as well as the average dispersion.

The original work to find the stable pulse energies was presented in reference [50], this paper finds stable enhanced power dispersion managed solitons by letting the pulse evolve over a long propagation distance and removing the dispersive radiation to help the pulse evolve. It was noticed that the energy enhancement of these pulses had empirical relationship with what is now known as the dispersion map strength. An empirical relationship for the energy enhancement is given by,

$$E_{sol} = E_0\left[1+0.7\left(\frac{(\beta_{1n}-\beta_{aveg})l_1-(\beta_{12}-\beta_{aveg})l_2}{T^2}\right)^2\right] \tag{4.2}$$

Where β_1 and β_2 are the dispersions of the fibre and the grating, l_1 and l_2 are the lengths of the fibre and grating respectively, β_{ave} is the average dispersion, T is the FWHM pulse width, S is the dispersion map strength. E_{sol} and E_0 are the energies of the dispersion managed soliton and the equivalent first order soliton respectively. The same paper first time indicated that the pulse shape also varies with dispersion map strength. The possibility of using stronger dispersion map was thus opened up development of averaging techniques to find the exact periodic solution to dispersion managed system, and hence has allowed further investigation of the energy enhancement.

4.4 Conclusions

In this chapter we have discussed the basic principles of dispersion managed soliton transmision. It is apparent that the development of dispersion managed solitons based fibre communication have entered the stage of commercial exploitation and real world soliton networks. Dispersion managed soliton systems are an attractive option to upgrade existing fibre networks to multigigabit regimes. Dispersion managed pulse propagating down the fibre line experiences rapid periodic variations of power fibre loss and amplification and periodic breathing like oscillations of pulse width and chirp due to nonuniform local dispersion. We have shown the behaviour of soliton when they propagate in the normal and anomalous sections of fibre. They can be clearly seen to acquire different type of chirps depending on the dispersion of the fibre. In both cases the pulse broadens as it propagates down the fibre but the bandwidth decreases in the case of fibre having anomalous dispersion and increases in the case of normal dispersion fibre. Map strength is also an important parameter in describing the dispersion map and solitons. It gives the measure of, the amount of dispersive broadening, pulse undergo in the dispersion map. In the case of dispersion managed system shown in figure 4.1, the pulse clearly recovers after each dispersion map.

After propagating through the fibre the pulse accumulates a negative chirp which gets compensated in the grating by positive chirp due to the normal dispersion of the fibre. In the alternating sections having anomalous and normal dispersions, dispersion dominates the evolution of these pulses however self phase modulation modulation modulation modulation modulation plays an important role in the formation of dispersion managed solitons.

In summary we have discussed the various parameters involved in the propagation of dispersion managed solitons in the standard fibre for powers well below the ones required for the first order soliton.

Chapter 5

10Gbit/s RZ transmission over standard fibre with unchirped input pulses

5.1 Introduction

Most of the world wide installed optical fibre has low loss in the 1.3 and 1.55 μm region called the second and third communication window. This fibre which is also called standard fibre has low dispersion in the 1.3 μm window. In order to maintain data over system length, current systems work in the second window using electronic regenerators to retime, reshape and amplify the signal periodically. The regenerators only operate at a fixed data rate. If the system is to be upgraded, it is necessary to replace the regenerators by EDFA's, which are data rate transparent due to wide bandwidth. The EDFA's have their own drawbacks, and since they do not retime or reshape the signal, it is required to address these system design problems due to the high dispersion of fibre in the third communication window. Various methods have been suggested to counter the dispersion problem, such as use of dispersion compensating fibre [3], optical phase conjugation, pulse chirping and use of fibre grating. The pulse chirping and duobinary coding are limited in the distance over which they can be effective to around 150 km, phase conjugation is a complex process to implement.

A great deal of interest [75] has been shown towards use of higher data rates in optical fibre communications with 10 Gbit/s now virtually a minimum base line rate in telecommunications. As the potential data rates have increased in purpose designed systems [76], attention has turned to what can be made of the existing fibre infrastructure. There are tens of millions of kilometres of optical fibre already installed throughout the world, generally operating at very low data rates and over "standard fibre" at 1.3 μm wavelengths. Here the question arises that how can it be reused, avoiding expensive and time-consuming fibre laying, at higher data rates. The use of dispersion managed solitons decreases the path averaged dispersion of transmission line, thus reducing the timing jitter. Computer simulation and experiments have shown that stable pulses in a fibre with dispersion maps [54] that have larger deviation of local dispersion from average have enhanced energy relative to solitons in fibre with uniform dispersion that is equal to path averaged dispersion of the map.

Due to the emergence of the erbium doped fibre amplifier (EDFA) one solution to this problem is to replace the data rate specific electronic regenerators employed at 1.3 μm and replace them with essentially data rate transparent EDFAs. However, as the EDFA operates around 1.55 μm, whilst standard fibre was designed to have a dispersion minimum at the original 1.3 μm operating wavelength, there is high dispersion in the EDFA window causing significant problems, particularly temporal spreading of the pulses. There are also other problems associated with this older fibre, such as polarisation mode dispersion (PMD) which is generally higher than for newer fibres [77]. The dispersion is the correct sign for soliton transmission and solitons are resilient to PMD, plus they are compatible with all-optical processing technologies currently being proposed [78]. However such a high value of dispersion, typically 17 ps/nm/km limits the propagation distance for the short pulses required for high data rates.

In this chapter problems associated with using solitons to upgrade already installed standard fibre systems using EDFAs and fibre grating were studied. In particular systems were considered, where existing amplifier spacing are >25 km with a view to upgrading the data rate to 10 Gbit/s, which is a specific but important technological challenge relevant to current European optical network [79]. The soliton system design constraints are discussed and investigated by numerical simulation. The soliton propagation was shown to be possible in standard fibre systems to distances of around 5000 km, and that phase modulation and alternating amplitude coding are detrimental in such highly perturbed systems. To extend this distance a novel method of improving soliton propagation in standard fibre systems is examined. This investigates the use of Fibre grating to reduce the average dispersion of each system link. This scheme should lead to soliton propagation for distances greater than 5000 km.

5.2 System Description

For short-haul systems such as this considered here, the effects of Gordon-Haus jitter was kept to minimum by keeping low the average dispersion of the system. The soliton interaction and average soliton constraints must however be balanced to give a stable propagation. The average power requirements can also be an issue, due to the high dispersions of these systems. These constraints are illustrated and assessed using the following system.

It was assumed that EDFAs could provide the optical powers and gain necessary for soliton propagation, with amplifier output power in the range of 5-15 mW.

In this Chapter, an asymmetric map shown in figure 5.1 was used. The input pulse were taken to be sech shaped and is unchirped. The standard fibre was taken to have typical value of dispersion of -21.6821 ps^2/km, a loss of 0.2 dB/km at 1.55μm wavelength and Aeff is 50 μm^2. Dispersion compensation was performed prior to each amplification. The fibre grating was simulated to have a length of 10 cm and a dispersion of 2.142×10^7 ps^2/km and a 3dB loss.

The loss is chosen to allow double pass insertion loss of the circulator required, typically 0.8 dB port to port, and the loss of grating itself around 1-1.5 dB.

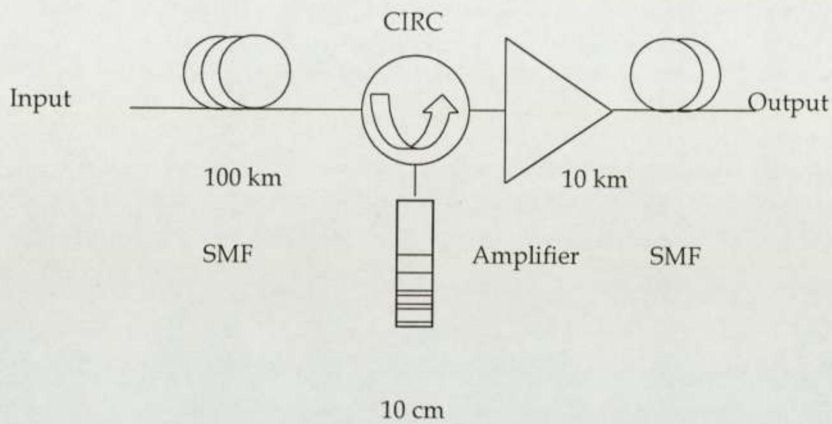

Figure 5.1: *Schematic diagram of the system under consideration*

Ideally original amplifier spacing should be maintained since the existing systems waas being upgraded, but more amplifier means more cost. In this section, the focus on the use of 100 km amplifier spacing. Since operation of soliton system at 10 Gbit/s necessarily prohibits soliton's width greater than approximately half the bit interval at 50 ps, the associated soliton periods in standard fibre are only a few tens of kilometres. As $L_a \cong Z_0$, average soliton perturbations are severe and the system design is closely squeezed between the competing requirements of the soliton-soliton interaction and average soliton constraints. Consequently, any potential system is highly perturbed. In order to probe the constraints and identify the limits, we have performed extensive set of numerical simulations using full NLSE propagation, as prescribed in the following section.

Various different maps were investigated by placing fibre grating and amplifier at different position in the span of standard fibre. The best results were obtained by using the schematic shown in figure 5.1. The amplifier provides 23 dB gain, which compensates for the loss of fibre and grating.

5.3 Optimisation Procedure

The dispersion map consists of 100 km long spans of standard fibre followed by a grating and an amplifier.

The launch position of soliton in the unit cell was set such that minimum pulse width variation is maintained and soliton repeat itself after each span. This type of launch position ensures the positioning of the grating in the unit cell at a point where minimum nonlinearity and hence dispersion compensation can be achieved independent of the nonlinearity effects. Fibre grating provides post dispersion compensation for the initial 90 km and acts as pre compensator for the rest of the 10 km in the unit cell. Since these pre compensation and post compensation sections were alternately positioned along the transmission line, there effect balanced each other error free transmission became possible.

The system was simulated by propagating a random bit sequence of 144 data bits, half of which were data 1's, at 10 Gbit/s using split-step NLS method, with the system under study as shown in figure 5.1. The standard fibre was taken to have typical values of dispersion of 17 ps/nm/km and loss of 0.2 dB/km at 1.55 μm wavelength and data rate was 10 Gbit/s. Dispersion compensation was performed prior to each amplification. For the purpose of simplification the fibre grating was simulated as a 10 cm piece of fibre with the appropriate dispersion (1680 ps/nm) and loss (3 dB) characteristics. The loss was chosen to allow for the double pass insertion loss of circulator required, typically 0.8 dB port to port, and the loss of grating itself, around 1-1.5 dB. Amplified spontaneous emission (ASE) noise was included, with noise figure is 4.5 dB. The impact of amplifier noise was expected to be significant in such long amplifier spans. A super Gaussian filter of 0.04 THz bandwidth was used to filter out this noise. The receiver was simulated as a fast photodiode followed by an electronic filter with bandwidth of half the data rate to convert the return-to-zero (RZ) soliton data to non-return-to-zero (NRZ) format.

The traditional soliton transmission lines have constraints such as timing jitter, interaction between adjacent pulses and collision induced frequency shift. Optimisation of the system performance assumes suppression of these factors in order to minimise the bit error rate (BER). However in practical transmission systems, many other factors such as boundary conditions and even the cost issues make it a complicated problem. The cost issue was taken into account in this system designby making the length of the SMF used long, which meant that less repeater sections were required. Secondly the use of passive element such as grating, for dispersion compensation, that can be incorporated into a single unit with the amplifier made the design simpler. Dispersion compensation makes the optimisation procedure more complex, as the introduction of new parameters (characterising the dispersion map) involved. The structure and propagation of the pulses in dispersion compensated system are different from those in conventional soliton systems. As discussed earlier the dispersion managed soliton is chirped, and the pulse width and chirp vary along the compensation section. Along with the other factors, it is important to diminish the energy shedding from the input pulse into a dispersion pedestal. This can be achieved by launching properly shaped pulses with optimum power into the fibre at an optimum position. The best system performance is achieved when an input signal fits the DM soliton (true periodic solution) corresponding to a given map. Initially the launch position of the pulse with in the dispersion map was varied until minimum deviation of pulse width was obtained.

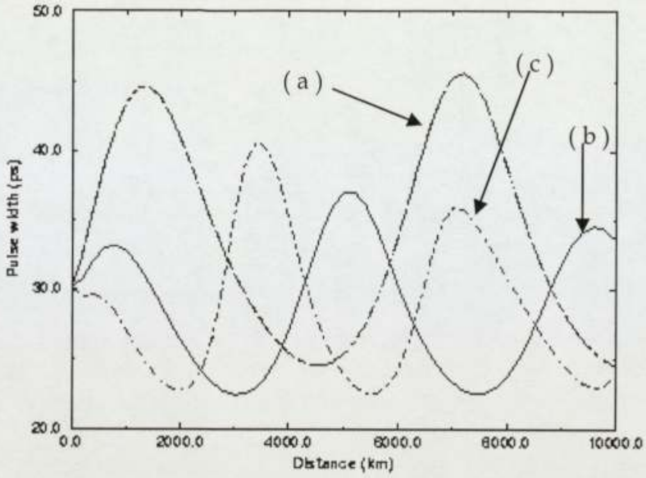

Figure 5.2: The pulse width variation verses distance for grating placed (a) dashed line: at start of 100 km span (b) solid line: after 90 km of standard fibre followed by 10 km of standard fibre (c) dot-dashed line: at the end of the span

After launching the pulse at this point, the peak power of the pulse was optimised for minimum pulse width variation from the original value for thousands of kilometres of propagation.

Figure 5.3 shows the pulse width variation by varying the value of input power. The plot shown with solid line represents the optimum peak power (12.5 mW), the other two plots represented by dotted and dot-dashed line having powers of 8.5 mW and 17 mW respectively.

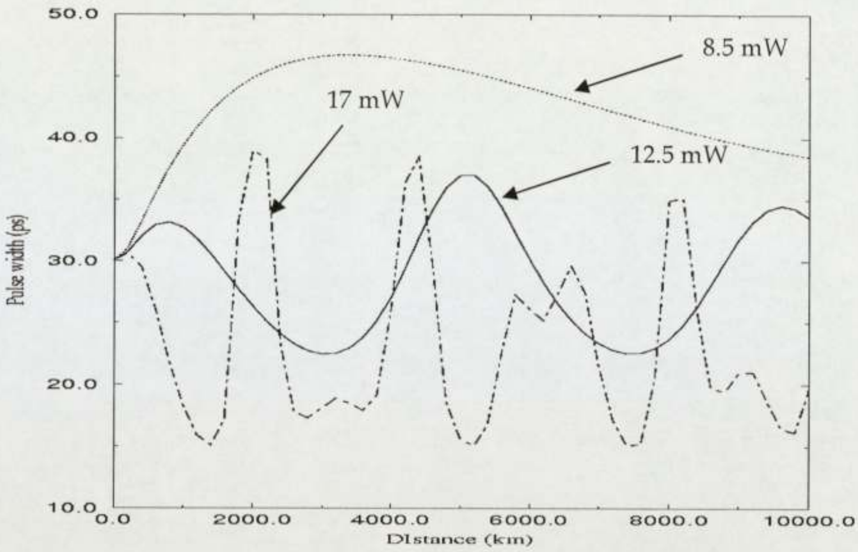

Figure 5.3: The pulse width against propagation distance for schematic shown in figure 5.1 for a input chirp of 0.0015 THz and peak powers 12.5 mW (solid line) 8.5 mW (dotted line) and 17 mW (dot-dashed line)

5.3.1 Result of Optimisation

Simulations were performed for pulse widths 20-50 ps to test the maximum transmission distance for which data could be recovered. Figure 5.4 shows a typical simulation result taken at each amplifier output for 30 ps pulses propagating to 500 km. After only a few amplifications the pulse begins to distort and by the end of the simulation the data has been lost.

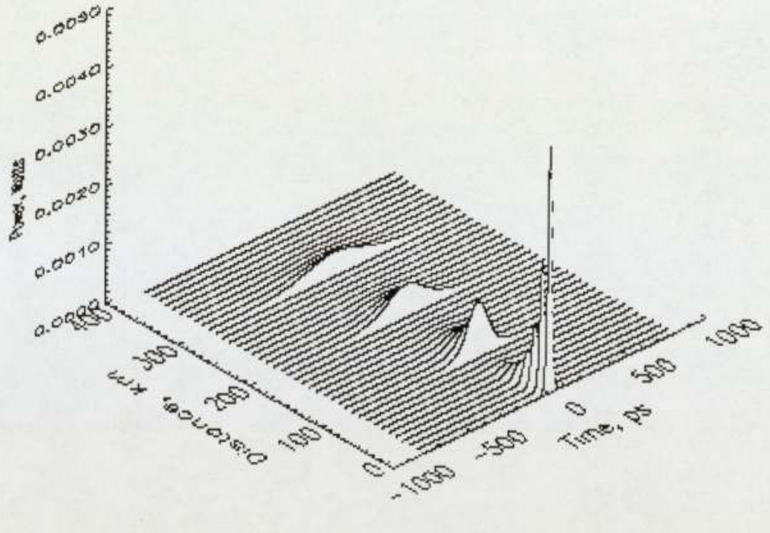

(a)

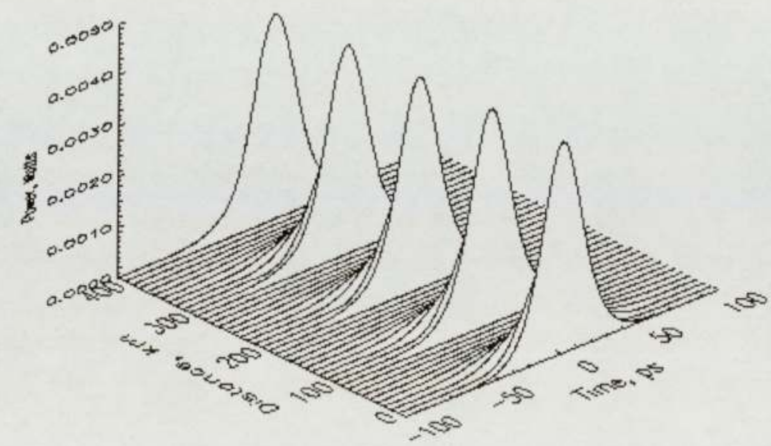

(b)

Figure 5.4: Single pulse propagating to 400 km (a) without dispersion compensation (b) with dispersion compensation.

These optimised pulses as discussed in previous section are now used in a direct simulation of standard fibre transmission. The system was simulated by propagating a random bit sequence of 144 data bits, half of which were data 1's, at 10 Gbit/s using split-step NLS method,

With the system under study as shown in figure 5.1. Amplified spontaneous emission (ASE) noise was included, with noise figure is 4.5 dB. The impact of amplifier noise is expected to be significant in such long amplifier spans. A filter of 0.0325 THz bandwidth is used to filter out this noise. The receiver was simulated as a fast photodiode followed by an electronics filter with bandwidth of half the data rate to convert the return-to-zero (RZ) soliton data to non-return-to-zero (NRZ) format. It was then possible to estimate the bit error ratio (BER) from the received eye diagram through the Q parameter method [80]-[81] Where Q is given by,

$$Q = \frac{\mu_1 - \mu_0}{\sigma_1 + \sigma_0} \tag{5.1}$$

For means μ_0 , μ_1 and standard deviations σ_0 , σ_1 of the data 1's and 0's. The BER is then estimated according to

$$\mathrm{BER} = \frac{1}{2\pi} \frac{\exp(-Q^2/2)}{Q} \tag{5.2}$$

For each BER computation, the 144 data bits were propagated in 9 sets of 16 bits for speed simulation, as it was found that the BER estimated was the same using this method or a single 144 bit propagation. We note that determination of the BER by this method is normally performed for a set of single, isolated pulses to avoid an under-estimate of the Q from patterning effects. However, in this work we expect strong soliton interactions, the nature of which will be pattern dependent, necessitating the inclusion of patterning in the BER estimate.

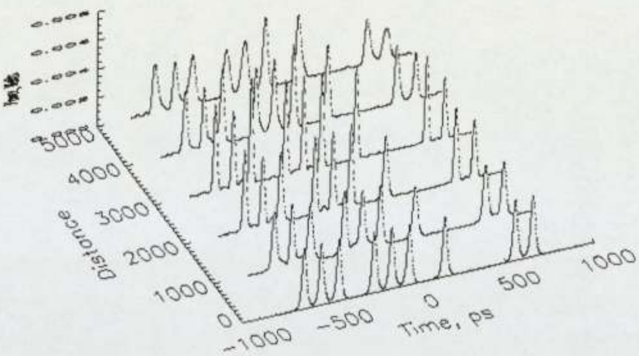

Figure 5.5: Simulation of 30 ps pulse train in a system compensated to –0.3 ps²/km, with data <0111011101000110>.

Figure 5.5 shows the 30 ps pulses propagating to 5000 km. After 5000 km propagation the pulses start interacting and BER falls bellow 10^{-9}.

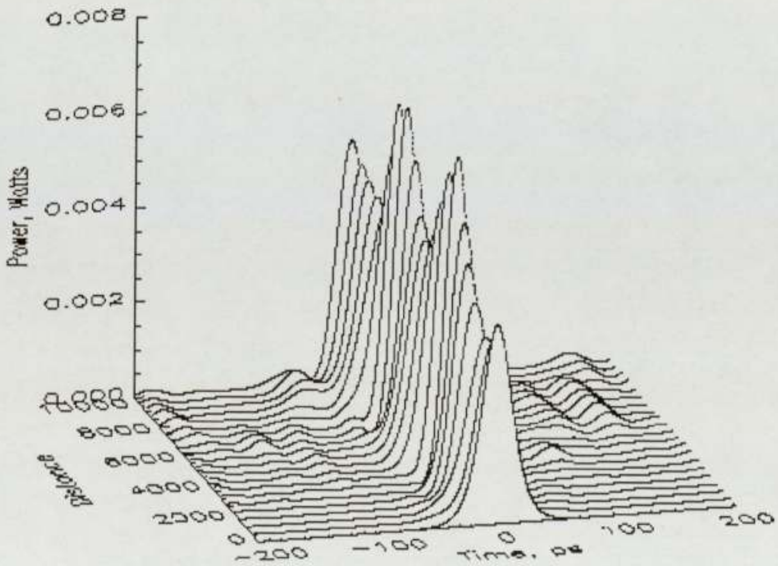

Figure 5.6: The pulse width evolution for the system shown in figure 5.1, the oscillations are considerably reduced.

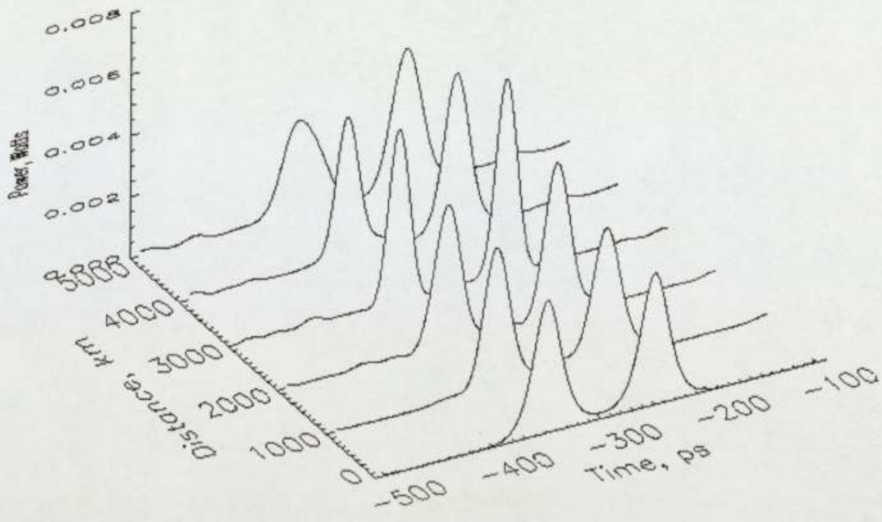

Figure 5.7: Two optimised pulses propagating over 5,000 km.

Figure 5.7 shows two of these optimised pulses propagating with a separation of 100 ps, making it equivalent to 10 Gbit/s over 5,000 km. These pulses don't undergo significant interaction even after several thousand of kilometres of propagation.

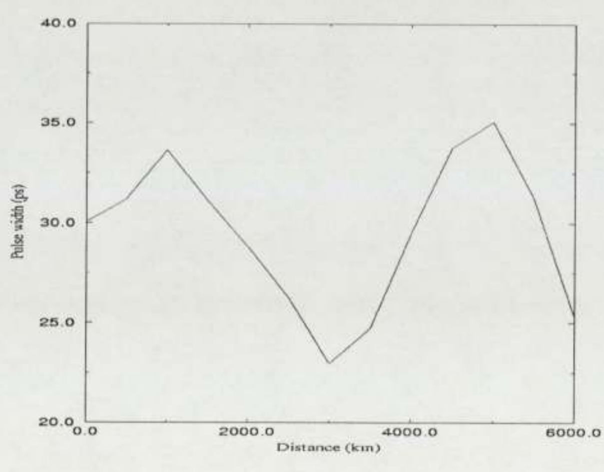

Figure 5.8: The pulse width against distance for system shown in figure 5.1.

The minimum in the pulse width relates to pulses with high peak powers and approximately coincides with the high Q-values. This can be seen as slight humps in the Q-values shown in figure 5.24. The maximum Qs are related to the minima in the time bandwidth product. The fluctuations in the pulse parameters such as chirp and width are due to the mismatch of the pulse shape with the dispersion map. The pulse under goes a long-term evolution as the pulse sheds dispersive radiations and all the parameters including pulse width, peak power, shape and chirp change. The chirp is highest at the start of the fibre and hence launching the chirped pulses at this point enhances this effect. The pulse is initially chirp free at the output point in the map, it soon accumulates complicated chirp. The points where the pulse width and Q are highest coincide with the points where chirp is at minimum.

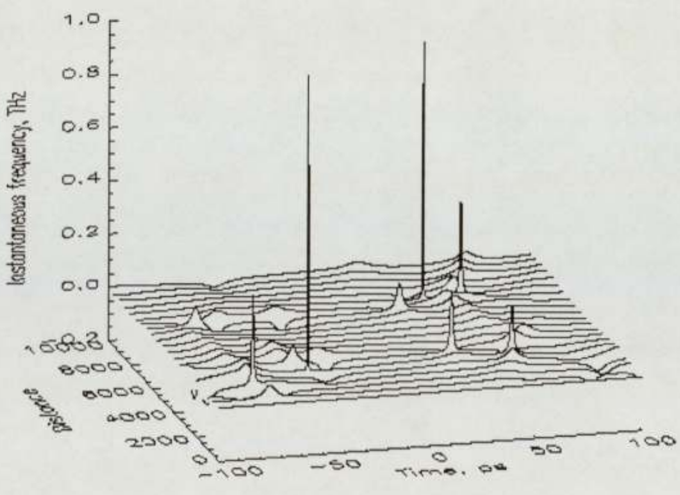

Figure 5.10: Instantaneous frequency for the system under consideration.

The chirp of the pulse can be examined by looking at the instantaneous frequency of given in figure 5.10, it is clear that even though it is chirp free at the output point in the map, it soon accumulates a complicated chirp. The pulse width shown in figure 5.8 varies a lot during the course of each dispersion map due to the high local dispersion but at the end of the dispersion map it returns close to its original value.

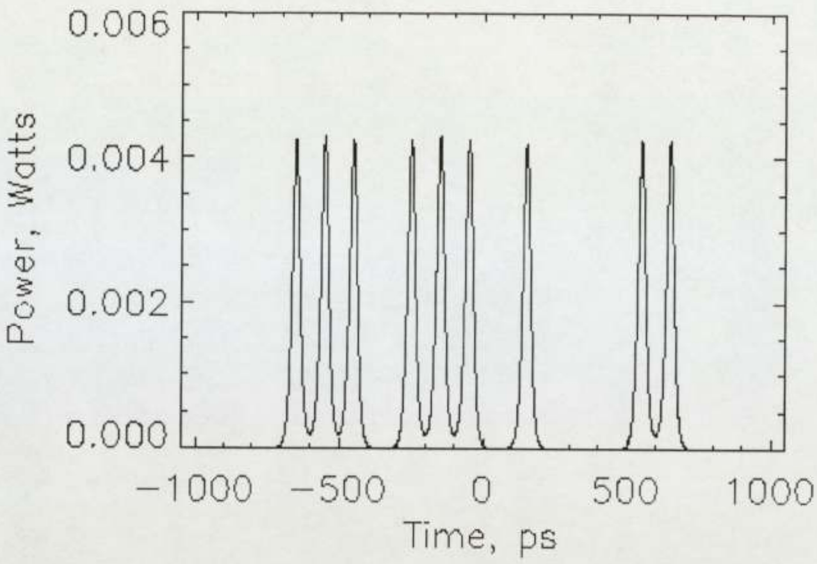

(a)

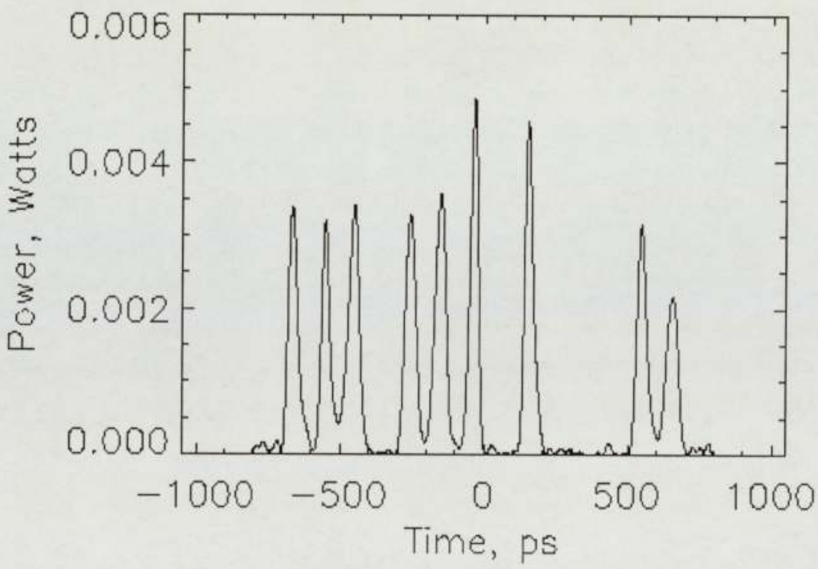

(b)

Figure 5.11: The top figure shows a section of a bit pattern at the start of the simulation. The lower picture shows the same bit pattern after it has propagated over 4000 km.

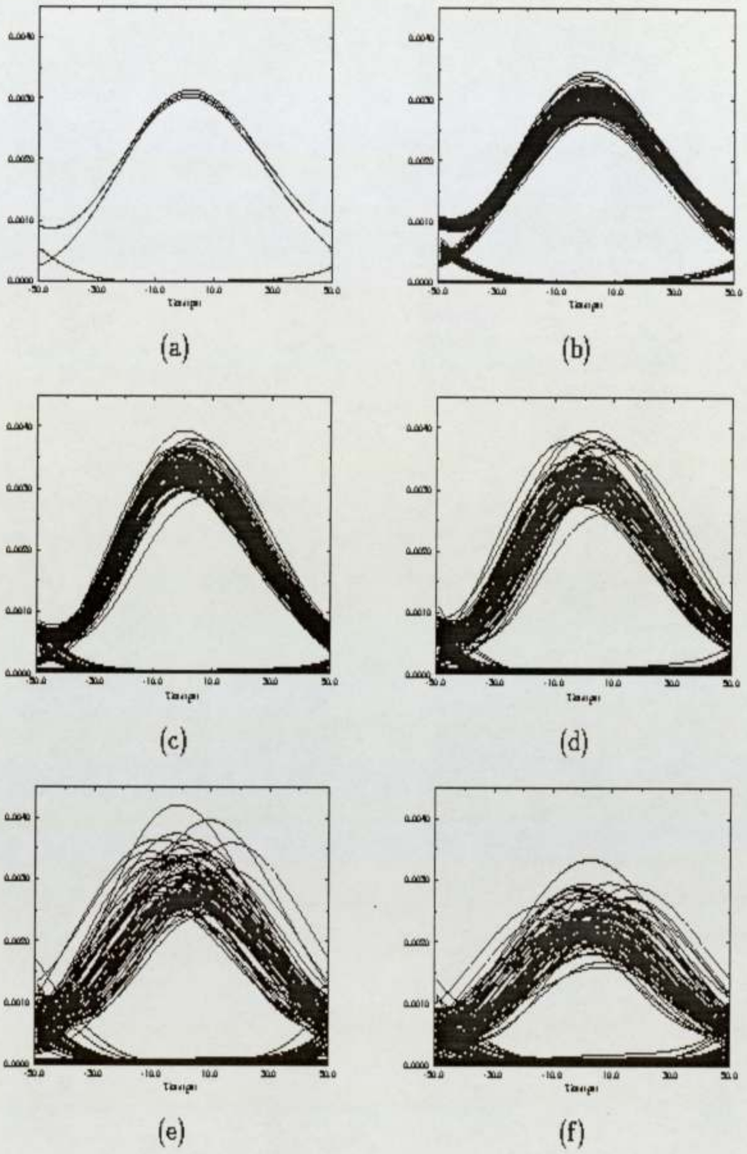

Figure 5.12: Simulation eye diagrams corresponding to figure 5.5, at distances (a) 0 km (b) 1000 km (c) 2000 km (c) 3000 km (d) 4000 km (e) 5000 km

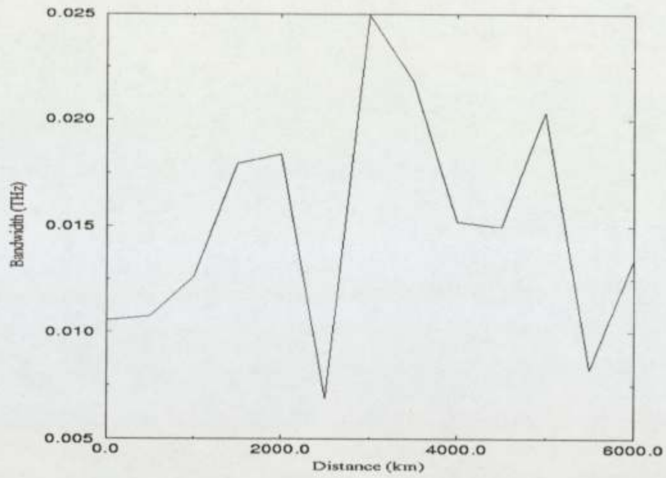

Figure 5.13: The bandwidth against distance for the map shown in figure 5.1.

By contrast bandwidth of the pulse as show in figure 5.13 reduces initially but recovers afterwards. Eventhough the bandwidth recover, on the whole it decreases. This recover does reduce the over all change in bandwidth, which in turns results in improvement in the performance of the system. The reduction in bandwidth is a critical factor, as it leads to long term changes in the pulse width, since the minimum pulse width is defined by the bandwidth of the pulse. Figure 5.12 show the simulation eye diagrams, and it can be clearly seen that even after 5000 km propagation the eye is open enough to give BER more than 10^{-9}.

The oscillations even though very low can be seen in the Q value. These oscillations normally occur as pulses are either not launched at the optimum place in the dispersion map, or the chirp in the input pulses is not completely optimised. The oscillations can also be seen in the plots of pulse shapes, which is shown in figure 5.7. They can be more clearly examined in the graphs of the pulse width evolution (figure 5.6) and time bandwidth product (figure 5.9).

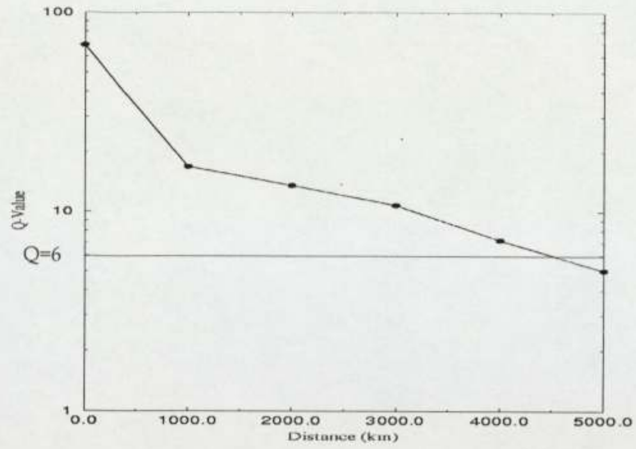

Figure 5.14: Q-value against distance for the system using the optimised pulses and system having optimised launch position.

Using 20 ps pulses in stead of 30 ps pulses the same simulations saw a clear improvement in the propagation distance. Figure 5.15 shows the pulse width variation for a single pulse as it propagates down the fibre.

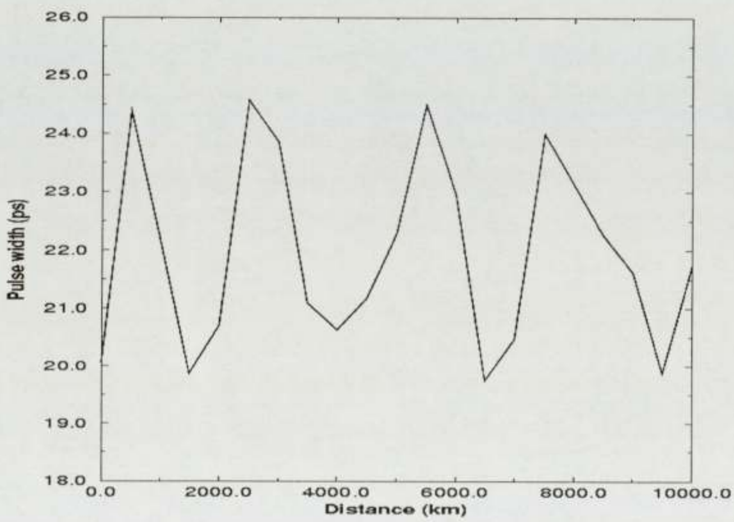

Figure 5.15: The pulse width against distance for the map shown in figure 5.1 for 20 ps input pulses.

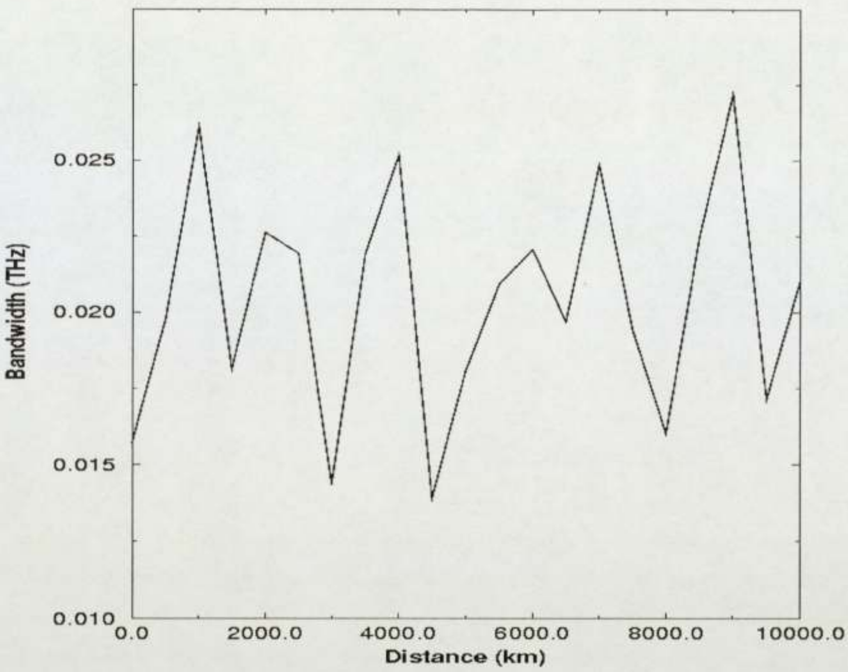

Figure 5.16: The bandwidth against distance for the map shown in figure 5.1 for 20 ps pulses.

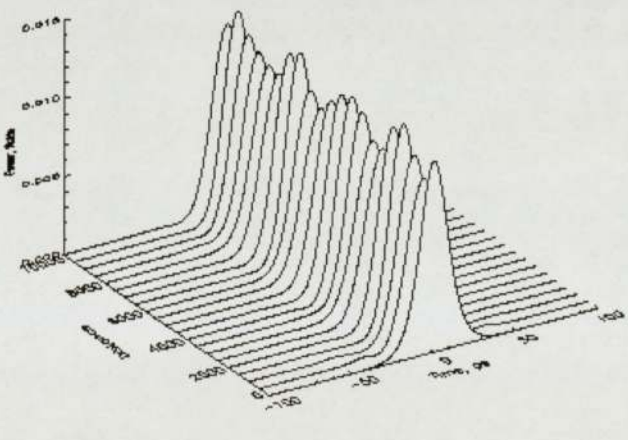

Figure 5.17: The pulse width evolution of a 20 ps pulse for the system shown in figure 5.1, the oscillations are considerably reduced

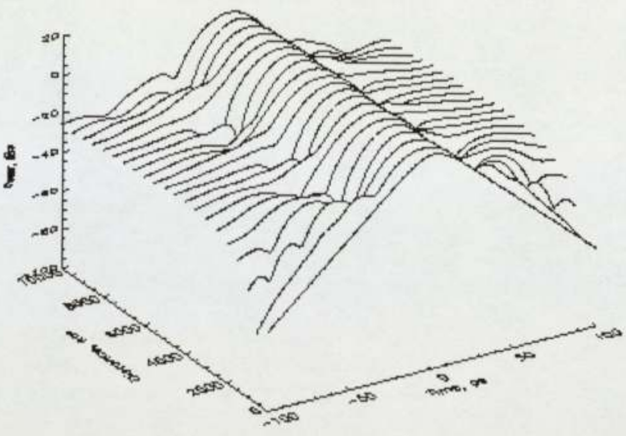

Figure 5.18: The pulsewidth against distance for the map shown in figure 5.1.

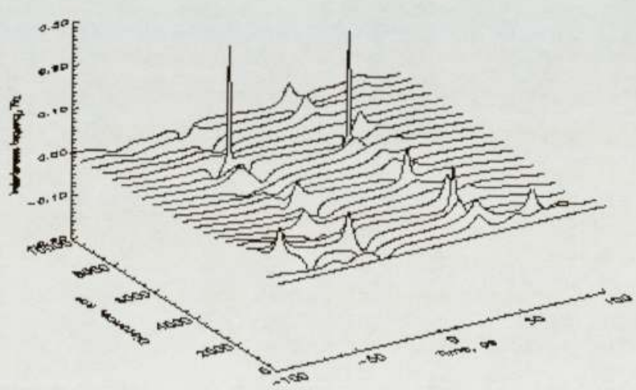

Figure 5.19: The instantaneous frequence against distance for the map shown in figure 5.1.

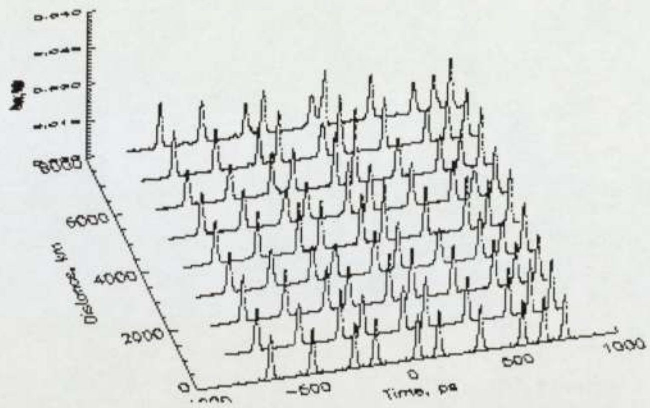

Figure 5.20: Simulation of 20 ps pulse train in a system compensated to –0.3 ps²/km, with data <0101011011010111>.

Figure 5.20 shows the 20 ps pulses propagating to 8000 km. After 7000 km propagation the pulses start interacting and BER falls bellow 10^{-9}.

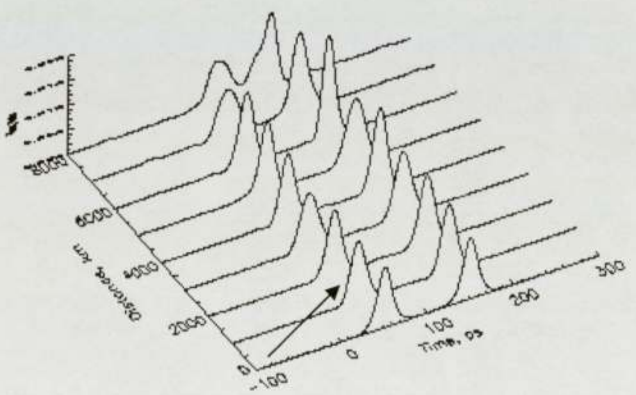

Figure 5.21: Two optimised 20 ps pulses propagating over 8,000 km.

Figure 5.21 shows two of these optimised pulses propagating with a separation of 100 ps, making it equivalent to 10 Gbit/s over 8,000 km. These pulses don't undergo significant interaction even after 7000 km of propagation distance.

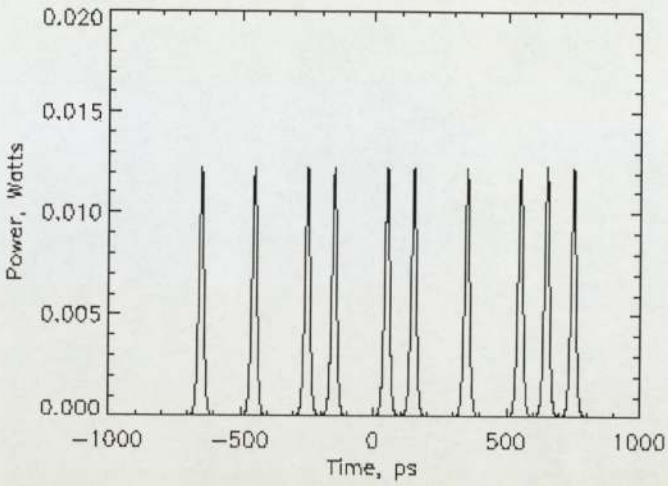

(a)

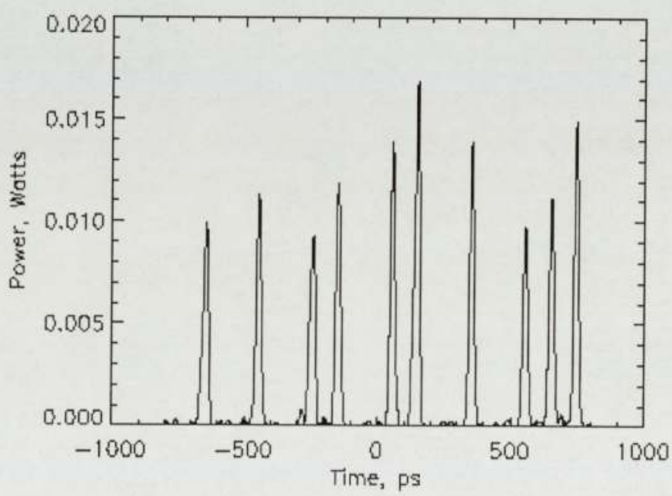

(b)

Figure 5.22: The top figure shows a section of a bit pattern at the start of the simulation. The lower picture shows the same bit pattern after it has propagated over 7000 km

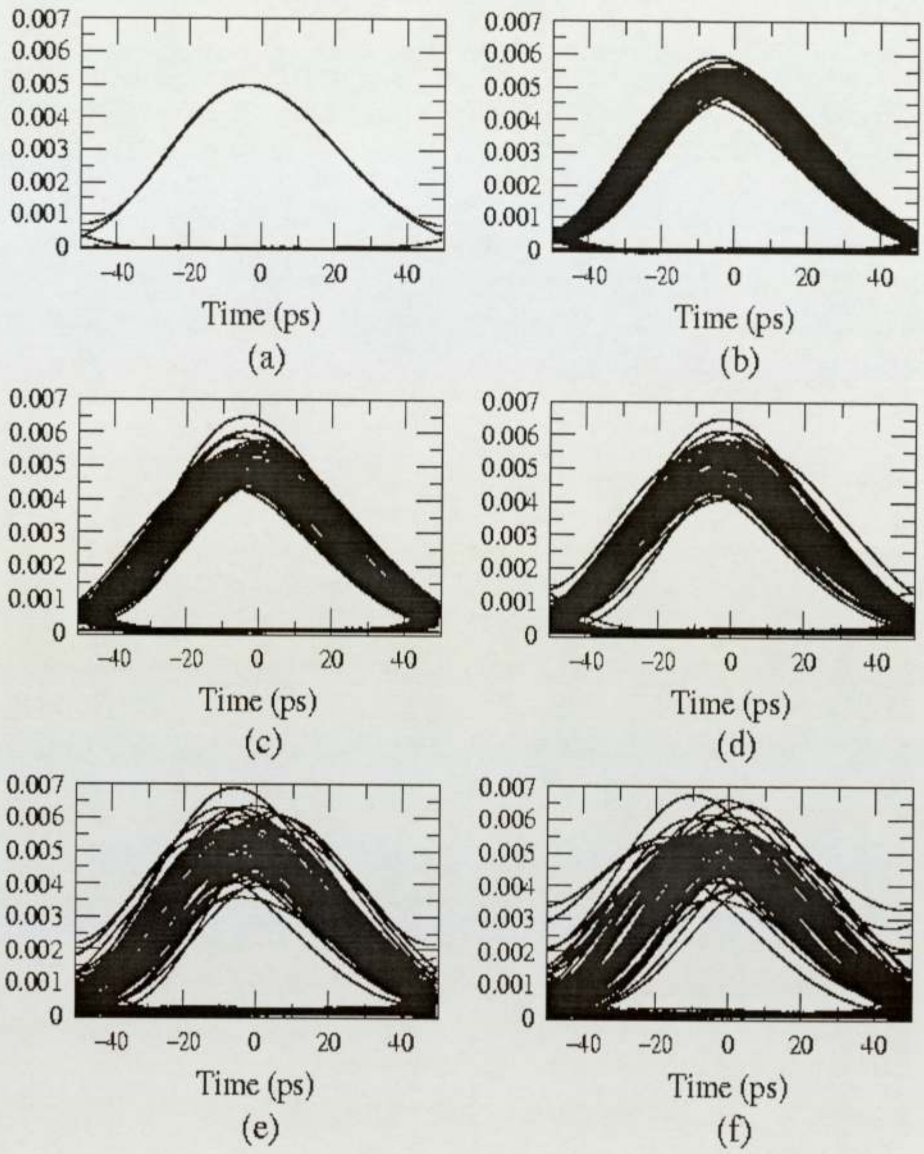

Figure 5.23: Simulation eye diagrams corresponding to figure 5.5, at distances (a) 0 km (b) 1500 km (c) 3000 km (c) 5000 km (d) 6500 km (e) 7000 km

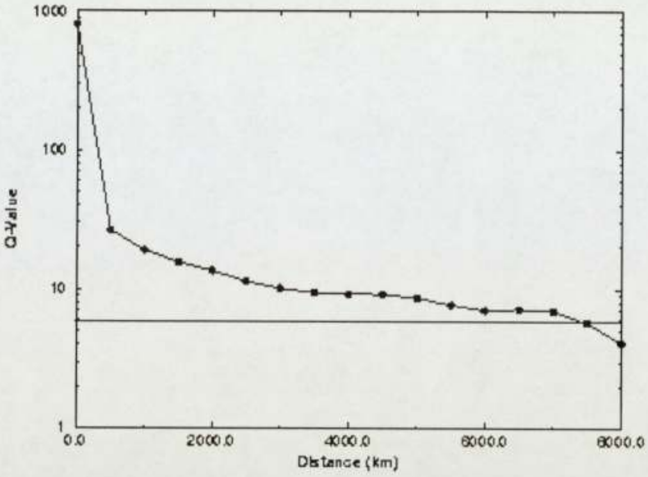

Figure 5.24: Q-value against distance for the system using the optimised 20 ps pulses and system having optimised launch position.

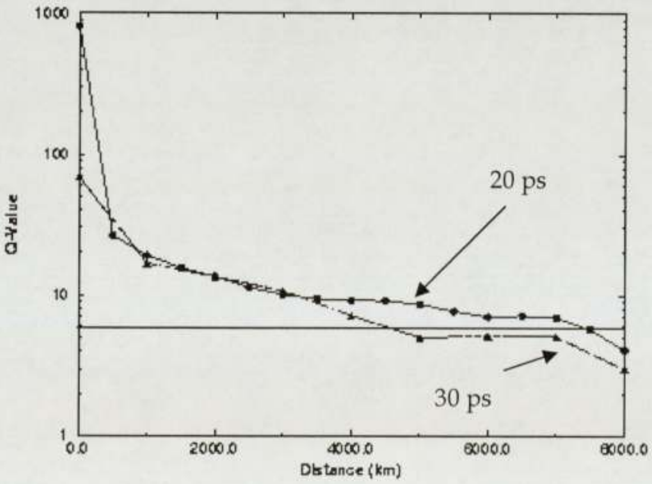

Figure 5.25: Comparison of Q-value against distance for systems with 20 ps input pulses (dots) and with 30 ps input pulses (upside triangles) at optimum position in the dispersion map.

Figure 5.25 shows comparison of Q-values for system with 20 ps input pulses (represented by dots) and with 30 ps input pulses (represented by up side down triangles) launched at optimum launch position in the dispersion map. A considerable improvement can be seen in the total propagation distance.

5.4 Conclusions

In conclusions we have studied the behaviour of dispersion managed solitons using fibre grating for dispersion compensation and optimising the position of grating in the dispersion map. We have shown that by carefully choosing the position of grating in the map the overall system performance can be dramatically improved. The optimum launch position of soliton for chirp free pulses is 90 km before the grating and energy enhancement is reduced by inclusion of loss in the systems. Stable solutions are possible by alternative arrangement of the pre compensation and post compensation sections.

Figure 5.12 shows the system performance improvement by launching the input pulses at optimum position, in terms of eye opening and temporal and amplitude jitter. It is clear from the Q-value plot in figure 5.24 that total propagation distance is over 4000 km. As found else where, whilst a traditional soliton system would require a mark to space ratio of 5 or 6, making 20 ps pulses the long pulse width limit, this constraint is reduced in dispersion managed systems [59] and longer pulse widths (30 ps in this case) are possible.

The results presented in this chapter demonstrate that proper choice of launch position in the dispersion map and peak power can improve the stability of dispersion managed soliton systems.

Chapter 6

10Gbit/s RZ transmission over standard fibre with chirped input pulses

6.1 Introduction

The importance of pulse chirping to reduce the chromatic dispersion penalty and to improve the transmission capacity of the dispersion managed systems has been pointed out in [82]. For systems with high dispersion map strength, the large variation of dispersion modifies the pulse propagation, including breathing like oscillations of the pulse width and chirp during the compensating period. Soliton propagation in the link with dispersion compensation is chirped in contrast to NLSE soliton. The most surprising feature of compensated solitons is their propagation stably along the fibre with zero and even normal average dispersion [60] (in contrast to the fundamental soliton that only propagates in anomalous dispersion region). This is extremely interesting because transmission of the finite energy pulse close to the zero dispersion point takes advantage of the suppressed timing jitter. On the other hand, in order to keep the signal to noise ratio large enough, one must not operate too close to zero dispersion point. Thus an optimum average dispersion is to be found with minimum timing jitter and maximised signal to noise ratio. The chirp is the most important feature of dispersion managed solitons [83]. Soliton chirp leads to rapid rotation of the relative phase shift between the neighbouring solitons, resulting in the suppression of the interaction.

This chapter examines the transmission of dispersion managed solitons, over standard fibre, with large amplifier spacing and chirped input pulses at 10 Gbit/s. Fibre grating is used for the dispersion compensation. It has been shown numerically and experimentally [84],[85],[86],[87],[88],[89],[90],[91],[92] the possibility of 10Gbit/s transmission using fibre gratings. A direct comparison is made between modelling of a system with unchirped input pulses launched at optimum launch position in the dispersion map. For a given dispersion map, the effects of changing the peak power and chirp of the input pulses is studied. Oscillations in the pulse width and peak power that lead to oscillation in the Q-values can be suppressed by appropriately choosing the chirp of the input pulses. These simulations can be used to compare the results of numerical simulations to experimental results.

The use of fibre amplifiers rather than repeaters means that the long-term effects of nonlinearly and dispersion has to be considered. Due to the use, EDFA's signal must propagate at 1.55 μm where dispersion of the standard fibre is high. High dispersion that leads to increases the power required to create a soliton also increases Gordon-Haus jitter and reduces the soliton period which causes problem with average soliton model and reduces the collapse length for adjacent solitons.

The average dispersion of the fibre link can be reduced by using dispersion management and hence possibility of large increase in the propagation distance [93], [94],[95],[96],[97],[98],[99],[100],[101],[102]. Dispersion management can be used for upgrading the current standard fibre network, as dispersion-compensating grating can be installed along with the amplifiers at the sites of repeaters in the current network and so upgrade will save us laying of large amount of fibre.

6.2 System Description

In this Chapter, we again consider the asymmetric map shown in figure 6.1. The input pulse is sech shaped and is chirped. The standard fibre was taken to have typical value of dispersion of -21.6821 ps^2/km, a loss of 0.2 dB/km at 1.55μm wavelength and Aeff is 50 μm^2. Dispersion compensation is perform prior to each amplification. The fibre grating is simulated to have a length of 10 cm and a dispersion of 2.142×10^7 ps^2/km and a 3dB loss. The loss is chosen to allow double pass insertion loss of the circulator required, typically 0.8 dB port to port, and the loss of grating itself around 1-1.5 dB.

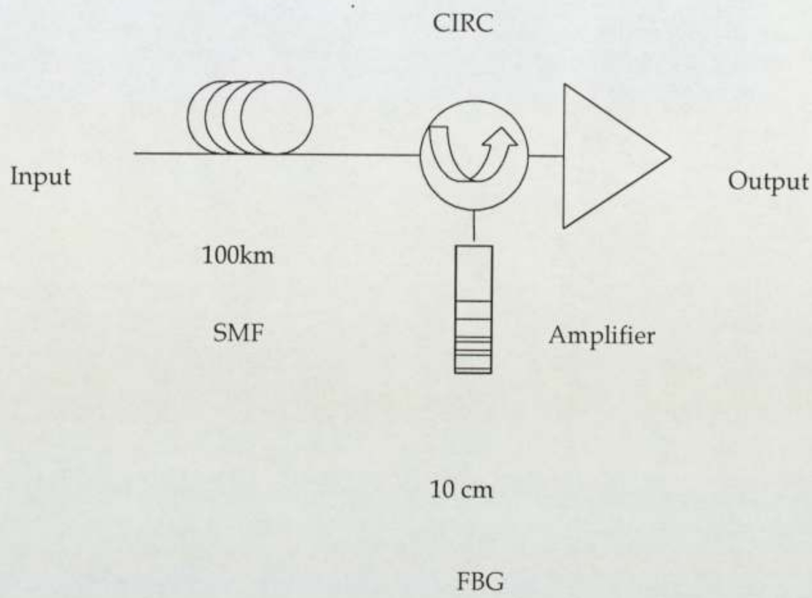

Figure 6.1: *Schematic diagram of the system under consideration*

Figure 6.1 shows the dispersion map used. The amplifier provides 23 dB gain, which compensates for the loss of fibre and grating.

6.3 Optimisation Procedure

The traditional soliton transmission lines have constraints such as timing jitter, interaction between adjacent pulses and collision induced frequency shift. Optimisation of the system performance assumes suppression of these factors in order to minimise the bit error rate (BER). However in practical transmission systems, many other factors such as boundary conditions and even the cost issues make it a complicated problem. The cost issue however is taken into account in this system design, as the length of the SMF used is long which makes the required number of repeater sections small. The use of passive element such as grating, for dispersion compensation, that can be incorporated into a single unit with the amplifier. One of the other benefits gained by using grating is the low loss as compared to 0.2 dB/km for the fibre. Dispersion compensation makes the optimisation procedure more complex, as the introduction of new parameters (characterising the dispersion map) involved. The structure and propagation of the pulses in dispersion compensated system are different from those in conventional soliton systems. As discussed earlier the dispersion managed soliton is chirped, and the pulse width and chirp vary along the compensation section. This leads to new important aspects of optimisation problem that are absent in the traditional soliton (i.e., unchirped and preserves its width with propagation). A new critical issue is the optimised soliton chirping. Along with the other factors, it is important to diminish the energy shedding from the input pulse into a dispersion pedestal. This can be achieved by launching properly shaped and chirped pulses with optimum power into the fibre. This chirping of the input pulses could be achieved by using an additional piece of fibre preceding the line edge or by properly phase modulation. The best system performance is achieved when an input signal fits the DM soliton (true periodic solution) corresponding to a given map. Initially the chirp of the input pulse was varied until minimum deviation of pulse width was obtained. Then using this value of chirp the peak power of the pulse was optimised for minimum pulse width variation from the original value for thousands of kilometres of propagation.

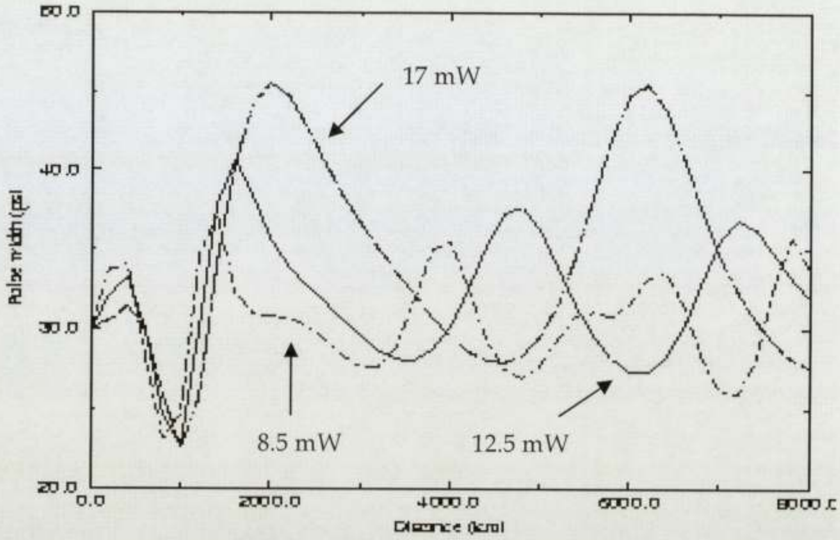

Figure 6.2: The pulse width against propagation distance for schematic shown in figure 6.1 for a input chirp of 0.0015 THz and peak powers 12.5 mW (solid line) 8.5 mW (dotted line) and 17 mW (dot-dashed line)

Figure 6.2 shows the pulse width variation by varying the value of input power. The plot shown with solid line represents the optimum peakpower (12.5 mW), the other two plots represented by dotted and dot-dashed line having powers of 8.5 mW and 17 mW respectively.

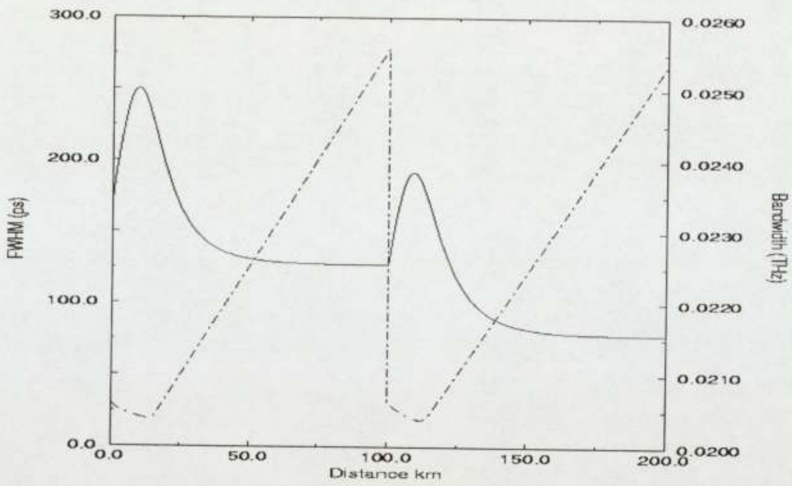

Figure 6.3: The pulse width (dashed line) and bandwidth (solid line) for an optimised pulse.

Figure 6.3 shows the bandwidth (solid line) and pulse width (dashed line) of the optimum pulse as it propagates over the dispersion map. It is clear that there are large changes in the pulse width (represented by solid line) during propagation, however at the beginning of the line the fibre bandwidth suffers a net increase, whereas over the later section of standard fibre the bandwidth suffers a net decrease. Two sections of the dispersion map are shown to show the net increase in the bandwidth at the beginning of the next section. This is due to the nonlinearly on the chirped pulse. This provides a considerable improvement in the performance of the earlier discussed system with unchirped input pulses. If the input pulses are not chirped, using the same dispersion map, no net increase in the bandwidth is obtained in the beginning of each section as shown in figure 6.4. This result in high net change in the bandwidth, hence degradation of the overall system performance. Thus by reduced net change in the bandwidth during each dispersion map improves the performance of the system.

The peak power and chirp of the input pulses is varied until the net change in the bandwidth of each section is minimised.

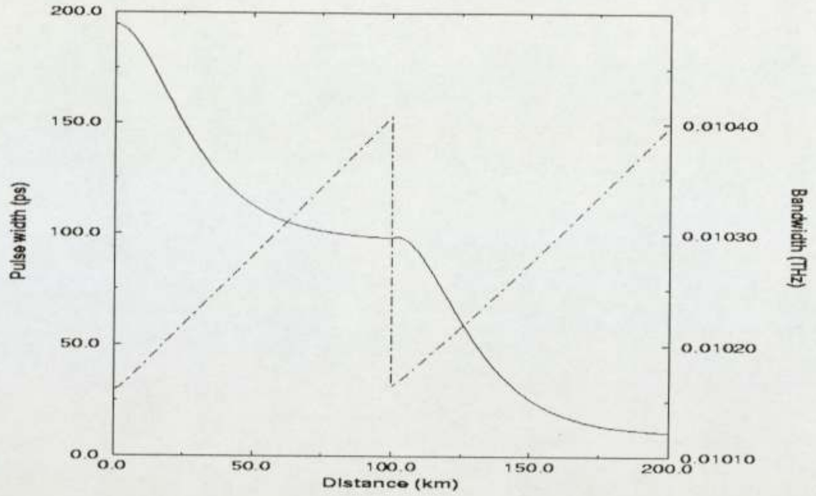

Figure 6.4: The pulse width (dashed line) and bandwidth (solid line) for an unchirped input pulse.

Figure 6.4 shows a comparison between the changes in bandwidth (solid line) and pulse width (dashed line). Note that the introduction of optimum chirp in the input pulse reduces the increase in pulse width where as it introduces the net increase in the beginning of each dispersion map.

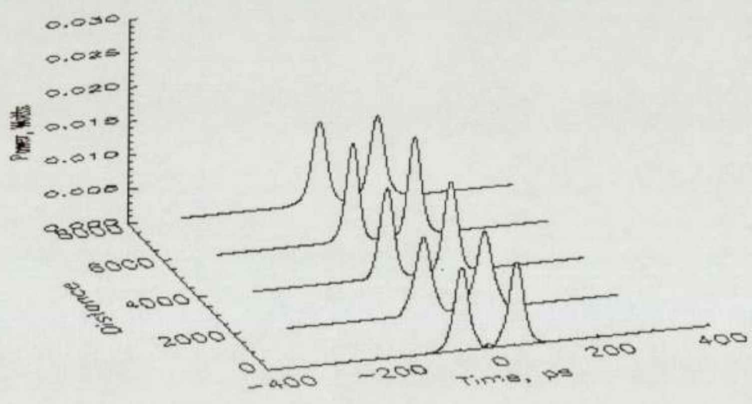

Figure 6.5: Two optimised pulses propagating over 8,000 km.

Figure 6.5 shows two of these optimised pulses propagating with a separation of 100 ps, making it equivalent to 10 Gbit/s over 8,000 km. These pulses don't undergo significant interaction even after several thousand of kilometres of propagation. This likely cause for this can be seen in the bandwidth shown in figure 6.3. Since interactions are a non-linear effect, the only occur where there is a large peak power, which is seen in figure 6.3 as changes in the bandwidth.

6.3.1 Result of Optimisation

These optimised pulses are now used in a direct simulation of standard fibre transmission. The system was simulated by propagating a random bit sequence of 128 data bits, half of which were data 1's, at 10 Gbit/s using split-step NLS method,

With the system under study as shown in figure 6.1. Amplified spontaneous emission (ASE) noise was included, with noise figure is 4.5 dB. The impact of amplifier noise is expected to be significant in such long amplifier spans. A filter of 0.04 THz bandwidth is used to filter out this noise. The receiver was simulated as a fast photodiode followed by an electronics filter with bandwidth of half the data rate to convert the return-to-zero (RZ) soliton data to non-return-to-zero (NRZ) format. It was then possible to estimate the bit error ratio (BER) from the received eye diagram through the Q parameter method [103]-[104] Where Q is given by, equation 5.1 and the BER is then estimated according to equation 5.2.

For each BER computation, the 128 data bits were propagated in 8 sets of 16 bits for speed simulation, as it was found that the BER estimated was the same using this method or a single 128 bit propagation. We note that determination of the BER by this method is normally performed for a set of single, isolated pulses to avoid an under-estimate of the Q from patterning effects. However, in this work we expect strong soliton interactions, the nature of which will be pattern dependent, necessitating the inclusion of patterning in the BER estimate.

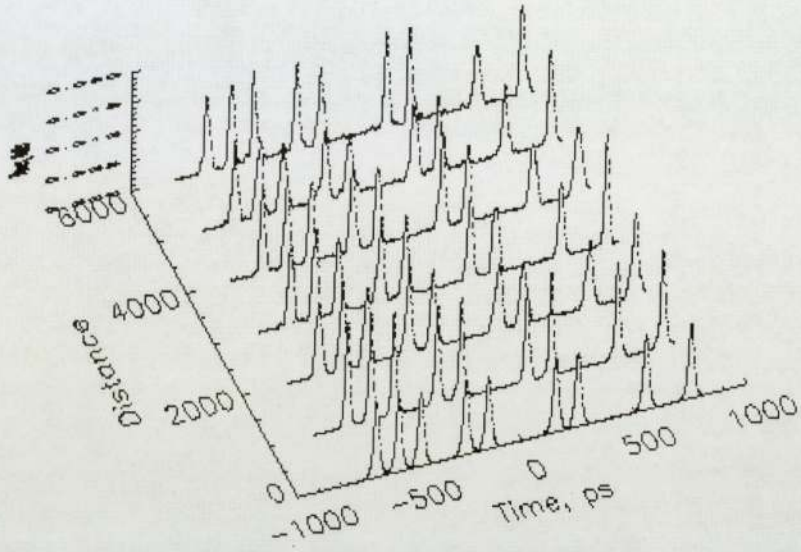

Figure 6.6: Simulation of 30 ps pulse train in a system compensated to -0.2 ps²/km, with data *<0111011101000110>.*

Figure 6.6 shows the 30 ps pulses propagating to 6000 km. Previously using the unchirped pulses the maximum propagation distance of more than 4000 km was possible. Now by using chirped input pulses with a peak power of 12.5 mW a maximum distance of more than 7800 km is possible.

The oscillations even though very low can be seen in the Q value. These oscillations normally occur as pulses are either not launched at the optimum place in the dispersion map, or the chirp in the input pulses is not completely optimised. The oscillations can also be seen in the plots of pulse shapes, which is shown in figure 6.8. They can be more clearly examined in the graphs of the pulse width evolution (figure 6.9) and time bandwidth product (figure 6.10).

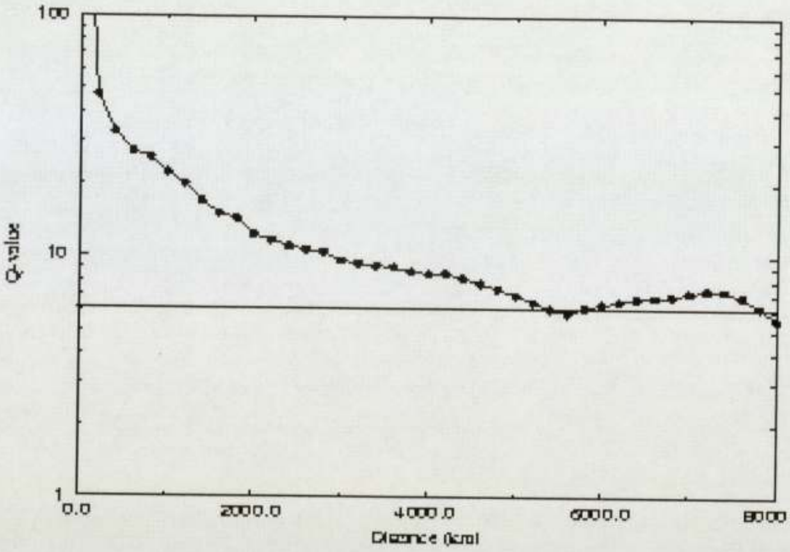

Figure 6.7: Q-value against distance for the system using the optimised pulses and system having optimised launch position.

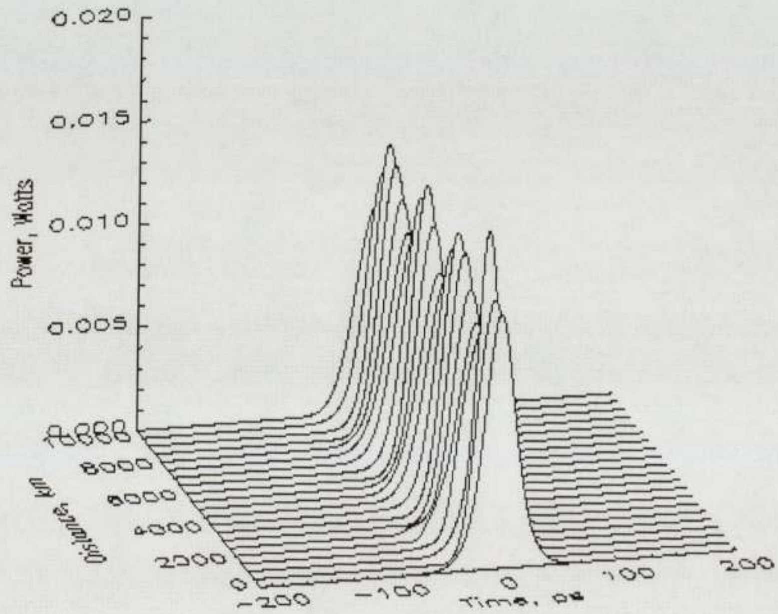

Figure 6.8: The pulse width evolution for the system shown in figure 6.1, the oscillations are considerably reduced.

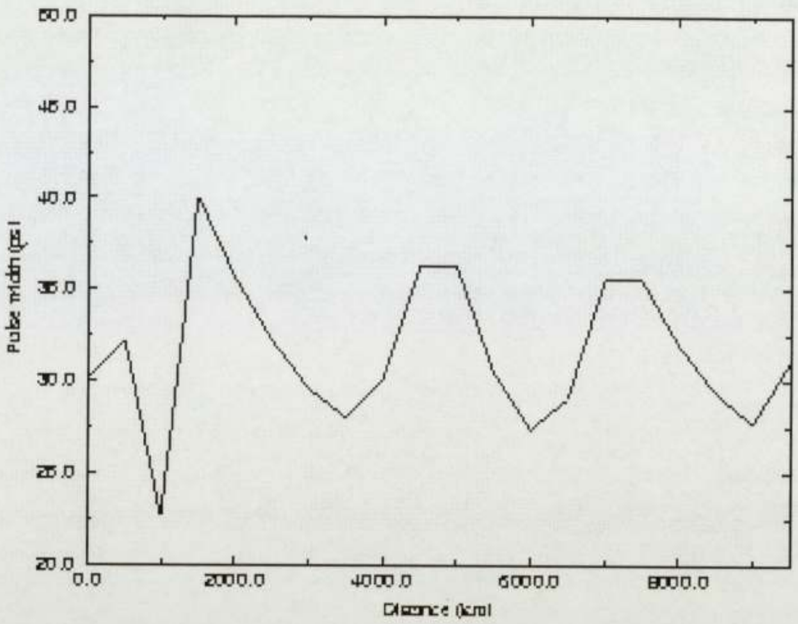

Figure 6.9: The pulse width against distance for system shown in figure 6.1.

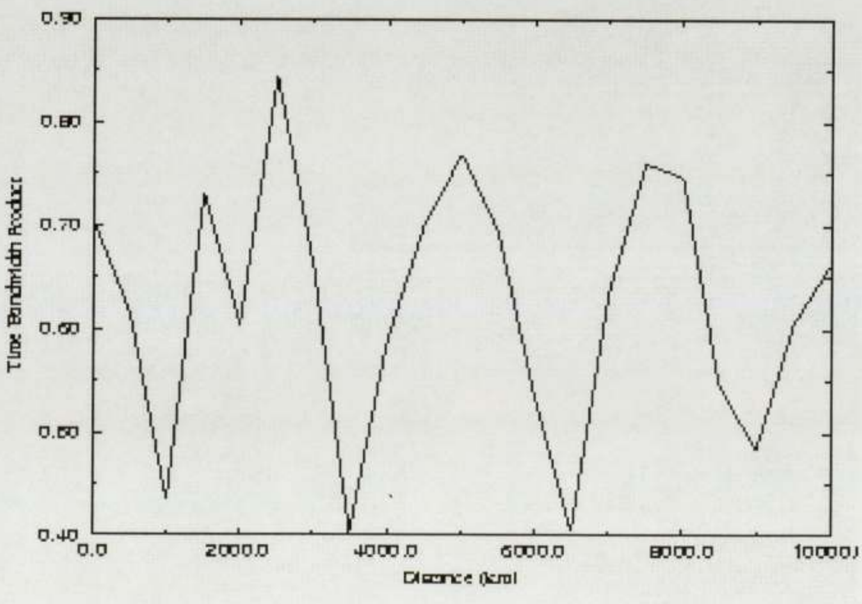

Figure 6.10: The time bandwidth product against distance for the map shown in figure 6.1.

The minimum in the pulse width relates to pulses with high peak powers and approximately coincides with the high Q-values. This can be seen as slight humps in the Q-values shown in figure 6.7. The maximum Qs are related to the minima in the time bandwidth product. The fluctuations in the pulse parameters such as chirp and width are due to the mismatch of the pulse shape with the dispersion map. The pulse under goes a long-term evolution as the pulse sheds dispersive radiations and all the parameters including pulse width, peak power, shape and chirp change. The chirp is highest at the start of the fibre and hence launching the chirped pulses at this point enhances this effect. The pulse is initially chirp free at the output point in the map, it soon accumulates complicated chirp. The points where the pulse width and Q are highest coincide with the points where chirp is at minimum.

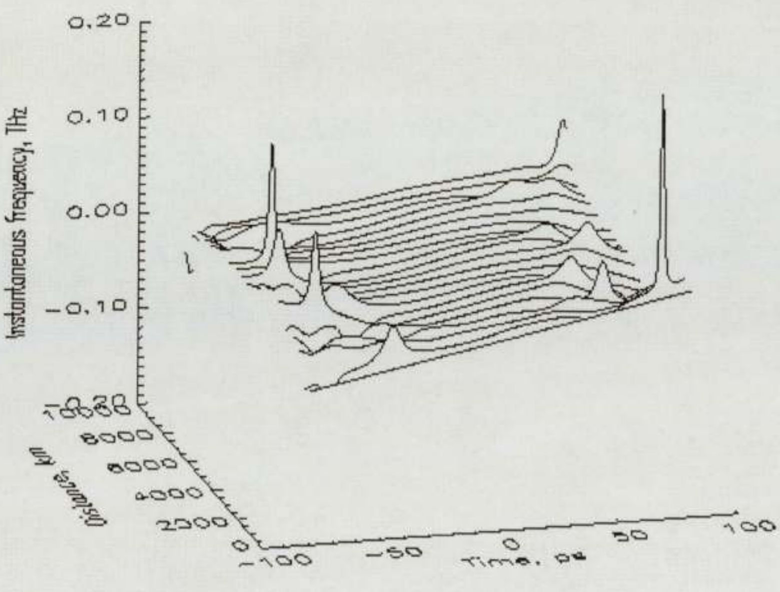

Figure 6.11: Instantaneous frequency for the system under consideration.

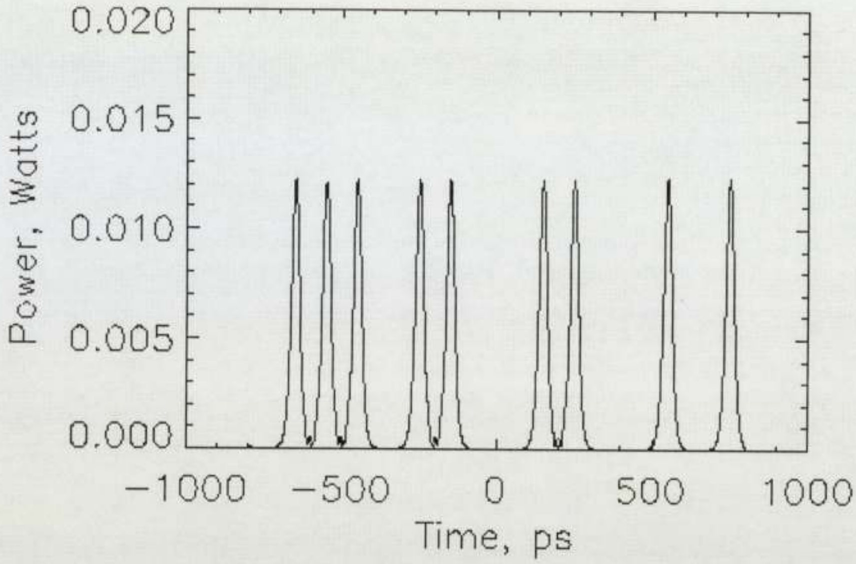

(a)

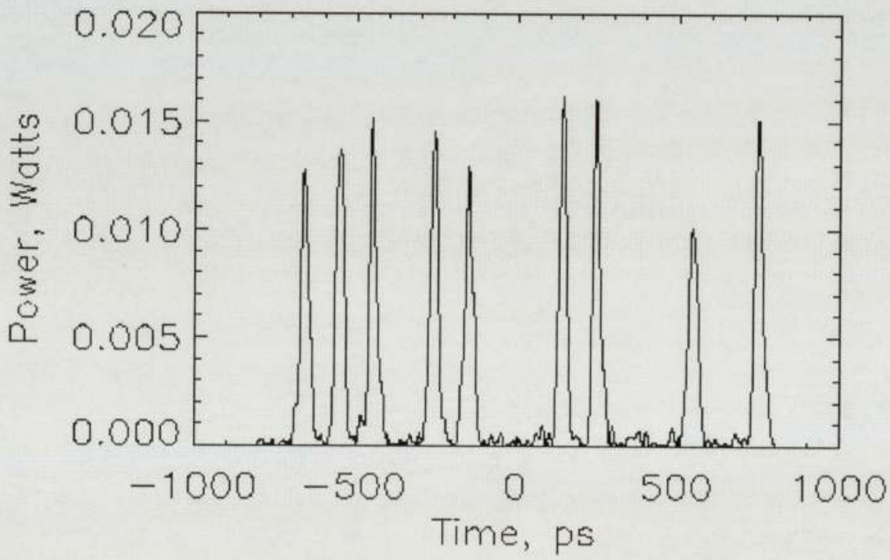

(b)

Figure 6.12: The top figure shows a section of a bit pattern at the start of the simulation. The lower picture shows the same bit pattern after it has propagated over 6000 km.

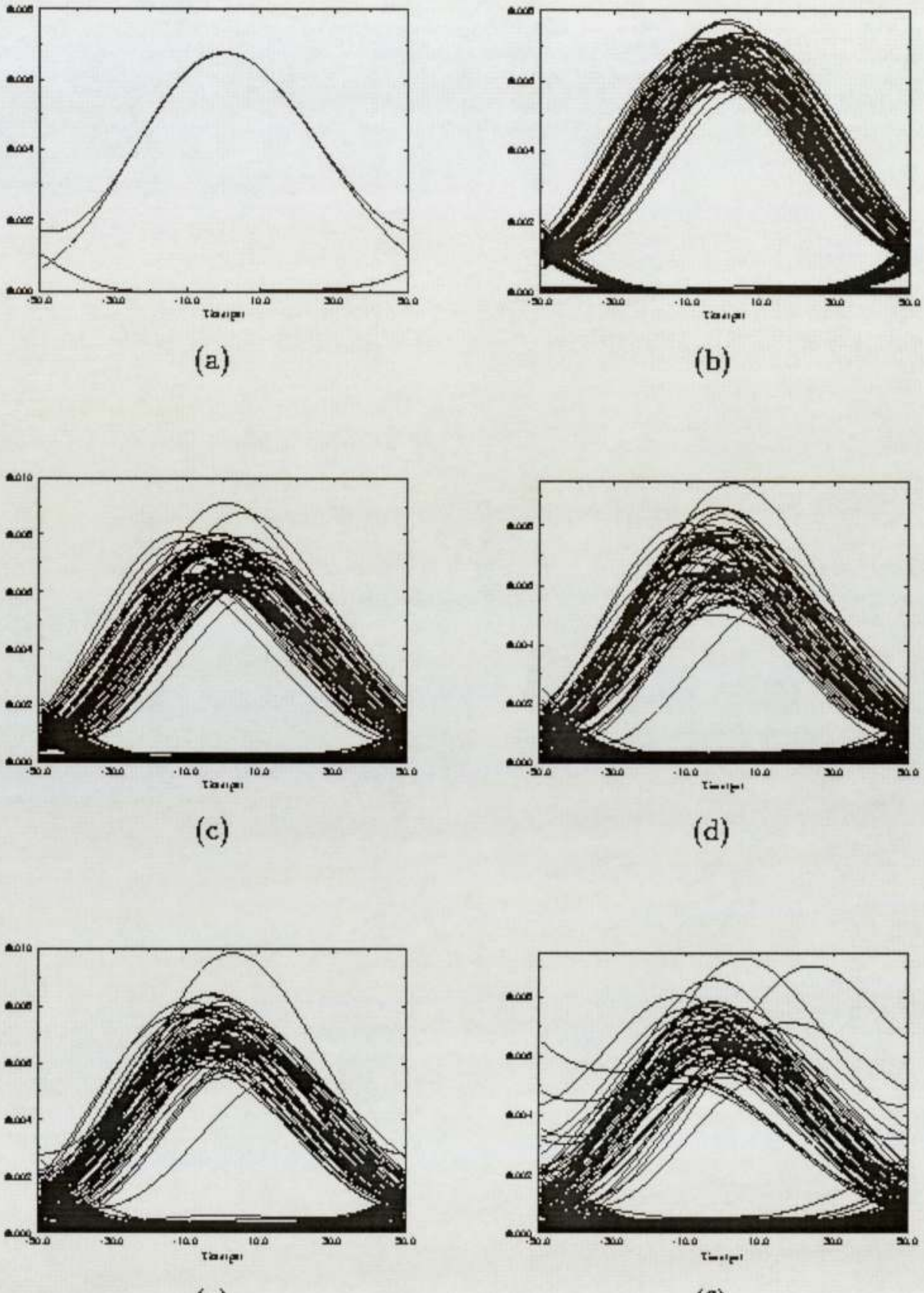

Figure 6.13: Simulation eye diagrams corresponding to figure 6.6, at distances (a) 0 km (b) 2000 km (c) 4000 km (c) 6000 km (d) 7000 km (e) 7800 km

The chirp of the pulse can be examined by looking at the instantaneous frequency of given in figure 6.11, it is clear that even though it is chirp free at the output point in the map, it soon accumulates a complicated chirp. The pulse width shown in figure 6.9 varies a lot during the course of each dispersion map due to the high local dispersion but at the end of the dispersion map it returns close to its original value.

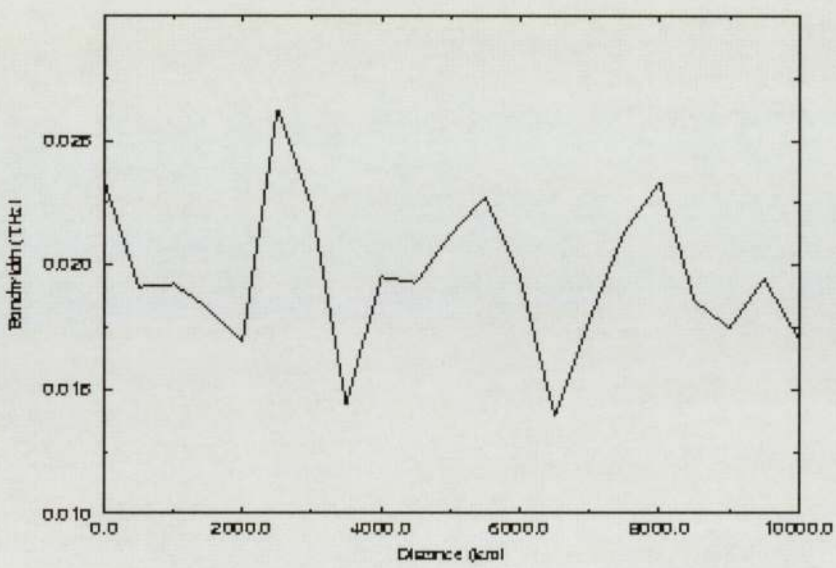

Figure 6.14: The bandwidth against distance for the map shown in figure 6.1.

By contrast bandwidth of the pulse as show in figure 6.14 reduces initially but recovers afterwards. Eventhough the bandwidth recover, on the whole it decreases. This recover does reduce the over all change in bandwidth, which in turns results in improvement in the performance of the system. The reduction in bandwidth is a critical factor, as it leads to long term changes in the pulse width, since the minimum pulse width is defined by the bandwidth of the pulse. This shows why systems with initially chirped pulses a better in contrast to the ones having unchirped input pulses where the bandwidth goes on decreasing due to the same sign of chirp.

Figure 6.13 show the simulation eye diagrams, and it can be clearly seen that even after 7800 km propagation the eye is open enough to give BER more than 10^{-9}.

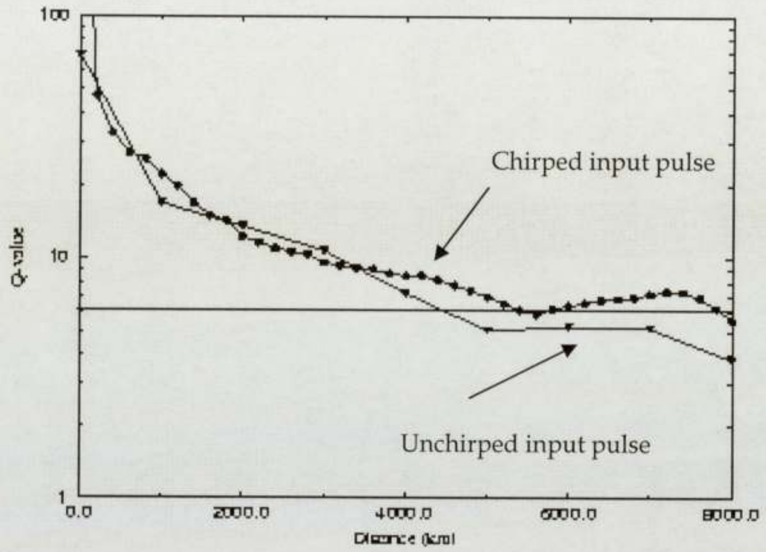

Figure: 6.15: Comparison of Q-value against distance for systems with chirped input pulses (dots) and system optimised by launching pulses (upside down triangles) at optimum position in the dispersion map.

Figure 6.15 shows comparison of Q-values for system with chirped input pulses (represented by dots) and system optimised by pulses launched at optimum launch position (represented by up side down triangles) in the dispersion map. A considerable improvement can be seen in the total propagation distance, which shows the robustness of the system.

6.4 Conclusions

In conclusions we have studied the behaviour of dispersion managed solitons in the deep dispersion mapped systems and have shown that by carefully choosing the input chirp (which found to be in this case 0.0015 THz) the overall system performance can be dramatically improved. Stable solutions are possible by alternative arrangement of the pre compensation and post compensation sections. With the increase in map strength [99], the pulse shape changes from secant hyperbolic to Gaussian.

Figure 6.13 shows the system performance improvement by using chirped input pulses, in terms of eye opening and temporal and amplitude jitter. It is clear from the Q-value plot in figure 6.15 that total propagation distance is increase from over 4000 km to over 7500 km. As found else where, whilst a traditional soliton system would require a mark to space ratio of 5 or 6, making 20 ps pulses the long pulse width limit, this constraint is reduced in dispersion managed systems and longer pulse widths (30 ps in this case) are possible.

The results presented in this chapter demonstrate that proper choice of chirped input pulses and peak power can improve the stability of dispersion managed soliton systems.

Chapter 7

40Gbit/s RZ transmission over standard fibre using grating for dispersion compensation

7.1 Introduction

Several experiments where transmission of data at 40 Gbit/s over distance greater than 1000 km in standard fibre have been performed already [105][106][107]. Due to the preliminary nature of these results, it is likely that the greater propagation distances could be obtained with parametric optimisation. The dispersion strength S is very large for these data rates, due to the short pulse widths, as compared to the one generally used [108]. It thus becomes very difficult to find optimal parameters in this regime to allow maximum transmission distance. In our optimisation we have limited our optimisation procedure to the variation of the signal power, pulse chirp and average dispersion within the dispersion map.

In the previous chapter the possibility of transmitting single channel data rates of 10Gbit/s over transoceanic distance, with chirped pulses was discussed. The next logical thing will be to investigate the propagation of soliton like RZ pulses at 40 Gbit/s. One of the main drives for this comes from the possibility to using such technique to upgrade the existing standard fibre network, even though we will be propagating the pulses to modest distances required for land bases communication. This chapter identifies the possibility of propagating soliton like pulses over distances more than 2000 km with single channel data rate of 40 Gbit/s. This distance was obtained using fibre grating for dispersion compensation and utilising a non symmetric dispersion map.

The number of experimental investigation of 40 Gbit/s transmission on standard fibre [105][107][109] has been very limited. Most of the work has been focused on maximising the performance at 10 Gbit/s. optical phase conjugation (OPC) and dispersion management are the two most successful techniques use for 40 Gbit/s transmission over standard fibre. Using OPC at the mid point of a transmission line, it has been possible to propagate over 434 km of standard fibre [109].

Increasing the data rate from 10 Gbit/s to 40 Gbit/s presents its own problems, most important of which is the increase in the map strength, which is caused by the necessary reduction in the pulsewidth. This increase map strength is well beyond the expected limit for stable soliton propagation. The map strength use in chapter is 172. The dispersion length for the system is short compared to the length of the fibre used. This is due to the short pulse width (5 ps) and high fibre dispersion (17 ps/(nm km)) that results in a dispersion length of ~ 0.3722 km. Due to this short dispersion length the pulse broadens substantially in the standard fibre. This in turn causes the pulse to exist only at chirp free points. This chirp free point moves throughout the standard fibre due to the relative high average anomalous dispersion, which leads to incorrect balance between the average dispersion and nonlinearity.

This chapter contains discussions relating to standard fibre propagation and the dispersion map used.

7.2 System Description

In this Chapter, we again consider the schematic shown in figure 7.1, as this is the mostly used scheme for upgrading the standard installed fibre [110]. The input pulse is 5 ps, sech shaped and are chirped. The reason for using chirped pulses is the nature of non-symmetric map, where either pulses have to be launched at optimum point or chirped input pluses must be used. As shown in the previous chapter that a considerable improvement can be gained by using chirped input pulses.

The standard fibre was taken to have typical value of dispersion of -21.6821 ps^2/km, a loss of 0.2 dB/km at 1.55μm wavelength and Aeff is 50 μm^2. Dispersion compensation is perform prior to each amplification. The fibre grating is simulated to have a length of 10 cm and a dispersion of 2.142×10^7 ps^2/km and a 3dB loss. The average dispersion can also be varied by varying the length of the standard fibre. The loss is chosen to allow double pass insertion loss of the circulator required, typically 0.8 dB port to port, and the loss of grating itself around 1-1.5 dB.

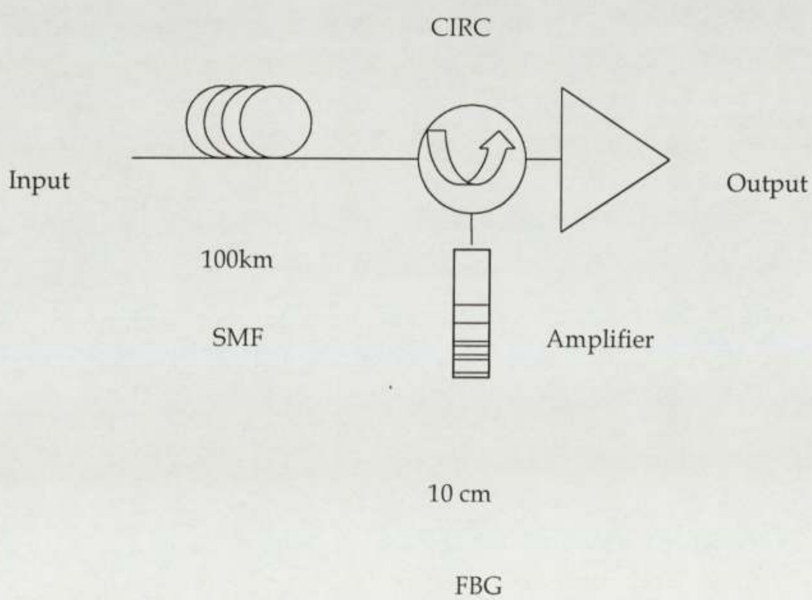

Figure 7.1: *Schematic diagram of the system under consideration*

Figure 7.1 shows the dispersion map used. The amplifier provides a gain of 23 dB, which compensates for the loss of fibre and grating and has a noise figure of 4.5 dB.

7.3 Optimisation Procedure

In order to find the best performance we kept the length of the standard fibre and the pulse width constant at 100 km and 5 ps respectively. By varying the signal peak power and the chirp of the input pulses we looked at the Q values at the output. The minimum acceptable value for the Q values was taken to be 6 (i.e., BER=10^{-9}). At the end of the optimisation the optimum chirp is found to be 0.007 s^{-1}. The optimum average dispersion is -0.002 ps^2/km, which is slightly anomalous. Figure 7.2 shows a single pulse with these parameters propagating through 3000 km of standard fibre in the dispersion map given in figure 7.1.

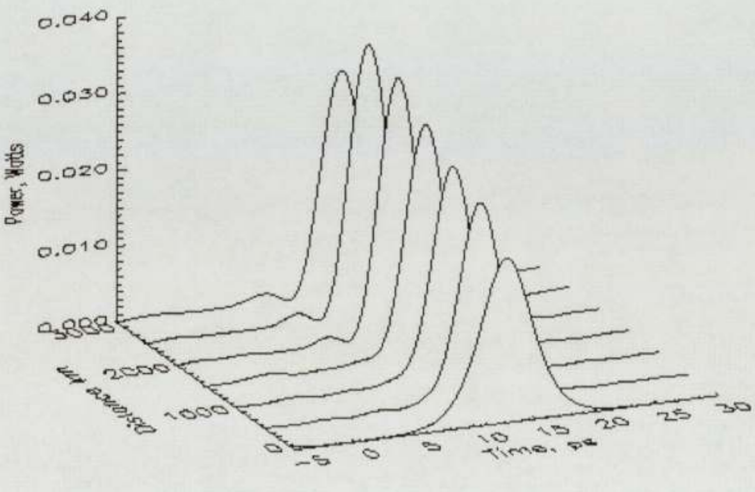

Figure 7.2: A single 5 ps pulse propagating through 3000 km of standard fibre in the dispersion map given in figure 7.1.

Figure 7.3 shows two of these optimised pulses propagating with a separation of 25 ps, making it equivalent to 40 Gbit/s over 3,000 km. These pulses don't undergo significant interaction even after several thousand of kilometres of propagation.

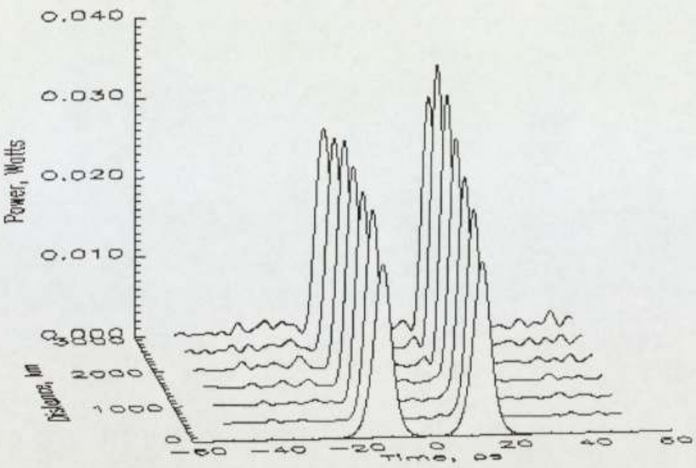

Figure 7.3: Two optimised pulses propagating over 3,000 km.

7.3.1 Result of Optimisation

These optimised pulses are now used in a direct simulation of standard fibre transmission. The system was simulated by propagating a random bit sequence of 128 data bits, half of which were data 1's, at 40 Gbit/s using split-step NLS method,

With the system under study as shown in figure 7.1. Amplified spontaneous emission (ASE) noise was included, with noise figure is 4.5 dB. The impact of amplifier noise is expected to be significant in such long amplifier spans. A filter of 0.04 THz bandwidth is used to filter out this noise. The receiver was simulated as a fast photodiode followed by an electronics filter with bandwidth of half the data rate to convert the return-to-zero (RZ) soliton data to non-return-to-zero (NRZ) format. It was then possible to estimate the bit error ratio (BER) from the received eye diagram through the Q parameter method [111]-[112] Where Q is given by equation 6.1 and BER is then estimated using equation 6.2.

For each BER computation, the 128 data bits were propagated in 8 sets of 16 bits for speed simulation, as it was found that the BER estimated was the same using this method or a single 128 bit propagation. We note that determination of the BER by this method is normally performed for a set of single, isolated pulses to avoid an under-estimate of the Q from patterning effects. However, in this work we expect strong soliton interactions, the nature of which will be pattern dependent, necessitating the inclusion of patterning in the BER estimate.

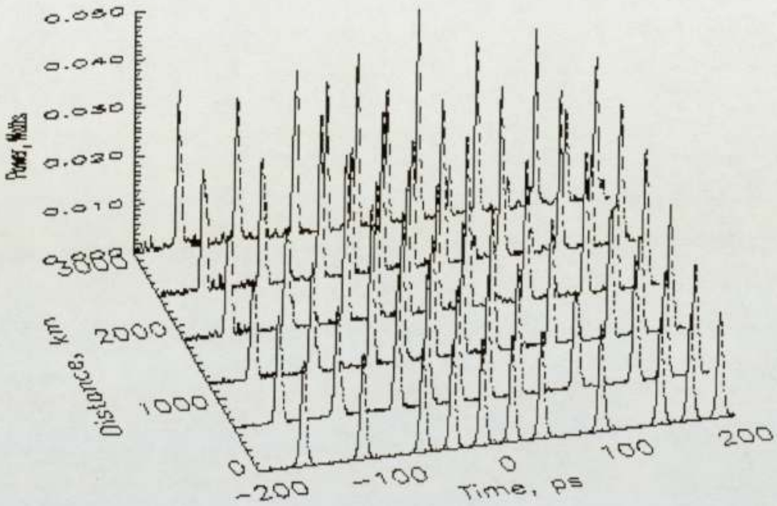

Figure 7.4: Simulation of 5 ps pulse train in a system compensated to -0.2 ps²/km, with data <0101011111010111>.

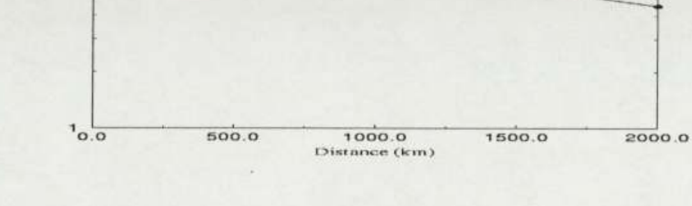

Figure 7.5: Q-value against distance for the system using the optimised pulses and system having optimised launch position.

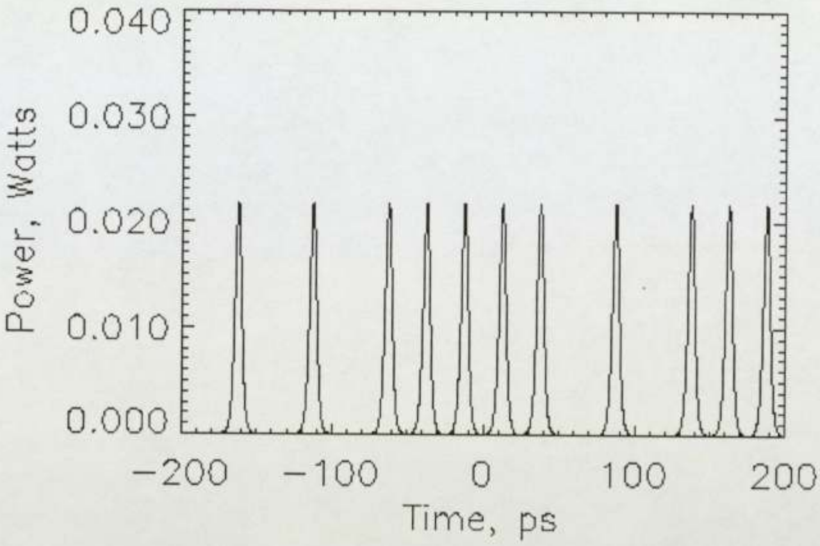

(a)

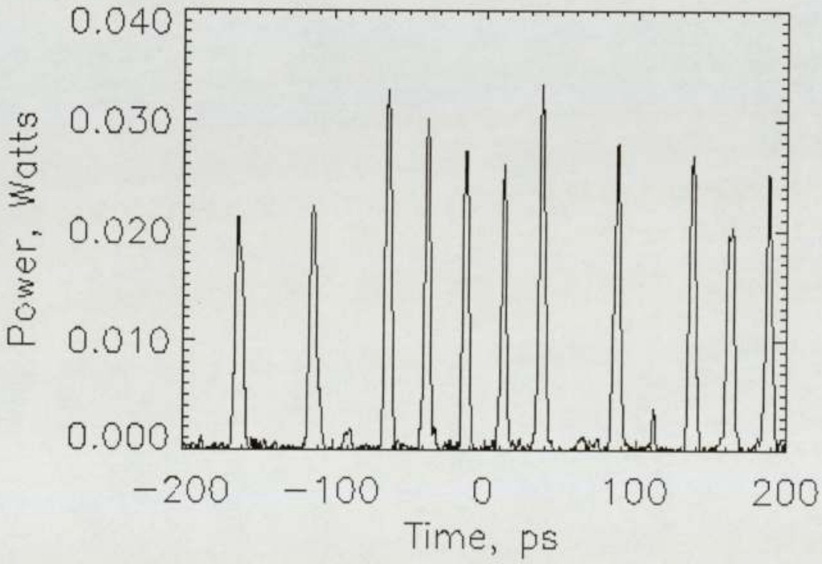

(b)

Figure 7.6: The top figure shows a section of a bit pattern at the start of the simulation. The lower picture shows the same bit pattern after it has propagated over 1500 km.

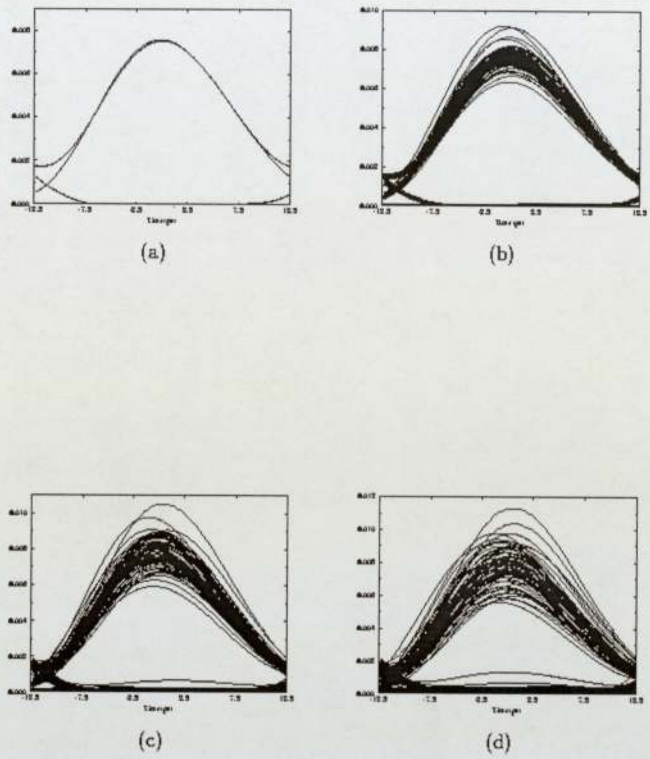

Figure 7.7: Simulation eye diagrams corresponding to figure 7.4, at distances (a) 0 km (b) 500 km (c) 1000 km (c) 1500 km

7.4 Conclusions

In conclusions we have studied the behaviour of dispersion managed solitons in standard fibre using fibre grating for dispersion compensation and have shown that by carefully choosing the input chirp (which found to be in this case 0.007 THz) the overall system performance can be dramatically improved. Stable solutions are possible by alternative arrangement of the pre compensation and post compensation sections. With the increase in map strength, the pulse shape changes from secant hyperbolic to Gaussian [50].

The results presented in this chapter demonstrate that proper choice of chirped input pulses and peak power can improve the stability of dispersion managed soliton systems.

Chapter 8

Conclusions

8.1 Thesis Conclusion

This thesis investigated various aspects of dispersion managed solitons for a single channel high bit rate system over longer distances. Initially an introduction to optical fibre and its properties was explained which was followed by a discussion on propagation in optical fibres (chapter 2). Propagation in optical fibre was explained with and without loss, followed by discussion on soliton system design features (chapter 3). After discussing dispersion managed solitons in chapter 4 a real system was introduced in chapter 5. Short-haul systems were considered, two of the constraints, the Gordon-Haus jitter and the required signal-to-noise ratio were unimportant, as neither had sufficient degree. The soliton interaction and average soliton constraints were however taken into account and balanced to give a stable propagation. The average power requirements were considered due to the high dispersions of these systems.

It was assumed that EDFAs could provide the optical powers and gain necessary for soliton propagation, with amplifier output power in the range of 5-15 mW.

The optimised pulses were used in a direct simulation of standard fibre transmission. The system was simulated by propagating a random bit sequence of 144 data bits, half of which were data 1's, at 10 Gbit/s using split-step NLS method, with the system discussed in chapter 6. Amplified spontaneous emission (ASE) noise was included, with noise figure is 4.5 dB. The impact of amplifier noise was expected to be significant in such long amplifier spans. A filter of 0.0325 THz bandwidth is used to filter out this noise. The receiver was simulated as a fast photodiode followed by an electronics filter with bandwidth of half the data rate to convert the return-to-zero (RZ) soliton data to non-return-to-zero (NRZ) format.

In chapter 5 we studied the behaviour of dispersion managed solitons using fibre grating for dispersion compensation at 10 Gbit/sec and optimising the position of grating in the dispersion map. We have shown that by carefully choosing the position of grating in the map the overall system performance can be dramatically improved. The optimum launch position of soliton for chirp free pulses is 90 km before the grating and energy enhancement is reduced by inclusion of loss in the systems. Stable solutions are possible by alternative arrangement of the pre compensation and post compensation sections.

In chapter 6 we studied the behaviour of dispersion managed solitons in the deep dispersion mapped systems at 10 Gbit/sec and showed that by carefully choosing the input chirp (which found to be in this case 0.0015 THz) the overall system performance can be dramatically improved. Stable solutions were possible by alternative arrangement of the pre compensation and post compensation sections. With the increase in map strength, the pulse shape changes from secant hyperbolic to Gaussian.

In chapter 7, we studied the behaviour of dispersion managed solitons in standard fibre using fibre grating for dispersion compensation at 40 Gbit/sec and have shown that by carefully choosing the input chirp (which found to be in this case 0.007 THz) the overall system performance can be dramatically improved. Stable solutions are possible by alternative arrangement of the pre compensation and post compensation sections. With the increase in map strength, the pulse shape changes from secant hyperbolic to Gaussian.

The results presented chapter 7 demonstrates that proper choice of chirped input pulses and peak power can improve the stability of dispersion managed soliton systems.

8.2 Future Work

We have looked at a few aspects of dispersion managed solitons there are however many still to be investigated. In this thesis a very simple grating was simulated, it will be interesting to add other parameters effecting the grating such as PMD and third order dispersion etc and investigate the effect on system performance. Further investigation into the position of amplifier and grating in the dispersion map is needed to understand the effect on the propagation distance and amplifier spacing. At present amplifier and grating are placed at the same point, investigation into the reasons for this might allow larger propagation distances. It would be interesting to look at using fibre grating in WDM systems.

Secondly in order to control the polarisation-mode dispersion (PMD,) it will be interesting to use saturable absorbers. It has been shown that saturable absorbers provide stabilising effect where stable pulse propagation is not possible. It should be noted that saturable absorbers can be more useful in stabilising propagation, rather than extending the propagation distance.

Further investigation into optimising the chirp will be quite useful, as we have shown that right choice of chirp in the input pulses considerably increases the propagation distance at high data rates.

8.3 Future of Optical Communication

The data rates of optical systems have increased in recent years through the use of both OTDM to increase the single channel data rate and WDM to increase the number of channels used. Single channel bit rates of 400Gbit/sec have been reported [113] using these techniques. Over Trans-oceanic distances 32, 5 Gbit/sec channels have been propagated [114] and experimental demonstrations of terabit/sec transmission have also been reported using a combination of these techniques [115, 116, 117]. Comparing these data rates with the single channel 5 Gbit/sec rate of Trans- Atlantic TAT12/13 systems, it can be easily seen that it is still possible to increase system data rates substantially. The advantages of WDM systems are that they allow single channels to be added and dropped [118] leaving the other channels unaltered. This finds its application in systems where several nodes need to be connected together and each pair of nodes can be given a particular wavelength. Nothing comes with a price, hence WDM systems do suffer from complication in design due to increased number of components involved, specially for long haul point to point systems. In dispersion managed systems WDM present slightly different kind of problem, where only a single channel can be optimally compensated, where as the other will suffer some penalty which can only be partially reduced by post transmission dispersion compensation. Finally all the channels will not be equally amplified at each EDFA due to the gain profile of the amplifier. This effect can be reduced by using gain flattened EDFA's [119], and the unequal gain can be compensated for by pre-emphasis or gain equalisation [120].

The possibility of soliton being used in the commercial communication systems is increased due to use of dispersion compensation. Several successful fields trials have shown that the dispersion managed solitons can be successfully operated in the already installed systems not designed for their use [121, 122, 123, 124, 125].

A study of limitations to error-free transmission distance as set by noise accumulation and nonlinear pulse interactions in dispersion-managed N40 Gbit / s transmission systems with either distributed backward Raman amplification or lumped erbium-doped fibre amplifiers [126] have shown significant performance improvement.

It has been shown through detailed numerical simulations that stable dispersion-managed solitons exist in short-period dispersion maps characterised by a dispersion-management period that is less than the amplifier spacing [127]. These pulses are shown to have regular dynamics within the amplifier span and have greater energy enhancement than the conventional dispersion-managed soliton, which results in greater interaction. Other numerical simulations have recently demonstrated N x 40Gbit/s single channel transmission over thousands of kilometres [128, 129, 130].

The possibility of achieving all optical passive regeneration and distance unlimited transmission, have also been numerically demonstrated using dispersion management and inline nonlinear loop mirrors over standard fibre [131].

Several experiments have recently demonstrated transmission of several hundred Gbit/s using WDM over modest distances [132, 133, 134, 135, 136, 137].

Dispersion management has found very beneficial in WDM systems in terms of suppressing the collision induced timing jitter between the wavelength channels. Thus while considering high data rates in WDM systems, effects of nonlinearity must be considered when operating at hundreds of Gbit/s data rates, which can be achieved using dispersion managed solitons. At higher data rates the strength of the dispersion maps are likely to increase, which will lead to necessary use of further control to get stable propagation. Dispersion managed solitons are currently the most successful method of transmitting data over standard fibre at high data rates.

The effect of PMD in fibres have been investigated numerically and soliton robustness to PMD has been shown to have strong dependence on both chromatic dispersion and soliton energy [138].

References

1 G. P. Agrawal. 'Non-linear fibre optics.', Academic Press Inc., 1989

2 H. Izadpanah, C. Lin, J. L. Gimlett, A. J. Antos, D. ~T. Hall, and D. K.Smith. 'Dispersion compensation in 1310 nm-optimised SMFs using optical equaliser fibre, EFDAs and 1310/15,50 nm WDM.', Electron.Lett.28(1a) pp.1469-1471, 1992.

3 M. Kakui, T. hato, T. Kashiwada, K. Nakazoto, C. Fukuda, I. Onishi, and I. Nishimura. '2.1 Gbit/s repeaterless transmission over 30km non-dispersion shifted fibre using directly modulated DFB-LD and dispersion compensating fibre.', Electron. Lett. 31(1)1995 pp.51-52

4 K. Sekine, S. Sasaki, and N. Kikuchi, '10 Gbit/s four-channel wavelength and polarisation-division multiplexing transmission over 340km with 0.5nm channel spacing.', Electron. Lett. . 31 (1) pp.49-50. 1995

5 S. G. Evangelides, L. F. Mollenauer. J. P. Gordon, and N. S. Bergallo, 'Polarisation multiplexing with solitons.', *IEEE J. Lightwave Technol. 10, 1992, pp.28-35*

6 C. D. Chen, J. M. P. Delavaux, B. W. Hakki, O. Mizuhara, T. V. Nguyen, R. J. Nuyts, K. Ogawa, Y. K. Park, R. E. Tench, L. D. Tzeng, and P. D. Yeates, 'Field experiment of 10 Gbit/s, 360 km transmission through embedded standard non-DSF fibre cables.', *Electron. Lett.*, **30 (14)**, 1994, pp.1159-1160

7 T. Widdowson, and D. J. Malyon. 'Error ratio measurements over transoceanic distances using recirculating loop', *Electron. Lett.*, **27 (24)**, 1991, pp.2201-2202

8 T. Morioka, S. Kawanishi, H. Takara, and O. Kamatani, 'Penalty-free, 100 Gbit/s optical transmission of < 2 ps supercontinuum transform-limited pulses over 40 km.', *Electron. Lett.*, **31 (2)**, 1995 pp.124-125

9 H.Bülow, 'Operation of digital optical transmission svstem with minimal degradation due to polariztion mode dispersion.', *Electron. Lett.*, **31 (3)**, 1995 pp.214-215

10 D. J. Malyon, T. Widdowson, and A. Lord, 'Assesment of polarization loss dependece of transoceanic systems using a recirculating loop.', *Electron. Lett.*, **29 (2)**, 1993 pp.207-209

11 F. Bruyere, and O. Audouin, 'Penalties in long-haul optical amplifier systems due to polarisation dependent loss and gain.', IEEE Photon. Technol. Lett.,1994, 6 (5):651-656. 1994

12 V. J. Mazurczyk, and J. L. Zyskind, 'Polarization dependence gain in erbium dopped fibre amplifiers.', IEEE Photon. Technol. Lett., 1994, 6 (5):616-618. 1994

13 T. Widdowson, A. Lord, and D. J. Malyon, 'Polaristion guiding in ultralong distance soliton transmission.', *Electron. Lett.,* **30 (11)**, 1994 pp.879-880

14 L. F. Mollenauer. K. Smith, and J. P. Gordon, 'Resisiteance of solitons to the effects of polarisation dispersion in optical fibres.', *Opt. Lett. 14 (21), 1989, pp.1218-1221*

15 L. F. Mollenauer. and J. P. Gordon, 'Birefringence-mediated timing jitter in soliton transmission.', *Opt. Lett. 19 (6), 1994, pp.375-377*

16 C. S. Gardner, J. M. Green, M. D. Kruskal, and R. M. Miura, Phys. Rev. Lett., 19 , 1967, pp.1095

17 V. E. Zakarov and A. B. Sabat, Sov. Phys. JETP, 34, 1972, pp.62

18 C. Desem, P. L. Chu, 'Effect of chirping on solution propagation in single mode fibres.' Opt. Lett., 11 (94), 1986, pp.248-251

19 D. Anderson, M. Lisak, and T. Relchel, 'Asymptotic propagation properties of pulses in a soliton based optical fibre communication system.', J. optical Society of America, B, 5 (2), 1988, pp.207-210

20 K. J. Blow, N. J. Doran, and D. Wood, ' Generation and stabilisation of short soliton pulses in the amplified nonlinear Schrödinger equation.' , J. optical Society of America, B, 5 (2), 1988, pp.381-391

21 S. V. Chernikov, J. R. Taytlor, and R. Kashap, 'Experimental demonstration of step like dispersion profiling in optical fibres for soliton pulse generation.' Electron. Lett., 30 (5), 1994, pp.433-435

22 H. Kubota and M,. Nakazawa, 'Long distance optical soliton transmission with Lumped Amplifiers.' IEEE J. Quantum Electron., 26, 1990, pp.692-700

23 A. Hasegawa, Y. Kodama, 'Guiding-centre soliton in optical fibres.' Opt. Lett., 15 (24), 1990, pp.1443-1445

24 A. Hasegawa, Y. Kodama, 'Guiding-centre soliton.' Phy. Rev. Lett., 66, 1991, pp.161-164

25 N. J. Smith, K. J. Blow, and I. Andonovic; 'Sideband generation through perturbation to the average soliton model.' IEEE J. Lightwave Technol., 10 , 1992, pp.1329-1333

26 K. J. Blow, and N. J. Doran, 'Average soliton dynamics and the operation of soliton systems with lumped amplifiers.' Electron. Lett., 30 (5), 1994, 433-435

27 A. F. Mitchell, J. V. Wright, S. F. Carter, A.D. Ellis, A. Lord, J. Lyle, and J. M. Scott, 'The future of optically amplified submarine systems.' Tech. Digest of 2nd Intern. Conf. on Optical Fibre Submarine Telecommun. Systems., Versailles, France, 1993, pp:49-54

28 J. P. Gordon, 'Interaction forces among solitons in optical fibres. ', Opt. Lett., 8 (11), 1983, pp:596-598

29 Y. Kodama and K. Nozaki, 'Soliton interactions in optical fibres.' Opt. Lett., 12 (12), 1987, pp:1038:1040

30 F. M. Mitschke, and L. F. Mollenauer, 'Experimental observation of interaction forces between solitons in optical fibres.' Opt. Lett., 12 (5), 1987, pp.355-357

31 R. P. Davey, N. Langford, and A. Ferguson, 'Interacting solitons in erbium fibre laser.' Electron. Lett., 27 (14), 1991, pp.1257-1259

32 T. Georges and F. Favre, 'Influence of soliton interaction on amplifier noise induced jitter: a first order analytic solution.' Opt. Lett., 16 (21), 1991, pp.1656-1658

33 M. Nakazawa, K. Suzuki, E. Yadama, and H. Kubota, ' Observations of non-linear interactions in 20 Gbit/s soliton transmission over 500 km using erbium doped fibre amplifiers.' Elect. Lett., 27 (18), 1991, pp.1662-1663

34 A. B. Aceves, C. D. Angelis, G. Nalesso, and M. Santagiustina, 'Higher-order effects in bandwidth limited soliton propagation in optical fibres.' Opt. Lett., 19 (24), 1994, pp. 2104-2106

35 W. H. Loh, A. B. Grudinin, V. V. Afansjev and D. N. Payne, 'Soliton interaction in the presence of a weak non soliton component.' Opt. Lett., 19 (10), 1994, pp.698-700

36 Y. Kodama, and S. Wabnitz 'Reduction of soliton interaction forces by bandwidth limited amplification. ' , Electron. Lett., 27 (21), 1991, pp.1931-1932

37 T. Georges, and F. Favre, 'Modulation, filtering and initial phase control of interacting solitons.', J. Optical Society of America, B., 10 (10), 1993, pp.1880-1889

38 P. L Francois and T. Georges, 'Reduction of averaged soliton interaction forces by amplitude modulation.', Opt. Lett., 18 (8), 1993, pp.583-585

39 C. Desem, and P. L. Chu, 'Optical solitons: theory and experiment.chapter soliton-soliton interaction.', Press syndicate of university of Cambridge., 1992, pp.107-151

40 P. A. Andrekson, N. A. Olsson, J. R. Simpson, T. Tanbun-Ek, A. Logan, and K. W. Wecht, 'Observation of collision induced temporary soliton carrier frequency shift in ultra long fibre transmission system.', IEEE J. Lightwave Technol.., 9 (9), 1991, pp.1132-1135

41 S. Chakrawarty, M. J.Abloitz, J. R. Sauer, and R. B. Jenkins, 'Multi-soliton interaction and wavelength division multiplexing.', Opt. Lett., 20 (2), 1995, pp.136-138

42 A. Mattheus, and S. Turitsyn, 'Pulse interaction in nonlinear communication systems based on standard mono-mode fibres.', Proceedings of 19th European conference on optical communications., 2 Paper MoC2.3, 1993, pp.37-40

43 M. Suzuki, N. Edagawa, H. Taga, M. H. Tanaka, S. Yamamoto, and S. Akiba, '10 Gbit/s over 12200 km soliton data transmission with alternating amplitude solitons.', IEEE Photon. Technol. Lett., 6 (6), 1994, pp.7557-7559

44 M. Nakazawa, E. Yoshida, E, Yadama, K. Suzuki, KT. Kitoh, and M. Kawachi, '80 Gbit/s soliton data transmission over 500 km with unequal amplitude solitons for timing clock extraction.', Electron. Lett., 30 (21), 1994, pp.1777-1778

45 K. Suzuki, N. Edagawa, H. Taga, M. H. Takaya, S. Yamamoto, and S. Akiba, 'Feasibility demonstration of 20 Gbit/s single channel soliton transmission over 11500 km using alternating amplitude soliton.', Electron. Lett., 30 (13), 1994, pp.1083-1084

46 J. P. Gordon, and H. A. Haus, 'Random walk of coherently amplified soliton in optical fibre transmission.', Opt. Lett., 11, 1986, pp.665-667

47 D. Marcuse, 'An alternative derivation of Gordon-Haus effect.', IEEE J. Lightwave Technol. , 10, 1992, pp.273-278

48 A. Hasegawa and Y. Kodama, 'Soliton in optical communications.', Clarendon press Oxford., 30 (13), 1995

49 C. Curtzki, 'Suppression of fibre nonlinearities by appropriate dispersion management.', *IEEE Photon. Tech. Lett.*, **5**, (10), 1993, pp: 1250-1253

50 N. J. Smith, F. M. Knox, N. J. Doran, K. J. Blow, and I. Bennion, Enhanced power solitons in optical fibres with periodic dispersion management.', *IEEE Photon. Tech. Lett.*, **32**, (1), 1996, pp: 54-55

51 M. Nakazawa, H. Kubota, A. Sahara, and K. Tamura 'Marked increase in the power margin through the use of disopersion allocated soliton.', *IEEE Photon. Tech. Lett.*, **8**, (8), 1996, pp: 1088-1090

52 J. H. B. Nijhof, N. J. Doran, W. Forysiak, and D. Bernston, 'Energy enhancement of dispersion-managed solitons WDM.', *Electron.. Lett.*, **34**, (5), 1998, pp: 481-482

53 T. Georges, 'Extended path average soliton regime in highly dispersive fibres.', *Opt. Lett.*, **22**, (10), 1997, pp: 679-681

54 A. Berntson, D. Anderson, N. J. Doran, W. Forysiak and J. H. B. Nijhof, 'Power dependence and accesible bandwidth for dispersion managed solitons in asymetric dispersion maps.', *Electron.. Lett.*, **34**, (21), 1998, pp: 2054-2056

55 M. Suzuki, I. Morita, N. Edagawa, S. Yamamoto, H. Taga, and S. Akiba, 'Reduction in Gordon-Haus timing jitter by periodic dispersion compensation in soliton transmission.', *Electron.. Lett.*, **31**, (23), 1995, pp: 2027-2029

56 G. M. Carter, J. B. Jacob, C. R. Menyuk, E. A. Golovchenko, and A. N. Pilipetskii, 'Timing jitter reduction for a dispersion managed soliton system: experimental evidence.', *Opt.. Lett.*, **22**, (8), 1997, pp: 513-515

57 S. Kumar, and F. Lederer, 'Gordon-Haus effect in dispersion manged soliton systems.', *Opt. Lett.*, **22**, (24), 1997, pp: 1870-1872

58 J. N. Kutz, and P. K. A. Wai, 'Ideal amplifier spacing for reduction of gordon-Haus jitter in dispersion manged soliton communications.', *Electron. Lett.*, **34**, (6), 1998, pp: 522-523

59 R. M. Mu, V. S. Grigoryan, C. R. Menuk, E. A. Golovchenko and A. N. Pilipetskii, 'Timing jitter reduction in a dispersion managed soliton system .', *Opt. Lett.*, **34**, (21), 1998, pp: 930-932

60 J. H. B. Nijhof, N. J. Doran, W. Forysiak, and F. M. Knox, 'Stable soliton-like propagation in dispersion managed systems with net anomalous, zero and normal dispersion.', *Electron.. Lett.*, **33**, (20), 1997, pp: 1726-1727

61 J. H. B. Nijhof, W. Forysiak , and N. J. Doran, 'Dispersion managed solitons in normal dispersion regime.', *Opt.. Lett.*, **23**, (21), 1998, pp: 1674-1676

62 J. N. Kutz, and S. G. Evangelides 'Dispersion managed breathers with average normal dispersion .', *Opt. Lett.*, **23**, (9), 1998, pp: 635-637

63 S. K. Turitsyn, E. G. Shapiro, 'Dispersion mamged solitons in optical amplifier transmission systems with zero average dispersion.', *Opt. Lett.*, **23**, (9), 1998, pp: 682-684

64 W. Forysiak, F. M. Knox and N. J. Doran 'Stepwise dispersion profiling of periodically amplified soliton systems.', *IEEE J. Lightwave. Technol. Lett.*, **12**, 1994, pp: 1330-1337

65 D. J. Richardson, R. P. Chamberlain, L. Dong, and D. N. Payne, 'High quality soliton loss-compemsation in 38km dispersion decreasing fibre.', *Electron. Lett.*, **31**, 1995, pp: 1681-1682

66 D. J. Richardson, L. Dong, R. P. Chamberlain, A. D. Ellis, T. Widdowson, and W. A. Pender, 'Periodically amplified system based on loss compensating dispersiom deceasing fibre.', *Electron. Lett.*, **34**, (4), 1996, pp: 373-374

67 W. Forysiak, K. J. Blow, and N. J. Doran 'Reduction in Gordon-Haus jitter by post-transmission dispersion compensation.', *Electron. Lett.*, **29**, 1993, pp: 1225-1226

68 J. P. Gordon, and L. F. Mollenauer, 'Scheme for the chracterization of dispersion managed solitons.', *Opt. Lett.*, **24**, (4) 1999, pp: 223-225

69 G. M. Carter, and J. M. Jacob 'Dynamics of Solitons in Filtered Dispersion Managed Systems.', *IEE Photon. Technol. Lett.*, **10**, (4) 1998, pp: 546-548

70 V. S. Grigoryan, T. Yu, A. Golovchenko, C. R. Menyuk and A. N. Pilipetskii, 'Dispersion/Managed Soliton Dynamics.', *Opt. Lett.*, **22**, 21,1997, pp: 1609-1611.

71 I. Gabitov and S. K. Turitsyn 'Breathing Solitons in Optical Fibre Links'.

.' JETP 63 (10) 1996 :pp 861-866.

72 S. K. Turitsyn, T. Schafer, and V. K. Mezentsev 'Self-Similar Core and Oscillatory Tails of a Path-Averageed Chirped Dispersion-Managed Optical Pulse'. .'OPT-Letters 23 *(17) 1998 :pp 1351-1353.*

73 A. Berntson, N, J, Doran, W. Forysiak and J. H , B Nijhof ' Power Dependance of Dispersion Managed Soliton for Anomulas,0 and Normal Path- Average Dispersion' , OPT-Letters,: 23 *(12) 1998 :pp 900-902.*

74 F. Favre, D. Le. Guen and T. Georges 'Experimental Evidance of Pseudo-Periodical Soliton Propagation In Dispersion Managed Link.' ,Electronic-Letters,: 34 *(19) 1998 :pp1868-1869.*

75 M. Suzuki, I. Morita, S. Yamamoto, N. Edagawa, H. Taga, and S. Akiba.

Timing jitter reduction by periodic dispersion compensation in soliton transmission. Electron. Lett., 23(7):2189-2197, 1995.

76 N. J. Smith, N. J. Doran, F. M. Knox, and W. Forysiak. Opt. Lett.,21:1996, 1981.

77 C. Das, U. Gaubatz, E. Gottwald, K. Kotten, L. Rapp, C. J. Weiske, B. Hein, F. Kuppers, and A. Mathews, 'Straightforward upgrading of transmission system to 4*10Gbit/s through 617 km and 8*10Gbit/s through 412 km of SMF.', *Electron. Lett.*, **31**, 1995, pp.1374-1375

78 N. J. Smith, F. M. Knox, N. J. Doran, K. J. Blow, and I. Bennion.

Enhanced power solitons in optical fibers with periodic dispersion management. Electron. Lett., 32:54-55, 1996.

79 A. Mattheus, and S. Turitsyn, 'Pulse interaction in nonlinear communication systems based on standard mono-mode fibres.', Proceedings of 19th European conference on optical communications., 2 Paper MoC2.3, 1993, pp.37-40

80 N. A. Olson, 'Lightwave systems with optical amplifiers', *IEEE J. Lightwave Technol.*, **7**, (7), 1989, pp.1071-1082

81 D. Marcuse, 'Calculation of bit error probability for a Lightwave system with optical amplifiers and post deduction Gaussian noise', , *IEEE J. Lightwave Technol.*, **9**, (4), 1991, pp.505-513

82 T. Georges, and B. Charbonnier, 'Reduction of the dispersive wave in periodically amplified links with initially chirped solitons', *IEEE Photon. Tech. Lett.*, **9**, (127), 1997

83 I. Gabitove and S. K. Turitsyn, 'Average pulse dynamics in cascaded transmission systems with a passive dispersion compensation.', *Optic. Lett., 21, 327,*

84 F. Matera, and M. settembre, '10 Gbit/s optically amplified single channel systems operating in links encompasing conventional step index fibres.', *optical Quantum Electron.*, **29**, 1997, pp.21-34

85 E. Yamada, H. Kubota, T. Yamamoto, A. Shara, sand M. Nakazawa, ''10 Gbit/s 10600 km, dispersion-allocated soliton transmission using conventional 1.3 μm singlemode fibres', *Electron. Lett.*, **33** **(7)** 1997, pp.602-603

86 P. A. Kurg, T. Stephens, G. Yoffe, F. Ouellete, P. Hill, and G. Dhosi, 'Dispersion comensation over 270 km at 10Gbit/s using an offset-sore chirped fibre Bragg grating.' , *Electron. Lett.*, **31** **(13)** 1995, pp.1091-1093

87 W. H. Loh, R. I. Lamming, A.D. Ellis, and D. Atkinson, '10Gb/s transmission over 700 km of standard single-mode fibre with 10-cm chirped fibre bragg grating compensator and duobinary transmitter.' , *IEEE Photon. Tech. Lett.*, **8**, (9) , 1996, pp.1258-1260

88 B. J. Eggleton, T. Stephens, P. A. Kurg, G. Dhosi, Z. Rodzeli, and F. Ouellete 'Dispersion comensation using a fibre grating in transmission.' , *Electron. Lett.*, **32** **(17)** 1996, pp.1610-1611

89 J. A. R. Williams, I. Bennion, K. Sugden, and N. J. Doran, 'Fibre dispersion compensation using a chirped infibre grating.', , *Electron. Lett.*, **30** **(12)** 1994, pp.985-987

90 J. A. R. Williams, L. A. Everall, I. Bennion, and N. J. Doran, 'Fibre Bragg grating fabrication for dispersion slope compensation.' , *IEEE Photon. Tech. Lett.*, **8**, (9) , 1996, pp.1187-1189

91 T. Stephens, P. A. Kurg, G. Dhosi, F. Ouellete, and L. Poladian, '257 km transmission at 10 Gbit/s in non dispersion shifted fibre using an unchirped fibre Bragg grating dispersion compensator.' , *Electron. Lett.*, **32 (17)** 1996, pp.1599-1600

92 W. H. Loh, R. I. Lamming, N. Robinson, A. Cavaciuti, F. Vaninetti, C. J Anderson, M. N. Zervas, and M. J. Cole., 'Dispersion compensation over distances in excess of 500 km for 10 Gb/s systems using chirped fibre grating.' , *IEEE Photon. Tech. Lett.*, **8**, (7) , 1996, pp.944-946

93 C. Das, U. Gaubatz, E. Gottwald, K. Kotten, L. Rapp, C. J. Weiske, B. Hein, F. Kuppers, and A. Mathews, 'Straightforward upgrading of transmission system to 4*10Gbit/s through 617 km and 8*10Gbit/s through 412 km of SMF.', *Electron. Lett.*, **31**, 1995, pp.1374-1375

94 F. M. Knox, W. Forsiak, and N. J. Doran, '10 Gbit/s soliton communication systems over standard fibre at 1.55 μm and the use of dispersion compensation.' *IEEE J. Lightwave Technol.*, **13**, 1995, pp.1955-1962

95 S. Alleston, I. Penketh, P. harper, A. Niculae, I. Bennion, and N. J. Doran, '16000 km 10 Gbit/s soliton transmission over standard fibre by reduction of interactions through optimum amplifier positioning.', *OFC 1999*, 1999, WC 4,pp.41-43

96 B. Dany, J. P. Hamaide, and F. Neddam, 'Numerical study of long-haul 16*10Gbit/s soliton transmission using dispersion management and narrow-band filtering.' *Electron. Lett.*, **34 (21)** 1998, pp.2053-2054

97 T. Georges, and B. Charbonnier, 'Prechirping and dispersion compensation for long hau; 20 Gbit/s soliton transmission at 1.55 μm on nondisperion shifted fibres. ', *OFC 1997*, 1997, WH2 ,pp.144-145

98 C. Das, U. Gaubatz, E. Gottwald, K. Kotten, L. Rapp, C. J. Weiske, B. Hein, F. Kuppers, and A. Mathews, 'Straightforward upgrading of transmission system to 4*10Gbit/s through 617 km and 8*10Gbit/s through 412 km of SMF.', *Electron. Lett.*, **31**, 1995, pp.1374-1375

99 F. M. Knox, W. Forsiak, and N. J. Doran, '10 Gbit/s soliton communication systems over standard fibre at 1.55 μm and the use of dispersion compensation.' *IEEE J. Lightwave Technol.*, **13**, 1995, pp.1955-1962

100 S. Alleston, I. Penketh, P. harper, A. Niculae, I. Bennion, and N. J. Doran, '16000 km 10 Gbit/s soliton transmission over standard fibre by reduction of interactions through optimum amplifier positioning.', *OFC 1999*, 1999, WC 4,pp.41-43

101 B. Dany, J. P. Hamaide, and F. Neddam, 'Numerical study of long-haul 16*10Gbit/s soliton transmission using dispersion management and narrow-band filtering.' *Electron. Lett.*, **34 (21)** 1998, pp.2053-2054

102 T. Georges, and B. Charbonnier, 'Prechirping and dispersion compensation for long haul 20 Gbit/s soliton transmission at 1.55 μm on nondisperion shifted fibres. ', *OFC 1997*, 1997, WH2 ,pp.144-145

103 N. A. Olson, 'Lightwave systems with optical amplifiers', *IEEE J. Lightwave Technol.*, **7**, (7), 1989, pp.1071-1082

104 D. Marcuse, 'Calculation of bit error probability for a Lightwave system with optical amplifiers and post deduction Gaussian noise', , *IEEE J. Lightwave Technol.*, **9**, (4), 1991, pp.505-513

105 S. B. Alleston, P. harper, I. S. Penketh, I. Bennion, N. J. Doran, and A. D. Ellis, '1000 km transmission of 40 Gbit/s single channel RZ data over dispersion managed standard (non-dispersion shifted) fibre .', Electron. Lett., 1999,35,pp.823-824

106 A. Sahara, K. Suzuki, H. Kubota, T. Komukai, E. Tamada, T. Imai, K. Tamaura and M. Nakazawa, *OFC 99.*, 1999, Paper TH12

107 K. Suzuki, H. Kubota, A. Sahara, Tamaura and M. Nakazawa,'40 Gbit/s single channel optical soliton transmission over 70 000 km using in line synchrounous modulation and optical filtering', *Electron. Lett.*, **34**, 1998, pp.98-99

108 J.H.B Nijhof, N. J. Doran, W. Forysiak, and A. Benston, 'Energy enhancement of dispersion managed solitons and WDM', *Electron. Lett.*, **34**, (5), 1998, pp.481-482

109 A. D. Allis, and D. M. Spirit, 'Unrepeated transmission over 80 km standard fibre at 40 Gbit/s', *Electron. Lett.*, **30**,(1), 1994, pp.72-74

110 S. K. Turytsyn, and E. G. Shapiro, 'Variational approach to the Design of Optical Communication Systems with Dispersion Management', *Opt. Fibre Tech.*, **4**, 1998, pp.151-188

111 N. A. Olson, 'Lightwave systems with optical amplifiers', *IEEE J. Lightwave Technol.*, **7**, (7), 1989, pp.1071-1082

112 D. Marcuse, 'Calculation of bit error probability for a Lightwave system with optical amplifiers and post deduction Gaussian noise', , *IEEE J. Lightwave Technol.*, **9**, (4), 1991, pp.505-513

113 S. Kawanishi, H. Takara, T. Morioka, O. Kamatani, T. Takahashi, T. Kitoh, and M. Saruwatari, 'single-channel 400 Gbit/s time-division-multiplexed transmission of 0.98 ps pulses over 40 km employing dispersion slope compensation. ', Elect. Lett. . 32 (10) pp.916-918. 1996

114 N. S. Bergano, C. R. Davidson, M. A. Mills, P. C. Corbet, S. G. Evangelides, B. Pedersen, R. Menges, J. L. Ziskind, J. W. Sulhoff, A. K. Srivastava, C. Wolf, and J. Judkins, 'Long-haul WDM transmission using optimum channel modulation: A 160Gb/s (32 x 5 Gb/s) 9,300km demonstration. ', Opt. Fibre. Comm. (OFC 97) - Dallas, pp.PD16. OSA 1997

115 S. Kawanishi, H. Takara, K. Uchiyama, I. Shake, O. Kamatani, and H. Takahashi, '14 Tbit/s (200Gbit/s x 7ch) 50 km optical transmission experiment. ', Elect. Lett. . 33 (20) pp.716-718. 1997

116 T. Morioka, H. Takara, S. Kawanishi, O. Kamatani, K. Takiguchi, K. Uchiyama, M. Saruwatari, H. Takahashi, M. Yamada, T. Kanamori, and H. Ono '1 Tbit/s (100Gbit/s x 10m channel) OTDM/WDM transmission using a simple supercontinum WDM source. ', Elect. Lett. . 32 (10) pp.906-907. 1996

117 A. R. Chraplyvy, A. H. Gnauck, J. L. Tkack, R. W. Ziskind, J. W. Sulhoff, A. J. Lucero, Y. Sun, R. M. Jopson, F. Forghieri, R. M. Derosier, C. Wolf, and A.R. Mccormick, '1-Tb/s trasmission experiment. ', IEEE Photon. Technol. Lett., 8(9) pp.1264-1266, 1996

118 S. Y. Kim, S. B. Lee, J. Chung, I. J. Park, J. Jeong, and S. S. Choi, ' Highly Stable optical add/drop multiplexer using polarization beam splitters and fibre Bragg grattings. ', IEEE Photon. Technol. Lett., 9(8) pp.1119-1121, 1997

119 H,. Taga, T. Miyakawa, K. Murashige, N. Edagawa, M. Suzuki, H. Tanaka, K. Goto, and S. Yamamoto, ' A half Tbit/s (50 x 10.66 Gbit/s) over 1600km transmission experiment using widely gain flattened EDFA chain. ', Eur. Conf. on Opt Comm. (ECOC'97) - Edinburgh, 5, pp.13-16, IEE 1997

120 T. Naito, T. Treahara, and N. Shimojoh, '128 Gbit/s WDM transmission of 24 5.3Gbit/s rz signals over 7828 km using gain equalization to compensate for asymmetry in EDFA gain characteristcs. ', Opt. Fibre. Comm. (OFC 97) - Dallas, pp.44-45. OSA 1997

121 M. Nakazawa, Y. Kimura, K. Suzuki, H. Kubota, T. Komukai, E. Yamada, T. Sugawa, E. Yoshida, T. Yamamoto, T. Amai, A. Sahara, H. Nakazawa, O. Yamaouchi, and M. Umizawa, 'Field demonstration of soliton transmission at 10 Gbit/s over 2000km in Tokyo metropolitan optical loop network. ', Elect. Lett. . 31 (12) pp.992-994. 1995

122 A. Sahara, K. Suzuki, H. Kubota, T. Komukai, E. Yamada, T. Amai, K. Tamara, and M. Nakazawa, '40Gbit/s soliton transmission field experiment over 1000 km in Tokyo metropolitan optical loop network using dispersion compensation. ', Elect. Lett. . 34 (22) pp.2154-2155. 1998

123 K. Suzuki, H. Kubota, T. Komukai, E. Yamada, T. Amai, K. Tamara, A. Sahara, and M. Nakazawa, '40Gbit/s soliton transmission field experiment over 1360 using in-line soliton control. ', Elect. Lett. . 34 (22) pp.2143-2145. 1998

124 A. Kolltveit, P. A. Anrekson, J. Brentel, B. E. Olsson, B. Bakhshi, J. Hansryd, P. O. Hedekvist, M. Karlsson, H. Sunnerud, and J. Li, 'Single-wavelength 40Gbit/s soliton field transmission experiment over 400 km of installed fibre. ', Elect. Lett. . 35 (1) pp.75-76. 1999

125 J. Hansryd, B. Bakhshi, B. E. Olsson, P. A. Anrekson, J. Brentel, A. Kolltveit, '80 Gbit/s single wavelength OTDM soliton transmission over 172 km installed fibre. ', Opt. Fibre. Comm. (OFC 99) , pp.PD6. 1999

126 Stefan Wabnitz, Gaelle Le Meur, 'Nonlinear and noise limitations in dispersion-managed soliton wavelength-division multiplexing transmissions with distributed Raman amplification. ', Optics Lett. . 26 (11) pp.777-779. June 2001

127 L. J. Richardson, W. Forysiak, N. J. Doran, 'Dispersion-managed soliton propagation in short-period dispersion maps. ', Optics Lett. . 25 (14) pp.1010-1012. July 2000

128 L. J. Richardson, W. Forysiak, K. J. Blow 'Single channel 320 Gbit/s short period dispersion managed transmission over 6000 km. ', Elect. Lett. . 36 (24) pp.2029-2030. November 2000

129 L. J. Richardson, W. Forysiak, 'Trans-oceanic 80 Gbit/s single channel transmission using short period dispersion mamgement. ', IEE proc.-Optostsctron., . 147 (6) pp.417-422. December 2000

130 V. K. Mezentsev, S. K. Turitsyn , N. J. Doran, 'System optimisation of 80 Gbit/s single channel transmission over 1000 km of standard fibre. ', Elect. Lett. . 36 (23) pp. 1949-1951. November 2000

131 S. Boscolo, S. K. Turitsyn, K. J. Blow 'All-optical passive regeneration of 40 Gbit/s soliton data stream using dispersion management and in-line NOLMs. ', Elect. Lett. . 37 (2) pp.112-113. January 2001

132 K. Tanaka, I. Morita, and N. Edagawa, '50 GHz spaced 40 Gbit/s × 25WDM transmission over 480 km using bandlimited RZ signals. ', Elect. Lett. . 37 (12) pp.775-777. June 2001

133 H. Takenouchi, T. Ishii, and T. Goh, '8 THz bandwidth dispersion-slope compensator module for multiband 40 Gbit/s WDM transmission systems using an AWG and spatial phase filter. ', Elect. Lett. . 37 (12) pp.777-778. June 2001

134 M. Gunkel· F. Küppers· J. Berger· U. Feiste· R. Ludwig· C. Schubert· C. Schmidt· H. G. Weber, 'Unrepeatered 40 Gbit/s RZ transmission over 252 km SMF using Raman amplification. ', Elect. Lett. . 37 (10) pp.646-648. May 2001

135 I. Morita, K. Tanaka, N. Edagawa, 'Benefit of Raman amplification in ultra-long-distance 40 Gbit/s-based WDM transmission using dispersion-flattened fibre span. ', Elect. Lett. . 37 (8) pp.507-509. April 2001

136 B. Zhu, P. B. Hansen, L. Leng, S. Stulz, T. N. Nielsen, C. Doerr, A. J. Stentz, D. S. Vengsarkar, Z.J. Chen, D. W. Peckham, L. Gruner-Nielsen, ' 800 Gbit/s (80 × 10.66 Gbit/s) transmission over 3200 km of non-zero dispersion shifted fibre with 100 km amplified spans employing distributed Raman amplification. ', Elect. Lett. . 36 (22) pp. 1860-1861. October 2000

137 Y. Zhu, W. S.Lee, C. Scahill, C. Fludger, D. Watley, M. Jones, J. Homan, B. Shaw, A. Hadjifotiou '1.28 Tbit/s (32 × 40 Gbit/s) transmission over 1000 km NDSF employing distributed Raman amplification and active gain flattening. ', Elect. Lett. . 37 (1) pp.507-509. January 2001

138 C. Xie, M. Karlsson, P. A. Andrekson, H. Sunnerud, 'Statistical analysis of soliton robustness to polarisation-mode dispersion. ', Elect. Lett. . 37 (1) pp.507-509. January 2001